US Army Corps of Engineers®

ENGINEERING AND DESIGN

Inspection, Evaluation, and Repair of Hydraulic Steel Structures

ENGINEER MANUAL

AVAILABILITY

Electronic copies of this and other U.S. Army Corps of Engineers (USACE) publications are available on the Internet at http://www.usace.army.mil/inet/usace-docs/. This site is the only repository for all official USACE engineer regulations, circulars, manuals, and other documents originating from HQUSACE. Publications are provided in portable document format (PDF).

Engineering and Design
INSPECTION, EVALUATION AND REPAIR OF HYDRAULIC STEEL STRUCTURES

1. Purpose. This manual describes the inspection, evaluation, and repair of hydraulic steel structures, including preinspection identification of critical locations (such as fracture critical members and various connections) that require close examination. Nondestructive testing techniques that may be used during periodic inspections or detailed structural inspections are discussed. Guidance is provided on material testing to determine the chemistry, strength, ductility, hardness, and toughness of the base and weld metal. Analyses methods that can be used to determine structure safety, safe inspection intervals, and expected remaining life of the structure with given operational demands are presented. Finally, considerations for various types of repair are discussed.

2. Applicability. This manual applies to all USACE commands having responsibilities for the design of civil works projects.

3. Distribution Statement. Approved for public release; distribution is unlimited.

4. Scope of the Manual. Chapter 1 describes the types of hydraulic steel structures. Chapter 2 discusses the causes of structural deterioration. Chapter 3 describes periodic inspection procedures, which are primarily visual. If the inspection indicates that a structure is distressed, nondestructive or destructive testing, described in Chapters 4 and 5, respectively, may be required. Chapter 6 describes the evaluation of the capability of a structure to perform its intended function. Chapter 7 discusses the determination of fracture toughness, and Chapter 8 describes repairs.

FOR THE COMMANDER:

1 Appendix
(See Table of Contents)

ROBERT CREAR
Colonel, Corps of Engineers
Chief of Staff

This manual supersedes ETL 1110-2-346, 30 September 1993, and ETL 1110-2-351, 31 March 1994.

Manual
No. 1110-2-6054

1 December 2001

Engineering and Design
INSPECTION, EVALUATION AND REPAIR OF HYDRAULIC STEEL STRUCTURES

Chapter 1
Introduction

1-1. Purpose

This engineer manual (EM) describes the inspection, evaluation, and repair of hydraulic steel structures, including preinspection identification of critical locations (such as fracture critical members and various connections) that require close examination. Nondestructive testing techniques that may be used during periodic inspections or detailed structural inspections are discussed. Guidance is provided on material testing to determine the chemistry, strength, ductility, hardness, and toughness of the base and weld metal. Analyses methods that can be used to determine structure safety, safe inspection intervals, and expected remaining life of the structure with given operational demands are presented. Finally, considerations for various types of repair are discussed.

1-2. Applicability

This manual applies to all USACE commands having responsibilities for the design of civil works projects.

1-3. Distribution

This publication is approved for public release; distribution is unlimited.

1-4. References

Required and related publications are provided in Appendix A.

1-5. Background

a. Structural evaluation. USACE currently operates over 150 lock and dam structures that include various hydraulic steel structures, many of which are near or have reached their design life. Structural inspection and evaluation are required to assure that adequate strength and serviceability are maintained at all sections as long as the structure is in service. Engineer Regulation (ER) 1110-2-100 prescribes general periodic inspection requirements for completed civil works structures, and ER 1110-2-8157 provides specific requirements for hydraulic steel structures. Neither provides specific guidance for structural evaluation. To conduct a detailed inspection for all hydraulic steel structures is not economical, and detailed inspection must be limited to critical areas. When inspections reveal conditions that compromise the safety or serviceability of a structure, a structural evaluation must be conducted; and depending on the results, repair may be necessary. This EM provides specific guidance on inspection focused on critical areas, structural evaluation with emphasis on fatigue and fracture, and repair procedures. Fatigue and fracture concepts are emphasized because it is evident that steel fatigue and fracture are real problems. Many existing hydraulic steel structures in several USACE projects have exhibited fatigue and fracture failures, and many others may be susceptible to fatigue and fracture problems (see *c* below and Chapter 8).

b. Types of hydraulic steel structures. Lock gates are moveable gates that provide a damming surface across a lock chamber. Most existing lock gates are miter gates and vertical-lift gates, with a small percentage being sector gates and submergible tainter gates. Spillway gates are installed on the top of dam spillways to provide a moveable damming surface allowing the spillway crest to be located below a given operating water level. Such gates are used at locks and dams (navigation projects) and at reservoirs (flood control or hydropower projects). Spillway gates are generally tainter gates, the most common, or lift gates, but some

projects use roller gates. Other types of hydraulic steel structures include bulkheads, needle beams, lock culvert valves, and stop logs.

(1) Spillway tainter gates. A tainter gate is a segment of a cylinder mounted on radial arms, or struts, that rotate on trunnions anchored to the dam piers. Numerous types of framing exist; however, the most common type of gate includes two or three frames, each of which consists of a horizontal girder that is supported at each end by a strut. Each frame lies in a radial plane with the struts joining at the trunnion. The girder supports the stiffened skin plate assembly that forms the damming surface. Spillway flow is regulated by raising or lowering the gate to adjust the discharge under the gate.

(2) Miter gates. The majority of lock gates are miter gates, primarily because they tend to be more economical to construct and operate and can be opened and closed more rapidly than other types of lock gates. Miter gates are categorized by their framing mechanism as either vertically or horizontally framed. On a vertically framed gate, water pressure from the skin plate is resisted by vertical beam members that are supported at the ends by a horizontal girder at the top and one at the bottom of the leaf. The horizontal girders transmit the loads to the miter and quoin at the top of the leaf and into the sill at the bottom of the leaf. Horizontally framed lock gates include horizontal girders that resist the water loads and transfer the load to the quoin block and into the walls of the lock monolith. Current design guidance as provided by EM 1110-2-2703 recommends that future miter gates be horizontally framed; however, a large percentage of existing miter gates are vertically framed.

(3) Sector gates. Another type of lock gate is the sector gate. This gate is framed similar to a tainter gate, but it pivots about a vertical axis as does a miter gate. Sector gates have traditionally been used in tidal reaches of rivers or canals where the dam may be subject to head reversal. Sector gates may be used to control flow in the lock chamber during normal operation or restrict flow during emergency operation. Sector gates are generally limited to lifts of 3 m (10 ft) or less.

(4) Vertical lift gates. Vertical lift gates have been used as lock gates and spillway gates. These gates are raised and lowered vertically to open or close a lock chamber or spillway bay. They are essentially a stiffened plate structure that transmits the water load acting on the skin plate along horizontal girders into the walls of the lock monolith or spillway pier. Lift gates can be operated under moderate heads, but not under reverse head conditions. Specific design guidance for lift gates is specified by EM 1110-2-2701.

(5) Submergible tainter gates. Submergible tainter gates are used infrequently as lock gates. This type of gate pivots similar to a spillway tainter gate but is raised to close the lock chamber, and is lowered into the chamber floor to open it. The load developed by water pressure acting on skin plate is transmitted along horizontal girders to struts that are recessed in the lock wall. The struts are connected to and rotate about trunnions that are anchored to each lock wall.

(6) Bulkheads, stop logs, needle beams, and tainter valves.

(a) Bulkheads are moveable structures that provide temporary damming surfaces to enable the dewatering of a lock chamber or gate bay between dam piers. Slots are generally provided in the sides of lock chambers or piers to provide support for the bulkhead.

(b) Stop logs are smaller beam or girder structures that span the desired opening and are stacked to a desired damming height. A number of stacked stop logs make up a bulkhead.

(c) A needle dam consists of a sill, piers, a horizontal support girder that spans between piers, and a series of beams placed vertically between the sill and horizontal support girder. The vertical beams are referred to as needle beams. These are placed adjacent to each other to provide the damming surface.

(d)   Tainter valves are used to regulate flow through lock chambers. Tainter valves are geometrically similar to tainter gates; however, the valves are generally oriented such that their struts are in tension as opposed to spillway gates that resist load with their struts in compression.

c.   Examples of distressed hydraulic steel structures. The following brief examples, all taken from a single District, illustrate the potential results of casual inspection combined with inattention to fatigue and fracture concepts during design. These examples represent only a few of the steel cracking problems that have occurred on USACE projects. Chapter 8 provides other examples with recommended repair procedures.

(1)   Miter gate anchorage.

(a)   This case involves a failure on a downstream, vertically framed miter gate that spanned a 33.5-m- (110-ft-) wide lock. The upper embedded gate anchorage failed unexpectedly while the chamber was at tail-water elevation. Failure occurred by fracture at the gudgeon pin hole. The anchor was a structural steel assembly composed of two channels and two 12-mm- (1/2-in.-) thick plates. The use of a channel with upturned legs resulted in ponding of water that caused pitting and scaling corrosion of the channel. Since the anchor is a nonredundant tension member, failure caused the leaf to fall to the concrete sill, though it remained vertical.

(b)   The failure surfaces were disposed of without an examination to determine the cause of failure. To make the lock operational as quickly as possible, repairs were implemented without any evaluation or recommendations from the District's Engineering Division. These repairs consisted of butting and welding a new channel section to the remaining embedded section and bolting a 25-mm (1-in.) cover plate to the channel webs. The bolt and plate materials are not known.

(c)   The same type of anchorage is used on at least two other projects with a total of 16 similar anchors.

(2)   Spare miter gate.

(a)   The project had a spare miter gate consisting of five welded modules stacked and bolted together. The spare gate had been used several times. One month after the last installation, cracks were discovered in the downstream flanges of three vertical girders. The cracks originated at the downstream face of the flange in the heat-affected zone at the toe of a transverse fillet weld. (This detail has low fatigue strength.) The cracks then propagated through the flange and into the web. After cracking, the downstream face of the flange was 12.5 mm (0.5 in.) out of vertical alignment.

(b)   Quick repairs were performed by operations personnel, without input from engineering personnel. The web crack was filled with weld metal. The flange cracks were gouged and welded, and two small bars were fillet welded across the crack. The bar material is unknown. These repairs served to get the gate back into service immediately. However, reliable long-term repairs should be developed and implemented. This example is further discussed in paragraph 8-6*b*.

(3)   Submersible lift gate.

(a)   This project includes a submersible lift gate as the primary upstream lock gate. The gate consists of two leaves with six horizontal girders spanning 33.5 m (110 ft). Several cracks were discovered in one leaf while the lock was out of service for other repairs. Subsequent detailed inspection identified over 100 cracks in girder flanges and bracing members. One crack extended through the downstream flange of a horizontal girder and 1 m (3 ft) into the 2.5-m- (8-ft-) deep web.

(b) This gate was subjected to a detailed investigation to determine the cause of the cracking. The study identified several contributing factors: the original design had ignored a loading case and had included improper loading assumptions; limit switches were improperly stopping the gate before it reached its supports; the design ignored higher stresses caused by eccentric connections on the downstream face; most of the original welds did not meet current American Welding Society (AWS) quality standards; the steel for the gate had a low fracture toughness, ranging from 6.8 J (5 ft-lb) at 0 ^{o}C (32 ^{o}F) to 20 J (15 ft-lb) at 21 ^{o}C (70 ^{o}F).

(c) Repair procedures were designed by engineering personnel for this gate. However, the specified weld procedures were not used by the contractor, and the welders were not properly qualified per AWS requirements. These factors may have caused inadequate repair welds, which duplicates part of the causes of the original cracking problem. This example is further discussed in paragraph 8-6*c*.

1-6. Mandatory Requirements

This manual provides guidance for the protection of USACE structures. In certain cases, guidance requirements are considered mandatory because they are critical to project safety and performance as discussed in ER 1110-2-1150. Structural inspection and evaluation (and repair if necessary) are critical. These are best carried out on a case-by-case basis, however, and general mandatory requirements are not provided. In the inspection, evaluation, and repair process, guidance contained herein should be used where appropriate.

Chapter 2
Causes of Structural Deterioration

2-1. Corrosion

a. Effects of corrosion. Corrosion can seriously weaken a structure or impair its operation, so the effect of corrosion on the strength, stability, and serviceability of hydraulic steel structures must be evaluated. The major degrading effects of corrosion on structural members are a loss of cross section, buildup of corrosion products at connection details, and a notching effect that creates stress concentrations.

(1) A loss of cross section in a member causes a reduction in strength and stiffness that leads to increased stress levels and deformation without any change in the imposed loading. Flexure, shear, and buckling strength may all be affected. Depending on the location of corrosion, the percentage reduction in strength considering these different modes of failure is not generally not the same.

(2) A buildup of corrosion products can be particularly damaging at connection details. For example, corrosion buildup in a tainter gate trunnion or lift gate roller guides can lead to extremely high hoist loads. At connections between adjacent plates or angles, a buildup of rust can cause prying action. This is referred to as corrosion packout and results from expansion during the corrosion process.

(3) Localized pitting corrosion can form notches that may serve as fracture initiation sites. Notching significantly reduces the member fatigue life.

b. Common types of corrosion. Corrosion is degradation of a material due to reaction with its environment. All corrosion processes include electrochemical reactions. Galvanic corrosion, pitting corrosion, crevice corrosion, and general corrosion are purely electrochemical. Erosion corrosion and stress corrosion, however, result from the combined action of chemical plus mechanical factors. In general, hydraulic steel structures are susceptible to three types of corrosion: general atmospheric corrosion, localized corrosion, and mechanically assisted corrosion (Slater 1987). For any case, the type of corrosion and cause should be identified to assure that a meaningful evaluation is performed.

(1) General atmospheric corrosion is defined as corrosive attack that results in uniform thinning spread over a wide area. It is expected to occur in the ambient environment of hydraulic steel structures but is not likely to cause significant structural degradation.

(2) Localized corrosion is the type of corrosion most likely to affect hydraulic steel structures. Five types of localized corrosion are possible:

(a) Crevice corrosion occurs in narrow openings between two contact surfaces, such as between adjoining plates or angles in a connection. It can also occur between a steel component and a nonmetal one (under the seals, a paint layer, debris, sand or silt, or organisms caught on the gate members). It can lead to blistering and failure of the paint system, which further promotes corrosion.

(b) Pitting corrosion occurs on bare metal surfaces as well as under paint films. It is characterized by small cavities penetrating into the surface over a very localized area (at a point). If pitting occurs under paint, it can result in the formation of a blister and failure of the paint system.

(c) Galvanic corrosion can occur in gate structures where steels with different electrochemical potential (dissimilar metals) are in contact. The corrosion typically causes blistering or discoloration of the paint and

failure of the paint system adjacent to the contact area of the two steels and decreases as the distance from the metal junction increases.

(d) Stray current corrosion may occur when sources of direct current (i.e., welding generators) are attached to the gate structures, or unintended fields from cathodic protection systems are generated.

(e) Filiform corrosion occurs under thin paint films and has the appearance of fine filaments emanating from one or more sources in random directions.

(3) Three types of mechanically assisted corrosion are also possible in hydraulic steel structures.

(a) Erosion corrosion is caused by removal of surface material by action of numerous individual impacts of solid or liquid particles and usually has a direction associated with the metal removal. The precursor of erosion corrosion is directional removal of the paint film by the impacting particles.

(b) Cavitation corrosion is caused by cavitation associated with turbulent flow. It can remove surface films such as oxides or paint and expose bare metal, producing rounded microcraters.

(c) Fretting corrosion is a combination of wear and corrosion in which material is removed between contacting surfaces when very small amplitude motions occur between the surfaces. Red rust is formed and appears to come from between the contacting surfaces.

c.   Factors influencing corrosion. The type and amount of corrosion that may occur on a hydraulic steel structure are dependent on many factors that include design details, material properties, maintenance and operation, environment, and coating system. In general, the primary factors are the local environment and the protective coating system.

(1) The pH and ion concentration of the river water and rain are significant environmental factors. Corrosion usually occurs at low pH (highly acidic conditions) or at high pH (highly alkaline conditions). At intermediate pH, a protective oxide or hydroxide often forms. Deposits of film-forming materials such as oil and grease and sand and silt can also contribute to corrosion by creating crevices and ion concentration cells.

(2) Corrosion of steel increases significantly when the relative humidity is greater than 40 percent. Corrosion is also aggravated by alternately wet and dry cycles with longer periods of wetness tending to increase the effect. Organisms in contact with steel also promote corrosion.

(3) Paint and other protective coatings are the primary preventive measures against corrosion on hydraulic steel structures. The effectiveness of a protective coating system is highly dependent on proper pretreatment of the steel surface and coating application. Sharp corners, edges, crevices, weld terminations, rivets, and bolts are often more susceptible to corrosion since they are more difficult to coat adequately. Any variation in the paint system can cause local coating failure, which may result in corrosion under the paint.

(4) The paint system and cathodic protection systems should be inspected to assure that protection is being provided against corrosion. If corrosion has occurred, ultrasonic equipment and gap gauges are available to measure loss of material.

2-2. Fracture

a.   Basic behavior.

(1)   Brittle fracture is a catastrophic failure that occurs suddenly without prior plastic deformation and can occur at nominal stress levels below the yield stress. Fracture of structural members occurs when a relatively high stress level is applied to a material with relatively low fracture toughness.

(2)   Fracture usually initiates at a discontinuity that serves as a local stress raiser. Structural connections that are welded, bolted, or riveted are sources of discontinuities and stress concentrations because members are discontinuous and abrupt changes in geometry occur where different members intersect. Welded connections include additional physical discontinuities, metallurgical structure variations, and residual stresses that further contribute to possible fracture. The fracture or cracking vulnerability of a structural component is governed by the material fracture toughness, the stress magnitude, the component geometry, and the size, shape, and orientation of any existing crack or discontinuity (see *b* and *c* below).

b.   Fracture mechanics concepts.

(1)   Fracture mechanics includes linear-elastic fracture mechanics (LEFM) and elastic-plastic fracture mechanics (EPFM). In LEFM analysis, it is assumed that the material in the vicinity of a crack tip is linear-elastic. EPFM methods, which include the crack tip opening displacement (CTOD) and J-integral methods, take into account plastic material behavior. Some fundamental concepts of LEFM are presented here. Additional information is provided in Chapter 6, and examples applying this methodology to hydraulic steel structures are located in Chapter 7.

(2)   When tensile stresses are applied to a body that contains a discontinuity such as a sharp crack, the crack tends to open and high stress is concentrated at the crack tip. For cases where plastic deformation is con-strained to a small zone at the crack tip (plane-strain condition), the fracture instability can be predicted using LEFM concepts. The fundamental principle of LEFM is that the stress field ahead of a sharp crack in a structural member can be characterized in terms of a single parameter, the stress intensity factor K_I. K_I is a function of the crack geometry and nominal stress level in the member, and K_I has the general form

$$K_I = C\sigma\sqrt{a} \tag{2-1}$$

where

C = nondimensional coefficient that is a function of the component and crack geometry

σ = member nominal stress

a = crack length

K_I is in units of Mpa-$\sqrt{m}$ (ksi-$\sqrt{in.}$) and, for a given crack size and geometry, is directly related to the nominal stress.

(3)   Another basic principal of LEFM is that fracture (unstable crack propagation) will occur when K_I exceeds the critical stress intensity factor K_{Ic} (or K_c depending on the state of stress at the crack tip). K_{Ic} represents the fracture toughness (ability of the material to withstand a given stress-field intensity at the tip of a crack and to resist tensile crack extension) of a component when the state of stress at the crack tip is plane strain and the extent of yielding at the crack tip is limited. This is generally the case for relatively thick

sections where a triaxial state of stress exists (due to the constraint in the through thickness direction) at the crack tip. Plane strain behavior occurs when

$$\beta_{Ic} = \frac{1}{t}\left(\frac{K_{Ic}}{\sigma_y}\right)^2 \leq 0.4 \tag{2-2}$$

where

β_{Ic} = Irwin's plane strain factor

t = thickness of the component

K_{Ic} = critical plane strain stress intensity factor

σ_y = yield stress

(4) K_{Ic} is a material property (for a given temperature and loading rate) that is defined by American Society for Testing and Materials (ASTM) E399 and is applicable only when plane strain conditions exist. When this requirement for plane strain conditions is not met, the fracture toughness of a component may be defined by the critical stress intensity factor K_c. K_c is the fracture toughness under other than plane strain conditions and is a function of the thickness of the component in addition to temperature and loading rate. K_c is always greater than K_{Ic}.

(5) For many structural applications where low- to medium-strength steels are used, the material thickness is not sufficient to maintain small crack-tip plastic deformation under slow loading conditions at normal service temperatures. Consequently, the LEFM approach is invalidated by the formation of large plastic zones and elastic-plastic behavior in the region near the crack tip. When the extent of yielding at the crack tip becomes large, EPFM methods are required. One widely used EPFM method is the CTOD method of fracture analysis (British Standards Institution 1980). The CTOD method is more applicable when there is significant plastification, since it is a direct measurement of opening displacement and is not based on calculated elastic stress fields. The LEFM and CTOD methods are discussed further in Chapter 6.

c. Factors influencing fracture. Many factors can contribute to fracture and weld-related cracking in hydraulic steel structures. These include material properties (fracture toughness), welding influences, and component thickness.

(1) Material properties. Material fracture toughness of steel is generally a function of chemical composition, thermomechanical history, and microstructure. Chemical composition affects the toughness of a steel, since the addition of solute (e.g., alloying and/or tramp elements) to a metal may inhibit plastic flow, which strengthens the material, but reduces its fracture toughness. Thermomechanical treatment can affect toughness by altering the phase composition of the material. The microstructure, particularly the grain size, also affects the fracture toughness. For a given steel, fracture toughness will generally tend to decrease with increasing grain size much the same as yield strength does. Fracture toughness will also vary significantly with temperature and loading rate (see Chapter 6). Structural steels exhibit a transition from a brittle behavior to a more ductile behavior at a certain temperature that is material dependent. Steel is also strain-rate sensitive, and fracture toughness decreases with increasing loading rate.

(2)   Welding influences.

(a)   Weld-related cracking is a result of welding discontinuities, residual stresses, and decreased strength and toughness in the weld metal and heat-affected zone (HAZ). Design and fabrication methods also affect weld integrity. Stress concentrations from notches, residual stresses, and changes in microstructure resulting in reduced toughness can also be caused by flame cutting.

(b)   Common weld discontinuities such as porosity, slag inclusion, and incomplete fusion (see Chapter 4) serve as local stress concentrations and crack nucleation sites. Discontinuities in regions near the weld are of special concern, since high tensile residual stresses develop from the welding process.

(c)   During welding, nonlinear thermal expansion and contraction of weld and base metal produce significant residual stresses. Near the weld, high tensile residual stresses may cause cracking, lamellar tearing in thick joints, and premature fracture of the welded connection. These stresses can also indirectly cause cracking by contributing to a triaxial stress state that tends toward brittle behavior. For example, at weld inter-sections (such as the corner of a girder flange, web, and transverse stiffener) a high triaxial state of residual tensile stress exists that is conducive to crack initiation and brittle fracture. (This detail can be improved using a coped stiffener or by not welding the stiffener to the flange.) The heat applied during the welding process also alters the microstructure in the vicinity of the weld or HAZ, which results in reduced toughness and strength in this area.

(d)   Welded details that have poor accessibility during fabrication are prone to cracking due to the increased difficulty in producing a sound weld. Tack welds used for positioning and alignment of components during the fabrication can be a source of problems, since they are not usually inspected and may include significant weld discontinuities and residual stresses. This may be especially true of welds on riveted structures, since the structural steels typically used in older structures are not characterized as steels for welding. A discussion of structural steels used in older spillway gates is provided in Chapter 7. Backup bars may also be a source of discontinuity if they are not welded continuously.

(3)   Thick plates. Thick plate material tends to be more susceptible to cracking, since during manufacturing the interior of a thick plate cools more slowly after rolling than that of a thin plate. Slow cooling of steel results in a microstructure with large grain size, and consequently, reduced toughness. The additional through-thickness constraint inherent in thick material also contributes to the susceptibility of cracking by promoting plane strain behavior. Weldments involving thick plates are particularly more susceptible to cracking than those of thin plates. In addition to the reduced toughness and additional through-thickness constraint inherent in thick plates, welding further increases the likelihood of cracking. Residual stresses due to welding are generally higher for weldments of increasing plate thickness simply because the increased thickness provides more constraint to weld shrinkage. Additionally, thick plate weldments require more weld passes so the number of thermal cycles (heating and cooling) and the probability of forming discontinuities increase. Another consideration for thick plate weldments is that a weld of a particular size will cool faster on a thick plate than a thin plate. Rapid cooling of the weld material and HAZ promotes the formation of martensite, which is a brittle phase of steel. Preheat and postheat requirements have been adopted (American National Standards Institute/American Welding Society (ANSI/AWS) D1.1) to minimize this effect.

2-3. Fatigue

Fatigue is the process of cumulative damage caused by repeated cyclic loading. Fatigue damage generally occurs at stress-concentrated regions where the localized stress exceeds the yield stress of the material. After a certain number of load cycles, the accumulated damage causes the initiation and propagation of a crack. Although the number of load cycles experienced by hydraulic steel structures does not, in general, compare to that of bridges, fatigue is a real concern for lock gates at busy locks and spillway gates with vibration problems.

    a.   Basic behavior.

    (1)   Like brittle fracture, fatigue cracking occurs or initiates at a discontinuity that serves as a stress raiser. Consequently, there are some parallels in the analysis of fatigue and fracture. Fatigue crack propagation is related to the stress intensity factor range ΔK, which serves as the driving force for fatigue (analogous to K_I considering fracture). More detailed information on fatigue crack propagation is given in Chapter 6. Here, the concept of fatigue life is introduced and will later be used to identify critical connections in Chapter 3.

    (2)   The fatigue life of a connection or detail is commonly defined as the number of load cycles that causes cracking of a component. The most important factors governing the fatigue life of structures are the severity of the stress concentration and the stress range of the cyclic loading. The fatigue life of a structure (member or connection) is often represented by an S_r-N curve, which defines the relationship between the constant-amplitude stress range S_r (σ_{max} - σ_{min}) and fatigue life N (number of cycles), for a given detail or category of details. The effect of the stress concentration for various details is reflected in the differences between the S_r-N curves. The S_r-N curves are based on constant-amplitude cyclic loading and are typically characterized by a linear relationship between $\log_{10} S_r$ and $\log_{10} N$. There is also a lower bound value of S_r, known as the fatigue limit, below which infinite life is assumed.

    b.   Fatigue strength of welded structures.

    (1)   Common welded details have been assigned fatigue categories (A, B, B', C, D, E, and E') and corresponding S_r-N curves. These curves have been derived from large amounts of experimental data and have been verified with analytical studies. S_r-N curves for welded details adopted by American Association of State Highway and Transportation Officials (AASHTO) for redundant structural members (AASHTO 1996) are shown in Figure 2-1. The dashed lines in Figure 2-1 represent the fatigue limit of the respective categories. Fatigue category A represents plain rolled base material and has the longest life for a given stress range and the highest fatigue limit. Categories B through E' represent increasing severity of stress concentration and associated diminishing fatigue life for a given stress range. Descriptions and illustrations of various welded details and their fatigue categories are given in Table 2-1 and Figure 2-1 (AASHTO 1996).
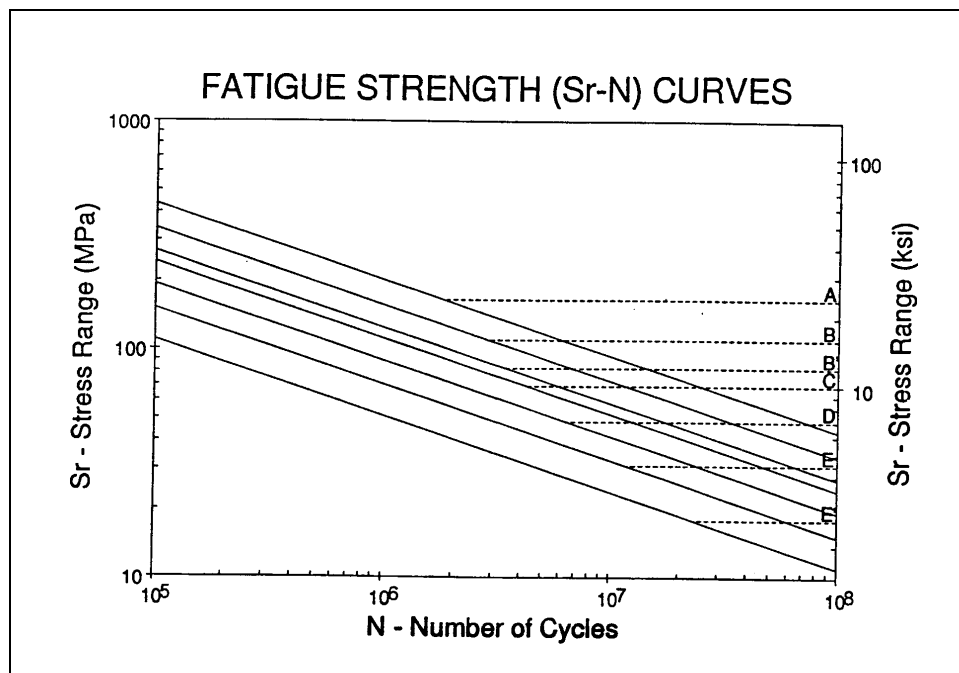

Figure 2-1. Current AASHTO S_r-N curves

Table 2-1
AASHTO Fatigue Categories

General Condition	Situation	Kind of Stress	Stress Category (See Table 10.3.1A)	Illustrative Example (See Figure 10.3.1C)
Plain Member	Base metal with rolled or cleaned surface. Flame-cut edges with ANSI smoothness of 1,000 or less.	T or Rev[a]	A	1,2
Built-Up Members	Base metal and weld metal in members of built-up plates or shapes (without attachments) connected by continuous full penetration groove welds (with backing bars removed) or by continuous fillet welds parallel to the direction of applied stress.	T or Rev	B	3,4,5,7
	Base metal and weld metal in members of built-up plates or shapes (without attachments) connected by continuous full penetration groove welds with backing bars not removed, or by continuous partial penetration groove welds parallel to the direction of applied stress.	T or Rev	B′	3,4,5,7
	Calculated flexural stress at the toe of transverse stiffener welds on girder webs or flanges.	T or Rev	C	6
	Base metal at ends of partial length welded coverplates with high-strength bolted slip-critical end connections. (See Note f.)	T or Rev	B	22
	Base metal at ends of partial length welded coverplates narrower than the flange having square or tapered ends, with or without welds across the ends, or wider than flange with welds across the ends:			
	(a) Flange thickness ≤ 0.8 in.	T or Rev	E	7
	(b) Flange thickness > 0.8 in.	T or Rev	E′	7
	Base metal at ends of partial length welded coverplates wider than the flange without welds across the ends.	T or Rev	E′	7
Groove Welded Connections	Base metal and weld metal in or adjacent to full penetration groove weld splices of rolled or welded sections having similar profiles when welds are ground flush with grinding in the direction of applied stress and weld soundness established by nondestructive inspection.	T or Rev	B	8,10
	Base metal and weld metal in or adjacent to full penetration groove weld splices with 2 ft radius transitions in width, when welds are ground flush with grinding in the direction of applied stress and weld soundness established by nondestructive inspection.	T or Rev	B	13
	Base metal and weld metal in or adjacent to full penetration groove weld splices at transitions in width or thickness, with welds ground to provide slopes no steeper than 1 to 2½, with grinding in the direction of the applied stress, and weld soundness established by nondestructive inspection:			
	(a) AASHTO M 270 Grades 100/100W (ASTM A 709) base metal	T or Rev	B′	11,12
	(b) Other base metals	T or Rev	B	11,12
	Base metal and weld metal in or adjacent to full penetration groove weld splices, with or without transitions having slopes no greater than 1 to 2½, when the reinforcement is not removed and weld soundness is established by nondestructive inspection.	T or Rev	C	8,10,11,12
Groove Welded Attachments— Longitudinally Loaded[b]	Base metal adjacent to details attached by full or partial penetration groove welds when the detail length, L, in the direction of stress, is less than 2 in.	T or Rev	C	6,15
	Base metal adjacent to details attached by full or partial penetration groove welds when the detail length, L, in the direction of stress, is between 2 in. and 12 times the plate thickness but less than 4 in.	T or Rev	D	15

(Sheet 1 of 4)

Note: Refer to AASHTO 1996 for Table 10.3.1A. For Figure 10.3.1C, see the last sheet of this table.
Taken from AASHTO 1996, Copyright 1996 by AASHTO, reproduced with permission.

Table 2-1 (Continued)

General Condition	Situation	Kind of Stress	Stress Category (See Table 10.3.1A)	Illustrative Example (See Figure 10.3.1C)
	Base metal adjacent to details attached by full or partial penetration groove welds when the detail length, L, in the direction of stress, is greater than 12 times the plate thickness or greater than 4 in.:			
	(a) Detail thickness < 1.0 in.	T or Rev	E	15
	(b) Detail thickness ≥ 1.0 in.	T or Rev	E′	15
	Base metal adjacent to details attached by full or partial penetration groove welds with a transition radius, R, regardless of the detail length:			
	—With the end welds ground smooth	T or Rev		16
	(a) Transition radius ≥ 24 in.		B	
	(b) 24 in. > Transition radius ≥ 6 in.		C	
	(c) 6 in. > Transition radius ≥ 2 in.		D	
	(d) 2 in. > Transition radius ≥ 0 in.		E	
	—For all transition radii without end welds ground smooth.	T or Rev	E	16
Groove welded Attachments— Transversely Loaded[b,c]	Detail base metal attached by full penetration groove welds with a transition radius, R, regardless of the detail length and with weld soundness transverse to the direction of stress established by nondestructive inspection:			
	—With equal plate thickness and reinforcement removed	T or Rev		16
	(a) Transition radius ≥ 24 in.		B	
	(b) 24 in. > Transition radius ≥ 6 in.		C	
	(c) 6 in. > Transition radius ≥ 2 in.		D	
	(d) 2 in. > Transition radius ≥ 0 in.		E	
	—With equal plate thickness and reinforcement not removed	T or Rev		16
	(a) Transition radius ≥ 6 in.		C	
	(b) 6 in. > Transition radius ≥ 2 in.		D	
	(c) 2 in. > Transition radius ≥ 0 in.		E	
	—With unequal plate thickness and reinforcement removed	T or Rev		16
	(a) Transition radius ≥ 2 in.		D	
	(b) 2 in. > Transition radius ≥ 0 in.		E	
	—For all transition radii with unequal plate thickness and reinforcement not removed.	T or Rev	E	16
Fillet Welded Connections	Base metal at details connected with transversely loaded welds, with the welds perpendicular to the direction of stress:			
	(a) Detail thickness ≤ 0.5 in.	T or Rev	C	14
	(b) Detail thickness > 0.5 in.	T or Rev	See Note[d]	
	Base metal at intermittent fillet welds.	T or Rev	E	—
	Shear stress on throat of fillet welds.	Shear	F	9
Fillet Welded Attachments— Longitudinally Loaded[b,c,e]	Base metal adjacent to details attached by fillet welds with length, L, in the direction of stress, is less than 2 in. and stud-type shear connectors.	T or Rev	C	15,17,18,20
	Base metal adjacent to details attached by fillet welds with length, L, in the direction of stress, between 2 in. and 12 times the plate thickness but less than 4 in.	T or Rev	D	15,17
	Base metal adjacent to details attached by fillet welds with length, L, in the direction of stress greater than 12 times the plate thickness or greater than 4 in.:			
	(a) Detail thickness < 1.0 in.	T or Rev	E	7,9,15,17
	(b) Detail thickness ≥ 1.0 in.	T or Rev	E′	7,9,15

(Sheet 2 of 4)

Table 2-1 (Continued)

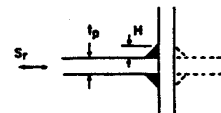| General Condition	Situation	Kind of Stress	Stress Category (See Table 10.3.1A)	Illustrative Example (See Figure 10.3.1C)
	Base metal adjacent to details attached by fillet welds with a transition radius, R, regardless of the detail length:			
	—With the end welds ground smooth (a) Transition radius ≥ 2 in. (b) 2 in. > Transition radius ≥ 0 in.	T or Rev	D E	16
	—For all transition radii without the end welds ground smooth.	T or Rev	E	16
Fillet Welded Attachments— Transversely Loaded with the Weld in the Direction of Principal Stress[b,e]	Detail base metal attached by fillet welds with a transition radius, R, regardless of the detail length (shear stress on the throat of fillet welds governed by Category F):			
	—With the end welds ground smooth (a) Transition radius ≥ 2 in. (b) 2 in. > Transition radius ≥ 0 in.	T or Rev	D E	16
	—For all transition radii without the end welds ground smooth.	T or Rev	E	16
Mechanically Fastened Connections	Base metal at gross section of high-strength bolted slip resistant connections, except axially loaded joints which induce out-of-plane bending in connecting materials.	T or Rev	B	21
	Base metal at net section of high-strength bolted bearing-type connections.	T or Rev	B	21
	Base metal at net section of riveted connections.	T or Rev	D	21
Eyebar or Pin Plates	Base metal at the net section of eyebar head, or pin plate	T	E	23, 24
	Base metal in the shank of eyebars, or through the gross section of pin plates with: (a) rolled or smoothly ground surfaces (b) flame-cut edges	 T T	 A B	 23, 24 23, 24

[a] "T" signifies range in tensile stress only, "Rev" signifies a range of stress involving both tension and compression during a stress cycle.

[b] "Longitudinally Loaded" signifies direction of applied stress is parallel to the longitudinal axis of the weld. "Transversely Loaded" signifies direction of applied stress is perpendicular to the longitudinal axis of the weld.

[c] Transversely loaded partial penetration groove welds are prohibited.

[d] Allowable fatigue stress range on throat of fillet welds transversely loaded is a function of the effective throat and plate thickness. (See Frank and Fisher, Journal of the Structural Division, ASCE, Vol. 105, No. ST9, Sept. 1979.)

$$S_r = S_r^C \left(\frac{0.06 + 0.79H/t_p}{1.1 t_p^{1/6}} \right)$$
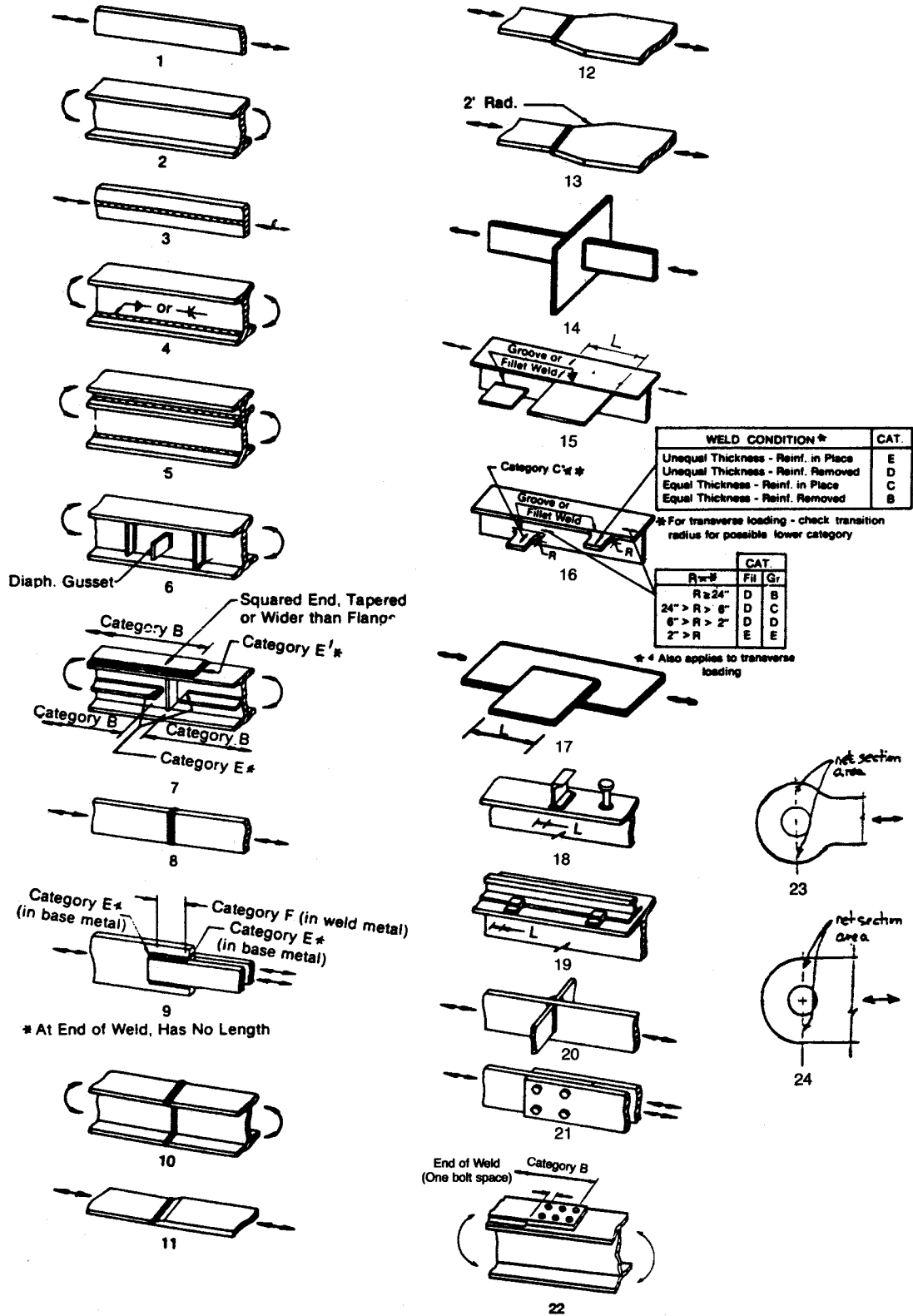
where S_r^C is equal to the allowable stress range for Category C given in Table 10.3.1A. This assumes no penetration at the weld root.

[e] Gusset plates attached to girder flange surfaces with only transverse fillet welds are prohibited.

[f] See Wattar, Albrecht and Sahli, Journal of Structural Engineering, ASCE, Vol. III, No. 6, June 1985, pp. 1235–1249.

(Sheet 3 of 4)

Table 2-1 (Concluded)

1

2

3

or

4

5

Diaph. Gusset 6

Category B — Squared End, Tapered or Wider than Flange

Category E'*

Category B

Category B — Category B

Category E*

7

8

Category E*
(in base metal) — Category F (in weld metal)
Category E*
(in base metal)

9

*At End of Weld, Has No Length

10

11

12

2' Rad.

13

14

Groove or Fillet Weld

L

15

Category C'* *

Groove or Fillet Weld

R   R

16

WELD CONDITION *	CAT.
Unequal Thickness - Reinf. in Place	E
Unequal Thickness - Reinf. Removed	D
Equal Thickness - Reinf. in Place	C
Equal Thickness - Reinf. Removed	B

* For transverse loading - check transition radius for possible lower category

R =	CAT.	
	Fil	Gr
R ≥ 24"	D	B
24" > R > 6"	D	C
6" > R > 2"	D	D
2" > R	E	E

* * Also applies to transverse loading

17   L

18   L

19   L

20

21

End of Weld
(One bolt space)   Category B

22

net section area

23

net section area

24

(2)   The American Institute of Steel Construction (AISC) has adopted AASHTO S_r-N curves for fatigue design (AISC 1989, 1994). The AWS has also adopted the S_r-N approach for design of welded structures and has published S_r-N curves and guidelines for categorization of welded details for redundant and nonredundant structural members (ANSI/AWS D1.1). The AWS S_r-N requirements vary slightly from those of AASHTO, which are adopted herein.

   c.   Fatigue strength of riveted structures.

   (1)   Fisher et al. (1987) compiled all the published data from fatigue testing of full-size riveted members. Based on these data, the fatigue strength of riveted members is relatively insensitive to the rivet pattern or type of detail (cover plate details, longitudinal splice plates, and angles or shear-splice details). The data are plotted in Figure 2-2 with the AASHTO fatigue strength (S_r-N) curves of Categories C and D, which have been developed for welded details. Based on the data shown in Figure 2-2, it is recommended that Category D be assumed for structural details in riveted members subjected to stress ranges higher than 68.95 MPa ($S_r \geq 68.95$ MPa (10 ksi)), and Category C be assumed for the lower stress range, high-cycle region. This recommendation is similar to the current American Railway Engineers Association (AREA) standards (AREA 1992). In cases where there are missing rivets or a significant number of rivets have lost their clamping force, Category E or E' strength should be assumed.
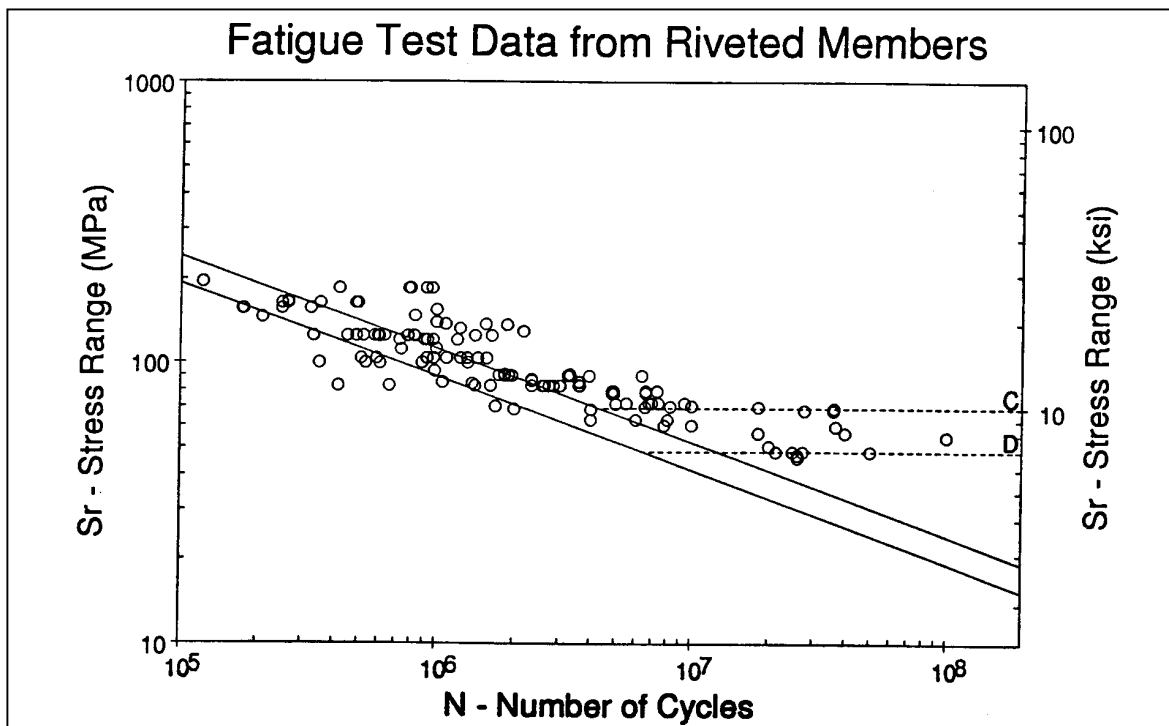

Figure 2-2. Fatigue test data from full-size riveted members

   (2)   There are insufficient data for a conclusion about the fatigue limit of riveted members. Fisher et al. (1987) state that no fatigue failure has ever occurred when the stress range was below 41.3 MPa (6 ksi) pro-vided that the member or detail was not otherwise damaged or severely corroded.

   (3)   A major advantage of riveted (or bolted) members is that they are internally redundant. Cracking that propagates from a rivet hole is the typical phenomenon of fatigue damage of riveted members as shown in Figures 2-3 and 2-4. Since cracks usually do not propagate from one component into adjacent components, fatigue cracking in riveted members is not continuous as in welded members. In other words, fatigue cracking in one component of a riveted structural member usually does not cause the complete failure of the member.
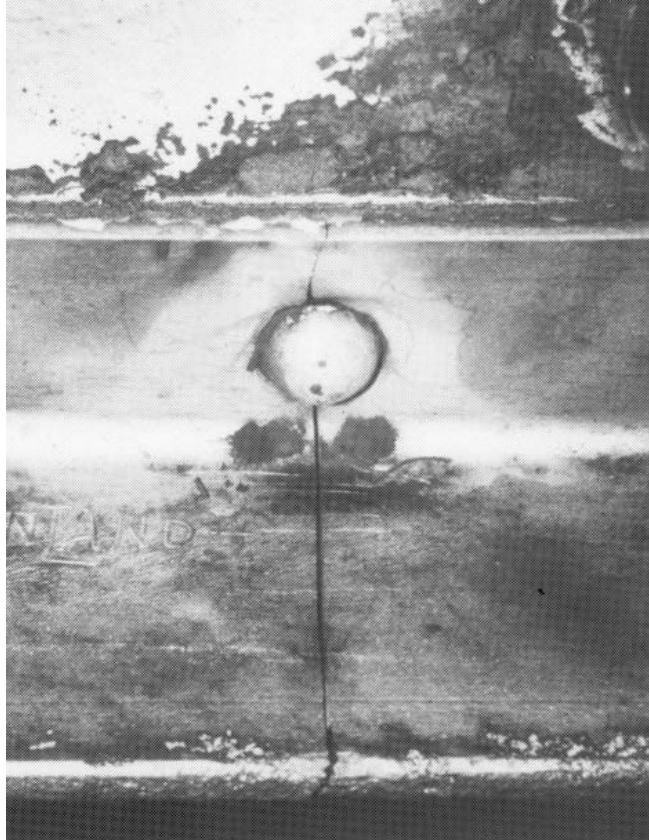
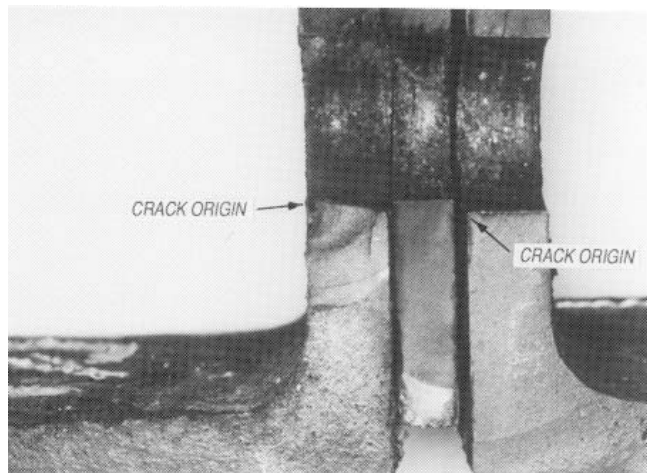**Figure 2-3. Typical fatigue cracking of riveted member**

Figure 2-4. Crack surface at the edge of rivet hole

Therefore, fatigue cracks would more likely be detected long before the load-carrying capacity of the riveted member is exhausted.

d. Fatigue strength of corroded members. For severely corroded members where corrosion notching has occurred, Category E or E' curves and the corresponding fatigue limits have been suggested for cases. When corrosion is severe and notching occurs, a fatigue crack may initiate from the corroded region as shown in Figure 2-5. In cases where corrosion has resulted in loss of more than 20 percent of the cross section, the corresponding increase in stress should also be considered.
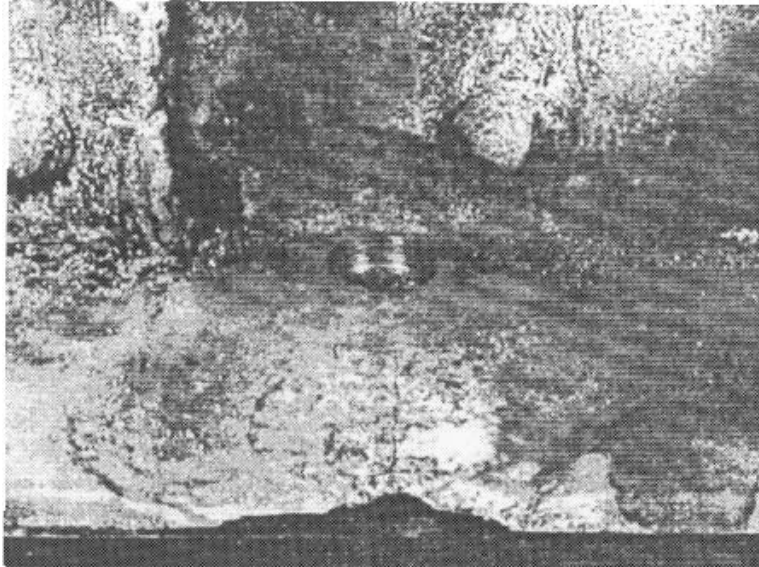
Figure 2-5. Fatigue crack from corrosion notch into rivet hole

e.   Variable-amplitude fatigue loading.

(1) Most of the fatigue test data and the S_r-N curves in Figures 2-1 and 2-2 were established from constant-amplitude cyclic loads. In reality, however, structural members are subjected to variable-amplitude cyclic loads resulting in a spectrum of various stress ranges. Variable-amplitude fatigue loading may occur on hydraulic steel structures.

(2) In order to use the available S_r-N curves for variable-amplitude stress ranges, an equivalent constant-amplitude stress range S_{re} can be determined from a histogram of the stress ranges (Figure 2-6). S_{re} is calculated as the root-mean-cube of the discrete stress ranges S_{ri}
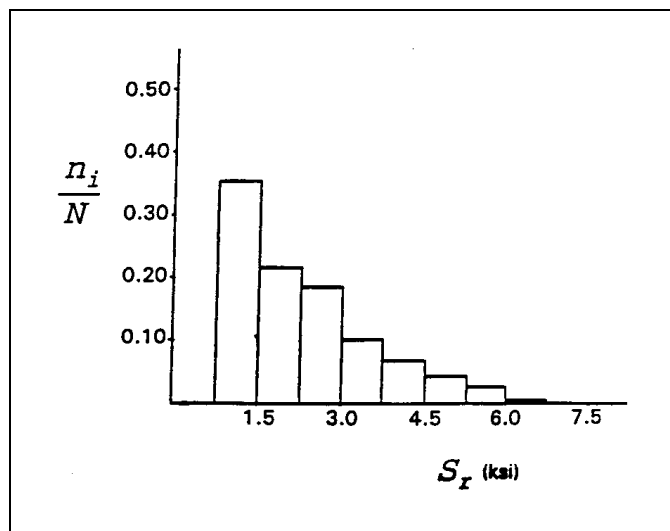

Figure 2-6. Sample stress range histogram

$$S_{re} = \sqrt[3]{\sum_{i=l}^{m} \frac{n_i S_{ri}^3}{N}} \qquad\qquad\qquad (2\text{-}3)$$

where

m = number of stress range blocks

n_i = number of cycles corresponding to S_{ri}

S_{ri} = magnitude of a stress range block

f.   Repeated loading for hydraulic steel structures. The general function of hydraulic steel structures is to dam and control the release of water. Sources of repeated loading include changes in load due to pool fluctuations, operation of the hydraulic steel structure, flow-induced vibration, and wind and wave action.

(1) Operation.

(a) Spillway gates. During the routine operation of actuating a spillway gate, cyclic loads are applied to structural members due to the change in hydrostatic pressure on the structure as the gate is raised and then lowered. Although this load case has the potential to produce large variation of stress in structural compo- nents, the frequency of occurrence (a very conservative assumption is one cycle per day) is too low to cause fatigue damage. One lifting/lowering operation per day results in only 18,000 cycles in a 50-year life. This is well below the number of cycles necessary for consideration of fatigue. Consequently, the possibility that repeated loads in spillway gates due to operations would cause fatigue damage is unlikely.

(b) Lock gates. Repeated loading for various structural components occurs due to variation in the lock chamber water level and to opening and closing of gates. The number of load cycles is a function of the number of lockages that occurs at the lock.   The number of load cycles due to gate operation or filling/emptying the lock chamber per lockage varies between 0.5 and 1.0 depending on barge traffic patterns. Gates at busy locks can easily endure greater than 100,000 load cycles within a 50-year life. Therefore, fatigue loading is significant and must be considered in design and evaluation.

(2) Flow-induced vibration. This phenomenon may produce significant cyclic loads on hydraulic steel structures because of the potential for the occurrence of high-frequency live load stresses above the fatigue limit. Spillway gates especially can experience some level of flow-induced vibration whenever water is being discharged, but severe vibration usually occurs only when the gate is open at a certain position. Vibration of tainter gates is heavily influenced by flow conditions (i.e., gate opening and tailwater elevation) and bottom seal details. Approximate measurements have indicated that a frequency of vibration of 5-10 Hz is reasonable (Bower et al. 1992). This frequency is large enough to cause fatigue damage in a short time even for relatively low stress range values. Although a hydraulic steel structure would rarely be operated in such a position for any length of time, flow-induced vibration should be considered as a possible source of fatigue loading. An example of the fatigue evaluation of a spillway gate including vibration loading is given in Chapter 7.

(3) Wind and wave action. This is a continuous phenomenon that has not caused fatigue problems in hydraulic steel structures probably due to the low magnitude of stress range for normal conditions.

2-4. Design Deficiencies

Many existing hydraulic steel structures were designed during the early and mid-1900's. Analysis and design technologies have significantly improved, producing the current design methodology. Original design loading conditions may no longer be valid for the operation of the existing structure, and overstress conditions may

exist. Current information, including modern welding practice and fatigue and fracture control in structures, was not available when many of the initial designs were performed. Consequently, low category fatigue details and low toughness materials exist on some hydraulic steel structures. In addition, the amount of corrosion anticipated in the original design may not accurately reflect actual conditions, and structural members may now be undersized. To evaluate existing structures properly, it is important that the analysis and design information for the structure be reviewed to assure no design deficiencies exist.

2-5. Fabrication Discontinuities

a. For strength and economic reasons, EM 1110-2-2703 recommends that hydraulic steel structures be fabricated using structural-grade carbon steel. Standards such as ASTM A6/A6M or ASTM A898/A898M have been developed to establish allowable size and number of discontinuities for base metal used to fabricate hydraulic steel structures. In addition, EM 1110-2-2703 also recommends that the steel structures be welded in accordance with the Structural Welding Code-Steel (ANSI/AWS D1.1). This code provides a standard for limiting the size and number of various types of discontinuities that develop during welding. Although these criteria exist, when a hydraulic steel structure goes into service, it does contain discontinuities.

b. Discontinuities that exist during initial fabrication are rejectable only when they exceed specified requirements in terms of type, size, distribution, or location as specified by ANSI/AWS D1.1. Welded fabrication can contain various types of discontinuities that may be detrimental (see paragraph 2-2). This is especially important when considering weldments involving thick plates, because thick plates are inherently less tough and welding residual stresses are high.

c. Frequently, plates 38 mm (1-1/2 in.) in thickness and greater are used as primary welded structural components on hydraulic steel structures. It is not uncommon to see such thick plates used as flanges, embedded anchorage used to support hydraulic steel structures, hinge and operating equipment connections, diagonal bracing, lifting or jacking assemblies, or platforms to support operating equipment that actuates the hydraulic steel structures. In addition, thick castings such as sector gears used for operating such structures as lock gates may be susceptible to brittle fracture. Hydraulic steel structures have experienced cracking during fabrication and after the thick assemblies are welded and placed into service.

2-6. Operation and Maintenance

Proper operation and maintenance of hydraulic steel structures are necessary to prevent structural deterioration. The following items are possible causes of structural deterioration that should be considered:

a. Weld repairs are often sources of future cracking or fracture problems, particularly if the existing steel had poor weldability as is often the case with older gates.

b. If moving connections are not lubricated properly, the bushings will wear and result in misalignment of the gate. The misalignment will subsequently wear contact blocks and seals, and unforeseen loads may develop.

c. Malfunctioning limit switches could result in detrimental loads and wear.

d. A coating system or cathodic protection that is not maintained can result in detrimental corrosion.

e. Loss of prestress in the gate leaf diagonals reduces the torsional stability of miter gates during opening and closing.

f. Proper maintenance of timber fenders and bumpers is necessary to provide protection to the gate and minimize deterioration.

2-7. Unforeseen Loading

a. Accidental overload or dynamic loading of a gate can result in deformed members or fracture. When structural members become plastically deformed or buckled, they may have significantly reduced strength and/or otherwise impair the performance of a hydraulic steel structure. The extent and nature of any noticeable plastic deformation should be noted and accurately described during the inspection process, and its effect on the performance of the structure should be assessed in the ensuing evaluation as further discussed in Chapter 6. Fractures that occur must generally be repaired. Considerations for repair are discussed in Chapter 8.

b. Dynamic loading due to hydraulic flow and impact loading due to vessel collision are currently unpredictable. The dynamic loading may be caused by hydraulic flow at the seals or may occur when lock gates are used to supplement chamber filling or skim ice and debris. Impact loading can occur from malfunctioning equipment on moving vessels or operator error. Fracture likelihood is enhanced with dynamic loads, since the fracture toughness for steels decreases with increasing load rate. Other unusual loadings may occur from malfunctioning limit switches or debris trapped at interfaces between moving parts. It is also possible that unusual loads may develop on hydraulic steel structures supported by walls that are settling or moving. These unusual loads can cause overstressing and lead to deterioration.

Chapter 3
Periodic Inspection

3-1. Purpose of Inspection

a. As discussed in Chapter 2, existing hydraulic steel structures are subjected to conditions that could cause structural deterioration and premature failure. Periodic inspection shall be conducted in accordance with ER 1110-2-100 and ER 1110-2-8157. Periodic inspections on hydraulic steel structures are primarily visual inspections. The inspection procedure should be designed to detect damage, deterioration, or signs of distress to avert any premature failure of the structure and to identify any future maintenance or repair requirements. The periodic inspection should assure that all critical members and connections are fit for service until the next scheduled inspection. Critical members and connections are those structural elements whose failure would render the hydraulic steel structure inoperable. Fitness for service means that the material and fabrication quality are at an appropriate level considering risks and consequences of failure. To be effective, the periodic inspection should be a systematic and complete examination of the entire structure with particular attention given to the critical locations. It should be done while the structure is in use and, to the extent possible, lifted out of the water. Ideally, inspections should be planned to coincide with scheduled dewatering of the structure.

b. If the periodic inspection indicates that a structure may be distressed, a more detailed inspection and evaluation may be necessary. This detailed inspection may require nondestructive and/or destructive testing as discussed in Chapters 4 and 5. The information obtained from the inspections and tests will then be used to perform a structural evaluation as discussed in Chapter 6 and make a recommendation for future action. This chapter will further discuss the visual inspection that should be performed during the periodic inspection.

3-2. Inspection Procedures

The following four primary steps are considered necessary to perform a periodic inspection adequately: preinspection assessment, inspection, evaluation, and recommendations.

a. Preinspection assessment.

(1) To conduct a detailed inspection over the entire hydraulic steel structure on a project is not economical, if at all possible. Prior to inspection, critical areas should be identified to determine which areas of the structure require the most attention (paragraph 3-3). The inspector should prepare by reviewing the design and drawings, previous inspection reports, and all operations/maintenance records since the most recent inspection.

(2) The inspector should review structural drawings to become familiar with the components and operation of each hydraulic steel structure. Locations and details on the structure prone to fracture or fatigue cracking or susceptible to corrosion should be identified. These locations should receive more attention during the inspection. The procedure for identifying critical areas and a checklist of locations (both specific and general) that are susceptible to fracture and corrosion are presented in paragraphs 3-3 and 3-5, respectively, to assist the inspector during the preinspection.

(3) Review of previous inspection reports and operations records will aid in defining occurrence of unusual circumstances or a history of problems. Distress may occur due operational problems (paragraph 2-6) or the occurrence of unusual loads (paragraph 2-7). These events could have imposed high-magnitude stresses and/or a large number of stress cycles, which may cause cracks to develop or members to buckle.

b. Inspection.

(1) Inspection is the activity of examining a structure to ascertain quality, detect damage or deterioration, or otherwise appraise a structure. Particular attention should be given to gate operation (and cathodic protection, if applicable) and the critical locations cited in the preinspection assessment. For the main structural elements, items to consider during inspection include occurrence of cracking or excessive deformation, excessive corrosion, loose rivets, fabrication defects, and damage due to impact from debris. Additionally, all previously reported conditions should be thoroughly inspected. Detailed procedures for inspecting hydraulic steel structures for occurrence of these items are presented in Chapter 4.

(2) Mechanical and electrical components such as seals, lifting mechanisms, bearings, limit switches, cathodic protection systems, and heaters are critical to the operation of hydraulic steel structures and should be inspected appropriately. These components should be checked for general working condition, corrosion, trapped debris, necessary tolerances, and proper lubrication. The structure should also be visually inspected for weld condition and surface defects.

(3) All observations of damage or unusual conditions should be documented in sufficient detail so that all necessary information for a structural evaluation is included and the severity of the condition can be quantitatively compared with previous and future observations.

c. Evaluation. Evaluation of the effects of existing cracks, excessive corrosion, excessive deformation, mechanical problems, weld bead noncompliance with the ANSI/AWS D1.1 standards, and the occurrence of unusual loads must be conducted. This requires qualitative as well as quantitative analysis of inspection data and unusual events reported in previous assessments and evaluations, considering loading and performance criteria required for the existing structure. The periodic inspection is the initial evaluation in the process of determining the structural adequacy of a structure. If surface cracks or fractured members are discovered during the periodic inspections, detailed inspection and evaluation shall be performed for the entire gate. The strength and stability of corroded members should be calculated. Information on evaluation and recommendation procedures is provided in Chapter 6.

d. Recommendations. This task is defined as the process of determining requirements pertaining to frequency of future inspection or remediation of problems, if required. Chapter 6 provides some general information on appropriate recommendations.

3-3. Critical Members and Connections

Critical structural members and connections can be determined from structural analysis of the hydraulic steel structure. This should include local stress concentrations and fatigue considerations. In addition, effects from existing corrosion and reduced weld quality or associated residual stresses should be considered. This analysis will require information pertaining to the existing mechanical properties of the structural material and weld (i.e., strength, toughness, ductility) and the location, type, size, and orientation of any known discontinuities.

a. Critical areas for fracture. Areas in a hydraulic steel structure that may be susceptible to fracture may be determined by considering the combined effect of nominal tensile stress levels and complexity of connection details. Connection details interrupt or change the flow of stress, resulting in stress concentrations; therefore, a moderate level of nominal tension stress occurring at a complex detail (stress concentration) may be amplified to a significant level. To identify critical areas for fracture, determine locations of moderate to high nominal tensile stress levels throughout the structure, identify locations or details where there are significant stress concentrations, and combine the effects of stress level and sensitive details.

(1)   Determination of stress levels.

(a)   In determining the critical locations for fracture, only nominal tensile stresses are considered since fracture will not occur under constant compressive stress. In contrast, fatigue cracking may occur under cyclic compressive loading when tensile residual stress is present. For example, if a residual tensile stress of 172.4 MPa (25 ksi) exists, a calculated stress variation from zero to 68.95 MPa (10 ksi) in compression would actually be a variation from 172.4 MPa (25 ksi) to 103.4 MPa (15 ksi), which could cause fatigue cracking. Welded members may include high tensile residual stress (near the yield stress in most cases) in the welded region. (EM 1110-2-2105 requires that fatigue design be considered for welded members subject to any computed stress variation, whether it is tension or compression.)

(b)   Stress levels in hydraulic steel structures can be determined from a variety of different analytical methods ranging from idealized two-dimensional (2-D) analysis to detailed three-dimensional (3-D) finite element analysis. In most cases, a simple 2-D analysis, such as that used in design, should be sufficient. A more detailed analysis may be required to determine the stress levels in a hydraulic steel structure if the gate has some history of unusual loading (unsymmetric loading or overload). The type of analysis to be performed is dependent on the particular stresses in question and the loading condition. In general, there will be common high-stress areas for a given type of hydraulic steel structure. For example, the following are typical locations of high-tension stress areas common to such hydraulic steel structures as roller, tainter, and lift gates:

- Roller gates are essentially simply supported and have high tensile stresses at midlength. High stress also occurs at the ends due to large shear forces, unintended flexural restraint, and lifting loads. Additionally, high tension stresses may exist at the junction between the apron assembly and the main tube.

- Tainter gates generally have significant tensile stresses in the downstream flanges at the midlength of the horizontal girders (lower girders are more critical), in the upstream flange of girders, in the outside flange of end frame struts near the girder-strut connections, and where the end frames join the trunnion assemblies (tensile stresses may occur in the end frame due to trunnion pin friction). High tensile stresses will also occur in the upstream flange of skin plate ribs at the horizontal girders.

- Lift gates resist horizontal (due to hydrostatic pressure) and vertical (due to hydrostatic pressure and structural weight) loads. Under horizontal loading, lift gates act essentially as simply supported stiffened plate structures, and significant tensile stresses are likely to occur in the downstream flange at the midlength of the horizontal girders, with highest stresses occurring in the lower girders. High tension stresses may also develop in the upstream flange near the ends of the girders if rotational restraint is imposed due to binding of the guide wheels (from debris or ice collecting at the slot in the pier). Because of displacement under vertical loading, significant tensile stresses may also develop in the bottom of downstream girder flanges and in various connections as discussed in *c* below.

(2) Detail categorization. The purpose of this task is to identify the severity of the stress concentration for various details. Since all details contain some level of stress concentration, a means of determining the relative stress concentration effect of the different connections is needed. For connections made up of welded details, this may be accomplished by determining the appropriate fatigue categories that reflect the severity of the stress concentration introduced by the particular detail.

(a) A complex welded connection will likely consist of several weld details, each with a corresponding fatigue category. For example, consider a gusset plate connection that joins bracing members to the downstream flange of a built-up girder (Figure 3-1). Evaluation of girder flexure includes the longitudinal web-to-flange weld, the attachment of the welded stiffener to the girder, and the attachment of the gusset plate to the girder flange. The fatigue category of the connection is determined by the most critical category detail in the connection. The fatigue category for a particular welded detail is based on the type of weld, geometry

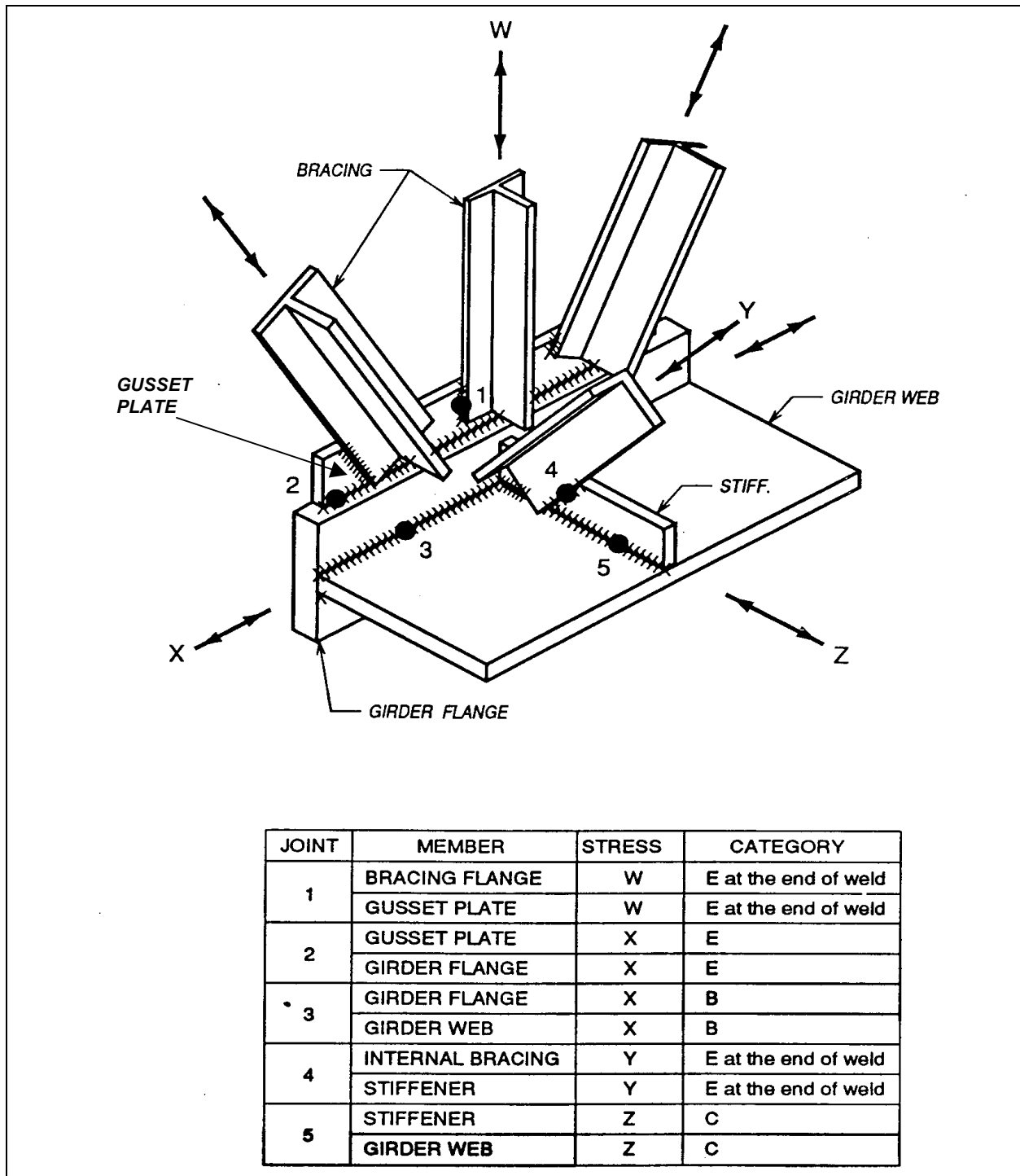| JOINT	MEMBER	STRESS	CATEGORY
1	BRACING FLANGE	W	E at the end of weld
	GUSSET PLATE	W	E at the end of weld
2	GUSSET PLATE	X	E
	GIRDER FLANGE	X	E
3	GIRDER FLANGE	X	B
	GIRDER WEB	X	B
4	INTERNAL BRACING	Y	E at the end of weld
	STIFFENER	Y	E at the end of weld
5	STIFFENER	Z	C
	GIRDER WEB	Z	C

Figure 3-1. Bracing-girder connection

of the detail, and the direction of the applied stress. The general procedure for determining the fatigue category of a welded connection is summarized in the following list. Examples that illustrate this process are provided in (4) and (5) below.

- Locate the main member being examined and define the structural action. At the intersection of two primary members, the structural action of each member must be considered independently and the weld

details categorized accordingly. A particular detail may have different fatigue category classifications when the structural action of the different members is considered.

- For each detail, determine the most appropriate example, general condition, and situation (geometry, weld type, loading direction, etc.) as described in Table 2-1.

- Select the appropriate fatigue category as specified in Table 2-1 for each detail.

- For the member and structural action considered, determine the fatigue category for the connection based on the most critical weld detail.

(b) All riveted details, regardless of particular configuration, may be classified as a Category C or D. Welded attachments, tack welds, seal welds, or repair welds that exist in riveted structures, however, may lower the fatigue category of a riveted detail from C or D to Category E or E'. Figure 3-2 shows a fatigue crack starting from a tack weld on a riveted bridge member. The crack initiated at the toe of the tack weld and grew into the riveted plate in the direction perpendicular to the primary tensile stress. Similar damage could occur on any riveted member. Figure 3-3(a) shows fatigue cracks initiating from the ends of welded stiffeners in the end shield of a riveted roller gate. Figure 3-3(b) shows cracks initiating from previous repair welds. In this instance, attempts to strengthen a riveted gate by adding welded stiffening plates created a detail susceptible to fatigue (high stress concentration).
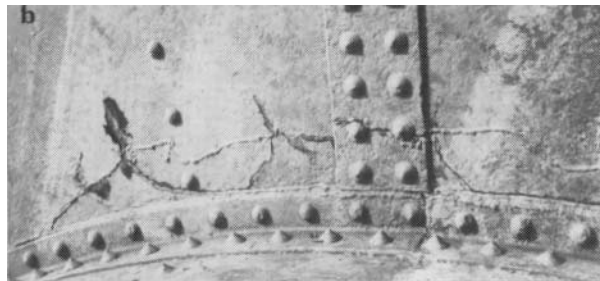

Figure 3-2. Fatigue crack at tack weld on a riveted member

(3) Identifying critical areas: Combining stress and detail.

(a) In determining the most critical areas susceptible to cracking, the combined effect of stress levels and stress concentration must be considered. For a structural component or detail subjected to fatigue loading, the combined effect of the stress range S_r and the stress concentration is reflected in the AASHTO S_r-N curves of Figure 2-1. The fatigue life N is a function of S_r and type of detail (fatigue category); N is lower for higher S_r and more severe stress concentration (lower fatigue category). In a comparison of two or more details, the one with the lowest fatigue life would be the most critical.

a. Fatigue cracks initiating from ends of welded stiffeners

b. Cracks initiating from previous repair welds

Figure 3-3. Fatigue cracks at end of stiffener and at weld repair

(b) This concept may also be applied for a structure under constant load to quantify the susceptibility to fracture. Fracture is most likely to occur at locations where high tension stress and/or severe stress concentration exist. Fatigue cracking due to repeated loading is more likely to occur (will occur sooner) at locations where high S_r and/or low fatigue categories exist. Tensile stress level is analogous to S_r, and severity of stress concentration is analogous to the particular fatigue category. Therefore, fatigue S_r-N relationships can be used to identify the areas most susceptible to fracture in a statically loaded structure by the following procedure. First, determine the fatigue category and nominal stress level for details subject to tensile loads. Second, determine N (with no consideration of fatigue limits) from Figure 2-1 for each detail by substituting the nominal stress level for S_r. Finally, rank the details according to their corresponding N values. The details with the lowest N would be considered most critical.

(c) In this application, N may be viewed as an index that indicates susceptibility to cracking. Index factors for various stress levels and categories are shown in Table 3-1 (lower values are more critical). These factors were derived by dividing N as determined by Figure 2-1 by 10^5. For riveted structures, except where welds exist, the highest stress areas will indicate the most critical locations since all details are Category D for stresses greater than 68.95 MPa (10 ksi).

(4) Fatigue categorization: Girder-rib-skin-plate connection example. To illustrate determining fatigue categories and combining stress and detail for a welded connection, a girder-rib-skin-plate connection that is common to tainter gates is examined. This connection and its fatigue categorization are illustrated in Figure 3-4. Two primary members (the horizontal girder and the vertical rib/skin plate) intersect at this connection.

Table 3-1
Index Factor for Stress and Detail

Stress Level MPa (ksi)	Fatigue Category						
	A	B	B'	C	D	E	E'
41 (6)	1,170	560.0	82.0	214.0	94.0	51.0	18.0
55 (8)	495	238.0	119.0	90.0	40.0	22.0	7.6
69 (10)	250	122.0	61.0	46.0	21.0	11.0	3.9
83 (12)	147	71.0	35.0	27.0	12.0	6.4	2.2
97 (14)	92	44.0	22.0	17.0	7.5	4.0	1.4
110 (16)	62	30.0	15.0	11.0	5.0	2.7	0.95
124 (18)	43	21.0	10.0	7.9	3.5	1.9	0.67
138 (20)	32	15.0	7.6	5.8	2.6	1.4	0.49
152 (22)	24	12.0	5.7	4.3	1.9	1.0	0.37
165 (24)	18	8.8	4.4	3.3	1.5	0.79	0.28
179 (26)	14	6.9	3.5	2.6	1.2	0.62	0.22
193 (28)	12	5.6	2.8	2.1	0.9	0.50	0.18

(a) The first member to be considered is the girder, and the structural action is flexure. Details to evaluate include the longitudinal web-to-flange weld, the attachment of the welded stiffener (if present) to the girder, and the attachment of the rib flange to the girder flange.

- Web-to-flange weld
  Illustrative example: No. 4 (Table 2-1)
  General condition: Built-up member
  Situation: Continuous fillet weld parallel to direction of the applied stress
  Fatigue category: B

- Welded stiffener

  Illustrative example: No. 6 (Table 2-1)
  General condition: Built-up member
  Situation: Toe of transverse stiffener welds on girder webs or flanges
  Fatigue category: C

- Rib flange to girder flange

  Illustrative example: No. 15 (Table 2-1)
  General condition: Fillet-welded attachments longitudinally loaded
  Situation: Base metal adjacent to details attached by fillet welds
  Fatigue category: C, D, E, or E' depending on weld length (rib flange width) and detail thickness (rib flange thickness)

Based on the most critical weld detail for flexural action of the girder (the rib-to-girder fillet weld), the connection is a fatigue category E or E' depending on the rib flange thickness. This assumes a continuous fillet weld across a rib flange of at least 10 cm (4 in.).

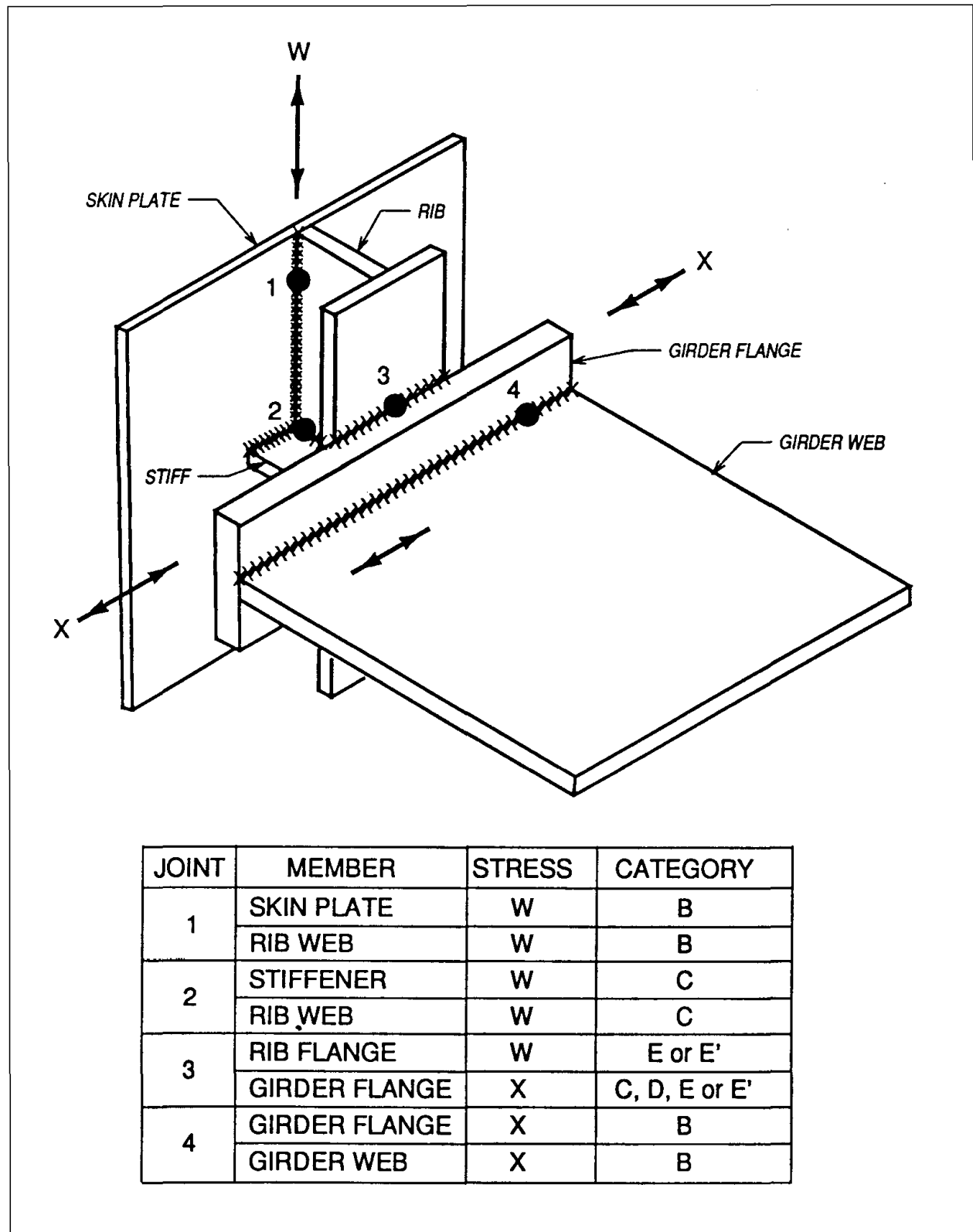| JOINT	MEMBER	STRESS	CATEGORY
1	SKIN PLATE	W	B
1	RIB WEB	W	B
2	STIFFENER	W	C
2	RIB WEB	W	C
3	RIB FLANGE	W	E or E'
3	GIRDER FLANGE	X	C, D, E or E'
4	GIRDER FLANGE	X	B
4	GIRDER WEB	X	B

Figure 3-4. Girder-rib-skin-plate connection

(b) The second member to be considered is the vertical rib/skin plate, and the structural action is flexure about the supporting girder. Details to be evaluated include the longitudinal rib-to-skin-plate weld, the attachment of the welded stiffener to the rib and skin plate, and the attachment of the rib flange to the girder flange. Since the structural action for the skin plate and rib is flexure, the rib-to-skin-plate weld is a Category B and the attachment of the welded stiffener to the rib and skin plate is a Category C, similar to the first two details evaluated for the girder. It is not obvious how to classify the fillet weld joining the rib to the girder. For this example, it is assumed that this weld is similar to one at the end of a cover plate that is wider than the flange.

<u>Rib flange to girder flange</u>

Illustrative example: No. 7 (Table 2-1)
General condition: Built-up member
Situation: Welded cover plate wider than flange with welds across the ends
Fatigue category: E or E' depending on rib flange thickness

Based on the most critical weld detail for flexural action of the rib/skin plate (the rib-to-girder fillet weld), the connection is a fatigue category E or E' depending on the rib flange thickness. If fatigue loading is not a concern, however, only nominal tensile stresses are significant, and these exist at the weld details attached to the skin plate. Under hydrostatic loading, compressive flexural stresses exist in the rib flange. Therefore, considering details subject to nominal tensile stresses that are not cyclic, this connection should be classified as a Category C. For fatigue loading, the connection is Category E or E′.

(5) Fatigue Categorization: Bracing-to-Girder Connection Example. To illustrate determining fatigue categories and combining stress and detail for a welded connection, a bracing-girder connection that is common on miter gates, tainter gates, and lift gates is examined. This connection and its fatigue categorization are illustrated in Figure 3-1. The main member for this connection is the girder, and the structural action is flexure. Details to be evaluated include the longitudinal web-to-flange weld, the attachment of the welded stiffener to the girder, and the attachment of the gusset plate to the girder flange. The web-to-flange weld is a Category B, and the attachment of the welded stiffener to the girder is a Category C, similar to the first two details evaluated for the girder connection presented in (4) above.

<u>Gusset-plate-to-girder-flange weld</u>

Illustrative example: No. 16 (Table 2-1)
General condition: Groove-welded attachments longitudinally loaded
Situation: Base metal adjacent to details attached by groove welds with a transition radius less than 50 mm (2 in.)
Fatigue category: E

Based on the most critical weld detail (the gusset-plate-to-girder-flange weld), the connection is a fatigue category E.

(6) Combining stress and detail example. The process of combining stress and detail for tainter gate connections described in (4) and (5) above will be discussed in general terms. For this example, it is assumed that fatigue loading is not a concern.

(a) For the girder-rib-skin-plate connection, the rib-to-girder weld was determined to be a Category E or E' for girder flexure (assume a Category E). This connection is located at each vertical rib on the upstream girder flange along the length of the girder. Without fatigue loading, only nominal tensile stresses should be considered. Along the length of the girder near midspan, the flexural stresses due to hydrostatic loading are

compressive in the upstream flange. Therefore, this connection is not critical near midspan. However, near the end frames, the flexural stress in the upstream flange is tensile with the highest stresses nearest the end frames. Assuming a structural analysis shows that the stress in the upstream flange near the end frames is about 103 MPa (15 ksi), the index factor for the rib-to-girder weld (Category E) is approximately 3.3 (Table 3-1). For rib/skin plate flexure, the most critical weld detail (stiffener attachment) under tensile stresses is a Category C. Under hydrostatic loading, compressive flexural stresses exist in the rib flange. Assuming that a structural analysis shows that the maximum tensile stress in the skin plate is 68.9 MPa (10 ksi), the index factor is 46.

(b) For the bracing-to-downstream-girder-flange connection, the most critical weld detail (the gusset-plate-to-girder-flange weld) is a fatigue category E. Under hydrostatic loading, tensile flexural stresses exist in the downstream girder flange at areas away from the end frames with the highest stresses at midspan. Assuming that bracing is located at midspan, and the stress in the downstream girder flange at midspan is about 124.1 MPa (18 ksi), the index factor for the gusset-plate-to-girder weld is 1.9 (Table 3-1).

(c) Based on the stress levels in this example, the most critical areas for inspection are at the gusset-plate-to-girder-flange weld on the downstream girder flange at midspan of the girder (index factor 1.9) and at the rib-to-girder weld on the upstream girder flange, near the end frame where the upstream flange of the girder is in tension (index factor 3.3). Although it depends on the size and geometry of individual girders, the lower girders generally have the highest stress levels and are, therefore, more critical.

b. Critical areas for corrosion damage. Chapter 2 discusses several types of corrosion that can occur on hydraulic steel structures. Corrosion can occur at any location on a structure, but certain areas are more susceptible to corrosion damage than others. Sensitivity to corrosion is enhanced at crevices, areas where dissimilar metals come in contact, areas subject to erosion, and areas where ponding water or debris may accumulate. Other areas often susceptible to corrosion are those where it is difficult to apply a protective coating adequately, such as at sharp corners, edges, intermittent welds, and rivets and bolts.

(1) Galvanic corrosion occurs at the contact surfaces of dissimilar metals or between steels with different electrochemical potential. For example, ASTM A7-67 steel is more electrochemically active than ASTM A588/A588M steel (a low-carbon weathering steel containing copper) and would corrode when coupled with A588/A588M steel. There may also be a potential difference between rivet steel and the adjoining plate or angle. If different steels have been used in the construction or repair of a structure, these locations should be inspected for galvanic corrosion.

(2) Other corrosion-susceptible areas are those where abrasion may occur. This type of corrosion may occur around moving parts such as at the guide wheels on vertical lift gates or at the trunnion assemblies or chain locations on tainter gates.

(3) Webs of the structural members on many gates, bulkheads, and valves are oriented horizontally or radially, providing corrosion-susceptible locations where ponding or debris accumulation may occur. To prevent ponding, the webs of these members are penetrated by drain holes. The hole locations can be corrosion-susceptible areas, especially if they are covered with debris. Areas where ponding may occur and the location of web drain holes should be determined prior to inspection.

(4) Seals on hydraulic steel structures are common locations of corrosion damage. Seals are subject to crevice corrosion between the contact surfaces of the structure and seal, galvanic corrosion if the seal plate is of a dissimilar metal to that of the structure itself, or erosion corrosion if abrasive sand and silt particles are passing through.

(5) Other areas susceptible to corrosion include heater locations (promotes oxidation) and the normal waterline (wetting and drying promotes corrosion).

(6) Areas with loose rivets or bolts are potential locations for crevice corrosion or fretting corrosion if the base components of the connection are loose.

(7) In addition to consideration of the previously described susceptible areas, certain findings during the physical inspection may indicate possibilities of corrosion. Generally, any failure of the paint system is an indication of underlying corrosion. A widespread failure of the paint system may indicate general corrosion resulting in a slow, relatively uniform thinning of the base metal. Moreover, some localized pitting corrosion may be present. If there is a localized failure of the paint system, localized corrosion may be occurring. Paint failure where the edges of two or more surfaces contact, such as at the edge of a rivet head or at the edge of an angle riveted to a plate, may indicate crevice corrosion. Paint failure near electrical connections may indicate stray current corrosion. If the paint failure is patterned or preferential in appearance, it may be due to filiform corrosion under the paint or to mechanically assisted corrosion, either fretting or erosion corrosion.

c. Critical areas for other effects. As discussed in Chapter 2, many factors other than nominal stress levels, severity of stress concentration, or corrosion aspects may contribute to the deterioration of a structure. These include effects of material thickness (affects residual stress, toughness, and constraint) and fabrication (i.e. weld quality, tack welds, intersecting welds, or poor accessibility), operational vibration or overload, displacement-induced secondary stress, and concentrated loads. The following paragraphs discuss some of these concerns.

(1) Details fabricated from thick plate sections and/or with large amounts of welding in a concentrated area are susceptible to cracking. Trunnion assemblies on tainter gates and lifting connections on all structures are examples. Locations where weld quality is poor are particularly susceptible to cracking. In welded joints there is a potential for many types of discontinuities, as illustrated in Chapter 4. Intersecting welds are often located on hydraulic steel structures at uncoped stiffeners and where diaphragm webs frame into girder webs and flanges.

(2) Where vibrational loads have been reported, components subjected to high-frequency flow-induced vibration may be critical. The lower sill of tainter gates and valves, the apron assembly of roller gates, and the end shield of roller gates are examples. Furthermore, any location where previous damage (buckling, plastic deformation, cracking, extreme corrosion) has been reported should be considered critical.

(3) Additional considerations are locations where extreme stresses occur in components subject to unforeseen secondary or displacement-induced stresses. One example is at the diaphragm-flange-to-girder-flange connections on welded lift gates. Under vertical loading, the horizontal girder flanges displace in a vertical plane similar to a uniformly loaded simple beam. The ends of diaphragm flanges are forced to rotate with the displaced girder flanges, which causes a large tensile force on one edge of the diaphragm; the girder flange rotation is greatest near the ends of the girders (Figure 3-5). Another example is at connections between a roller drum cylinder and the end shields (Figure 3-6). The rigidity of the connection prevents the movement of one component against the other. When a hydraulic steel structure is being opened or closed or when high-velocity water flows by the structure, relative local displacement may occur between two rigidly connected components and induce high stresses. Concentrated loads may induce high local stresses and/or displacements between connected components. Concentrated loads occur at support locations on all structures (i.e., trunnion assembly of gates and valves, end posts of lift gates, and end disks of roller gates), lifting connections, and areas where skin plate ribs are attached to horizontal girders on a tainter gate.
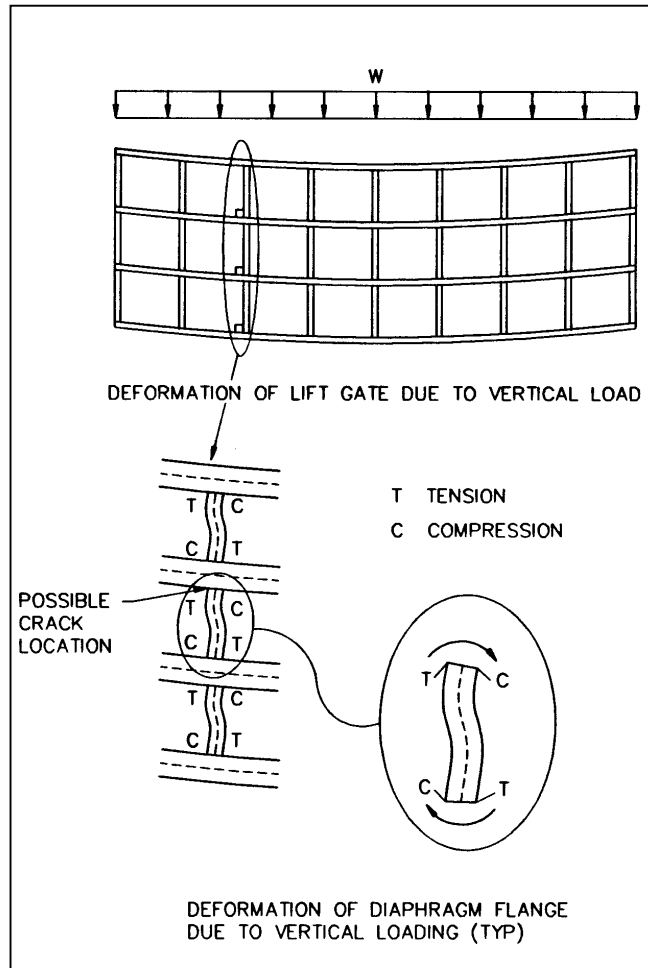
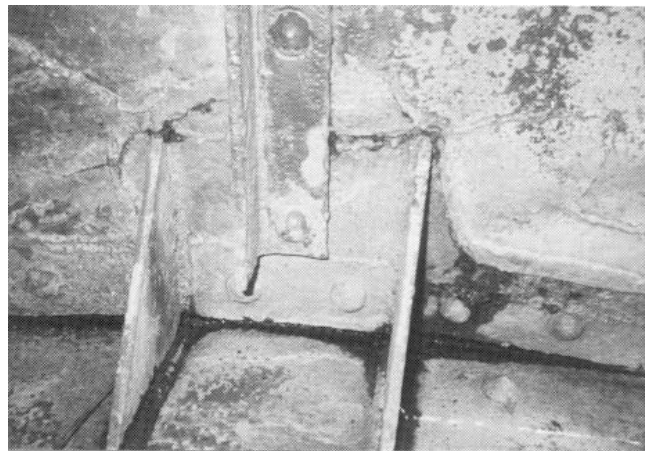**Figure 3-5. Distortion-induced high-stress location**

Figure 3-6. Fatigue crack at weld repair on roller gate end shield

3-4. Visual Inspection

a.   Visual inspection is the primary inspection method and shall be used to inspect all critical elements as determined according to paragraph 3-3.   A visual inspection is hands-on and requires careful and close examination. The inspector should look closely at the members and connections and not just view them from a distance. Inspectors should use various measuring scales, magnifying glasses, and other hand tools to identify, measure, and locate areas of concerns. Boroscopes, flashlights, and mirrors may be necessary to inspect areas of limited accessibility. Weld gauges should be available to check the dimensions of weld beads. Critical areas should be cleaned prior to inspection, and additional lighting should be used when necessary.

b.   Inspection methods other than visual inspection may be used for the periodic inspection of hydraulic steel structures, if necessary. These methods, discussed in Chapter 4, include dye penetrant, magnetic particle, or eddy-current methods for inspection of cracks, and ultrasonic methods for inspection of cracks or corrosion loss.

3-5. Critical Area Checklist

For the periodic inspection of any hydraulic steel structure, a critical area checklist should be developed prior to inspection as part of the preinspection assessment discussed in paragraph 3-2. Critical areas are likely common for a given type of hydraulic steel structure; however, detailed lists may be individually structure dependent.

a.   *General*. Based on the discussion in this chapter and Chapter 2, the following common areas should be inspected on all hydraulic steel structures:

(1) All nonredundant and/or fracture critical components. These typically include main framing members and lifting and support assemblies.

(2) Locations identified as susceptible to fracture or weld-related cracking as outlined in paragraph 3-3*a*.

(3) Corrosion-susceptible areas as outlined in paragraph 3-3*b* (normal waterline, abrasion areas, crevices, locations with dissimilar metals).

(4) Lifting connections or hitches. These are subjected to high concentrated loads, are often of welded thick-plate construction, and are fracture critical. The lifting chain or cable used to lift the gate is also critical.

(5) Support locations: trunnion (tainter gate, valves), end post (lift gate), top anchorage and pintle areas (miter gate), and end disk (roller gate) assemblies. These are subjected to high concentrated loads, are often of welded thick-plate construction, and are fracture critical.

(6) Intersecting welds. These occur at uncoped stiffeners and diaphragm web-to-girder welds.

(7) Previous cracks repaired by welding. Figure 3-6 shows an example of cracks redeveloped at weld repairs.

(8) Locations of previous repairs or where damage has been reported. This includes buckling or plastic deformation, cracking, or corrosion.

b.   Roller gates. Additional critical areas common for roller gates include the following (Figure 3-7):

(1) Attachments and connections at midspan (high tensile stress, stress concentration).

(2) The apron assembly connection to the roller (high stress, stress concentration).

(3) Connections between the roller drum cylinder and the end shields (displacement-induced stresses).

c.   Tainter gates. Additional critical areas common for tainter gates include the following (Figure 3-8):

(1) Girder-rib-skin-plate connection on the upstream girder flange near the end frames and the bracing-to-downstream-girder-flange connection near midspan (critical tension stress/detail combinations).

(2) Connections of main framing members such as the girder-to-strut connection (fracture critical, high moments).

(3) Seal lip plate if it is fabricated from stainless steel or other dissimilar metal (galvanic and/or crevice corrosion).

d. Lift gates. Additional critical areas common for lift gates include the following (Figure 3-9):

(1) Horizontal girder-to-end-box-girder connection and the bracing-to-downstream-girder-flange connection near midspan (critical tension stress/detail combinations).

(2) The ends of diaphragm flanges where attached to downstream girder flanges (displacement-induced stresses).

e. Miter gates. Additional critical areas common for miter gates include the following (Figure 3-10):

(1) Horizontal girder-to-miter and quoin post connections (thick plates, high constraint, high stress).

(2) The ends of diaphragm flanges where attached to downstream girder flanges (high stress, stress concentration).

(3) Connections at ends of diagonal members (high stress, fracture critical).

3-6. Inspection Intervals

The maximum time interval between periodic inspections of hydraulic steel structures is established in ER 1110-2-100. Visual inspections should also be performed if unusual loading situations occur. Such situations include barge impact, earthquake, excessive ice load, increase in frictional forces between seals and embedded plates, and movement of the supporting monoliths. Additional detailed inspections may be required to pursue concerns resulting from the periodic inspections or investigate reported distress from lock personnel. If discontinuities exist, fracture mechanics concepts can also be applied to determine appropriate inspection intervals as discussed in Chapter 6.
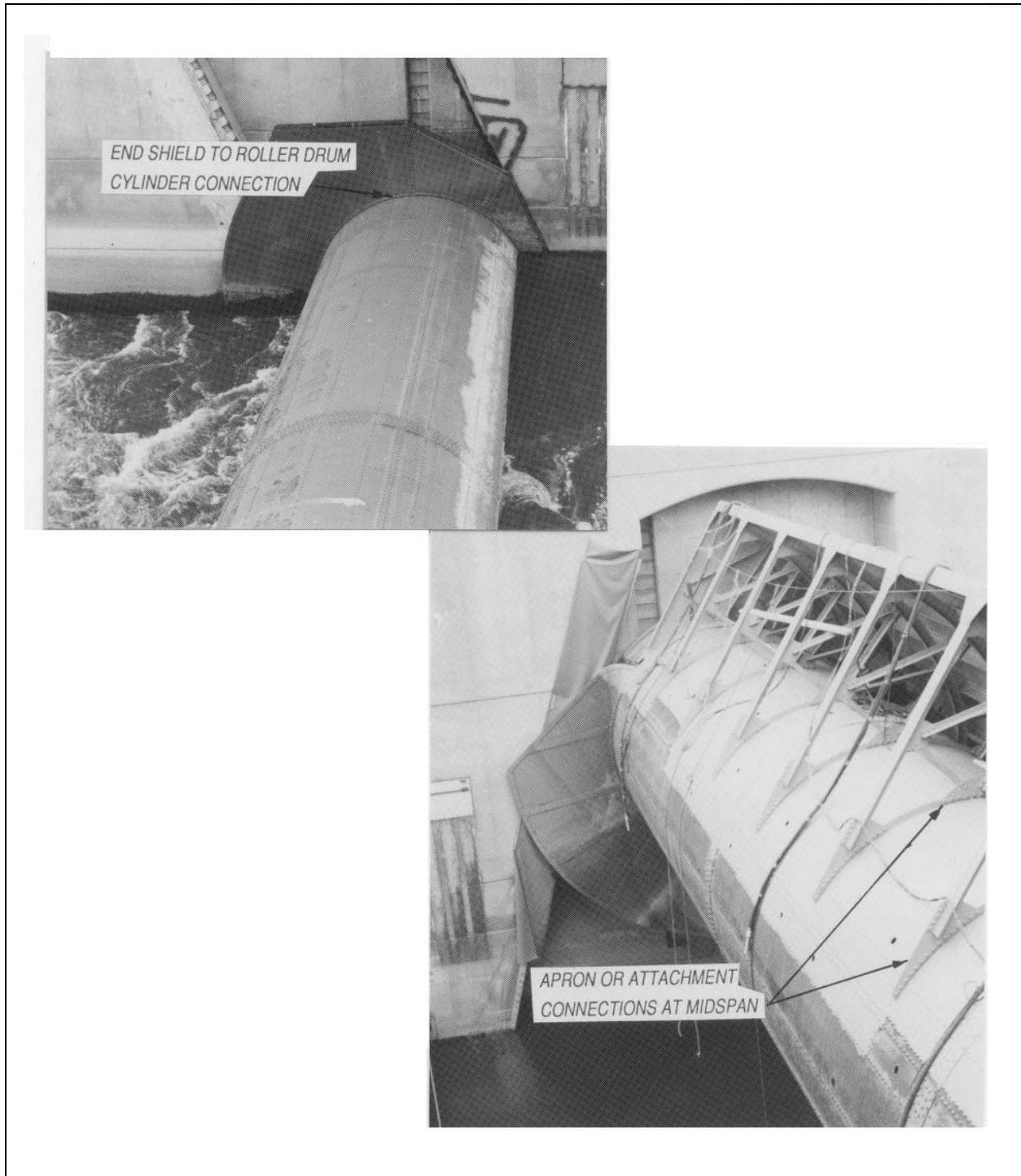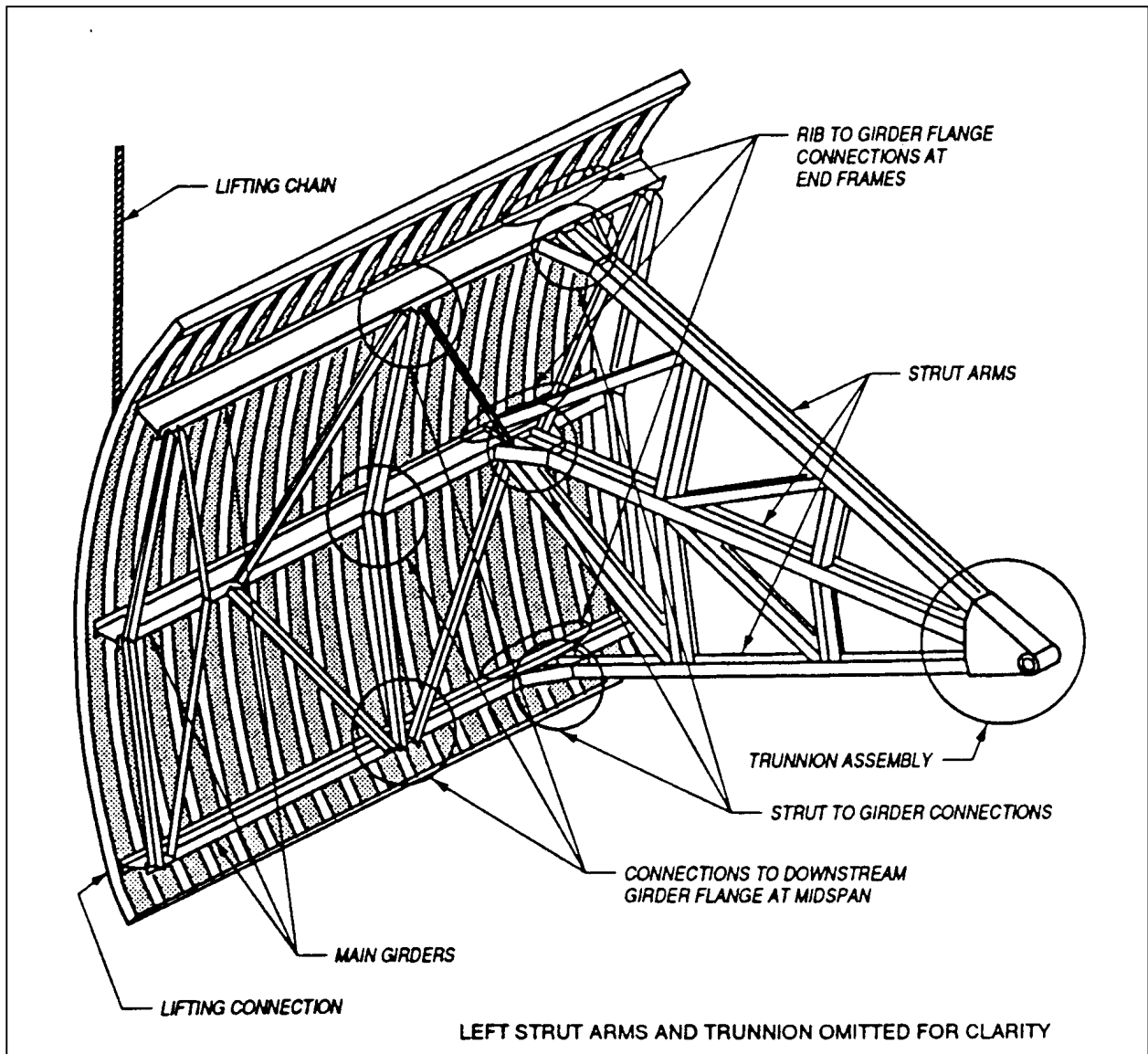
Figure 3-7. Critical areas for roller gates
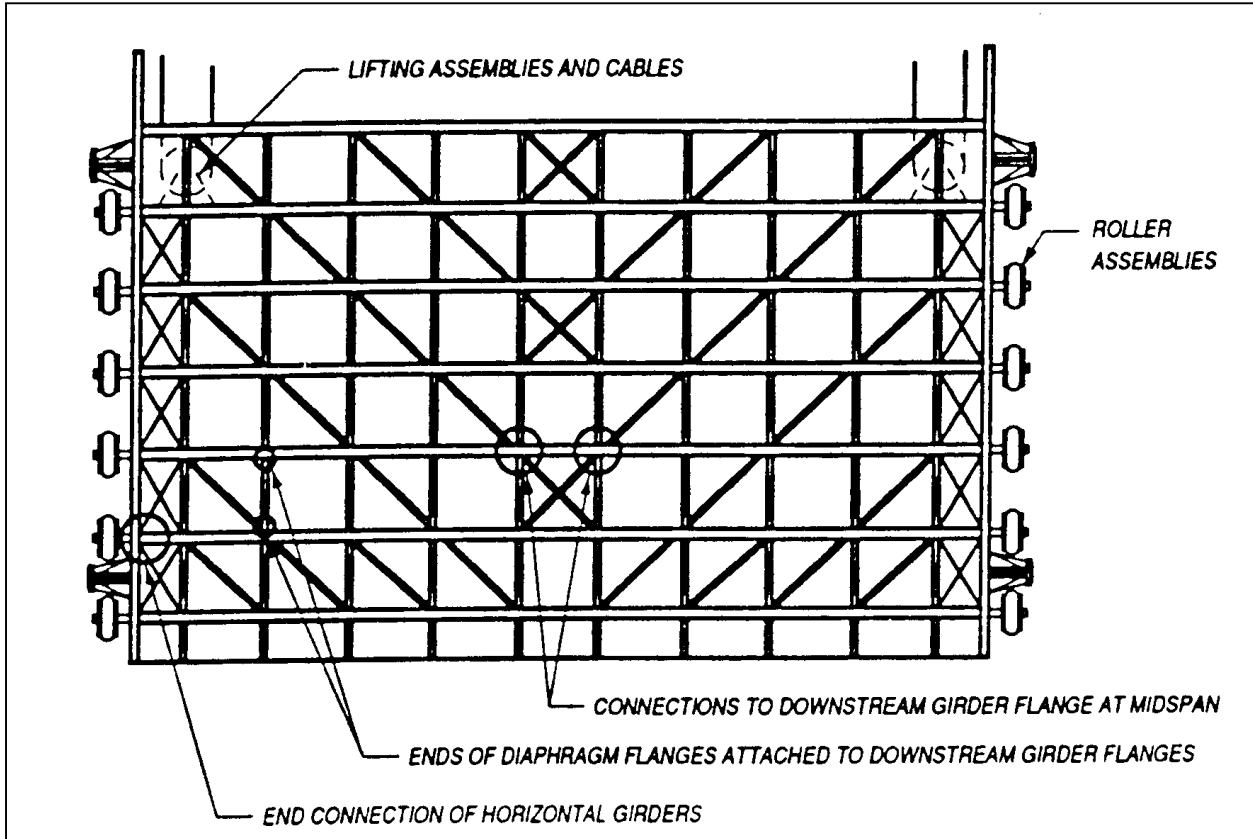
Figure 3-8. Critical areas for tainter gates
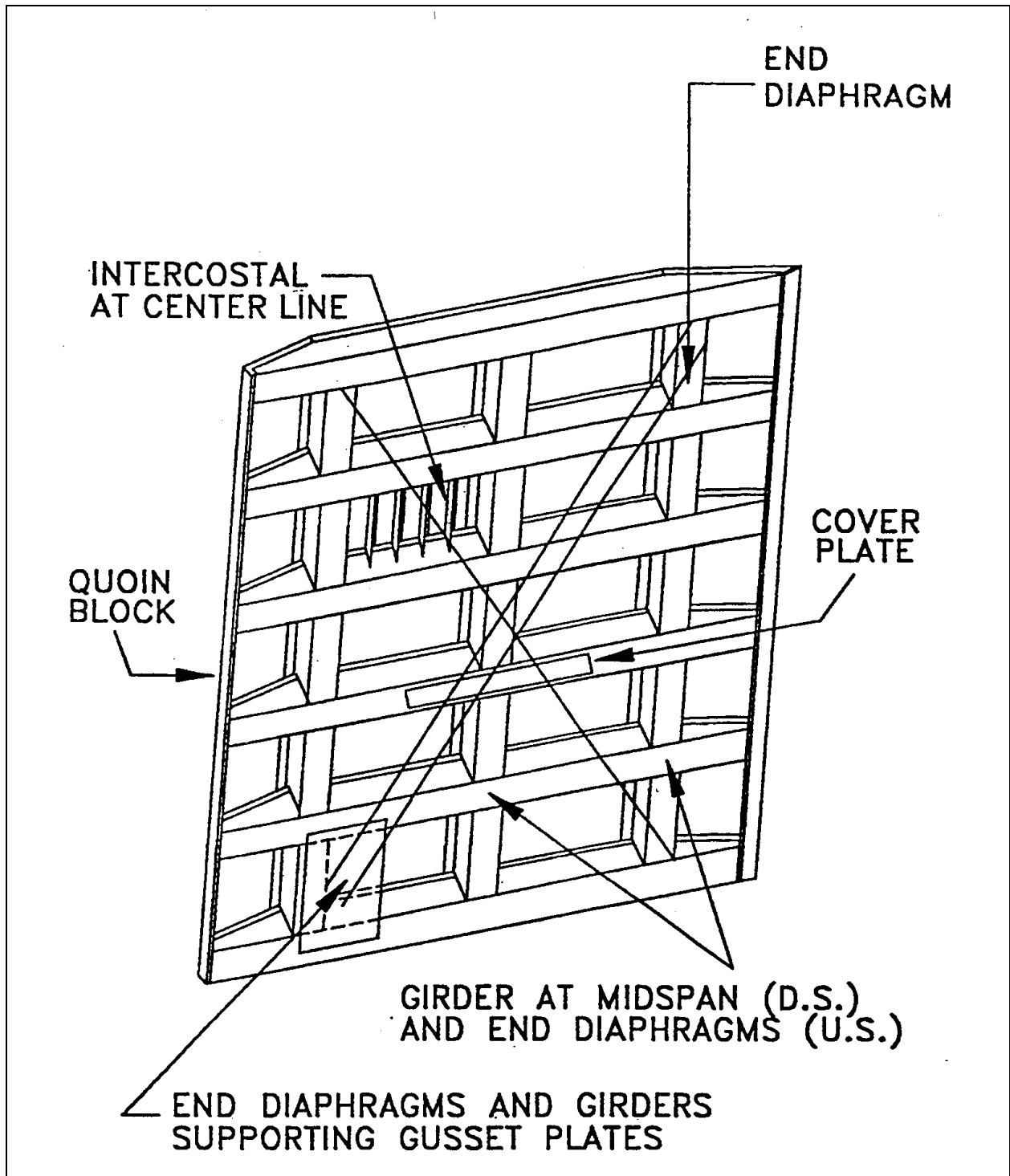
Figure 3-9. Critical areas for lift gates

Figure 3-10. Critical areas for miter gates

Chapter 4
Detailed Inspection

4-1. Introduction

This chapter summarizes appropriate inspection procedures, nondestructive testing (NDT) inspection methods, required inspector qualifications, and code acceptance criteria for defects in new weldments.

4-2. Purpose of Inspection

a. If distressed structural members or connections are identified in the periodic inspection or deterioration in structural performance is assessed from the initial evaluation, then the entire structure should receive a more detailed inspection. Detailed inspections may also be used as part of a damage-tolerance fracture control plan. This fracture control concept is based on the fact that presence of cracklike discontinuities in the structural members or connections does not necessarily mean the end of the service life of the structure. An integrated approach using scheduled inspections on the flawed members and analysis of fracture/fatigue resistance of the same members can assure satisfactory structural performance. The cost for repair or replacement of the flawed members can therefore be balanced against the inspection cost.

b. To develop schedules for inspection when the damage-tolerance fracture control plan is used, fracture mechanics theories must be applied. The inspection periods can be determined by fatigue propagation analysis of the cracked structural members. The crack growth history from a detectable size to the critical size can be predicted using the propagation laws (e.g., Paris's crack growth law). Time interval between inspections should be a fraction of this crack growth life. The optimum inspection intervals vary with service conditions and the discontinuity conditions. These inspection intervals should be short enough that the cracks that were not detectable at the preceding inspections do not have time to propagate to failure before the next scheduled inspection. A procedure for planning the inspection schedules from the crack growth analysis is presented in Chapter 6.

4-3. Inspection Procedures

a. Inspection of cracks. Field inspection for cracking on welded or riveted structures can be accomplished by various NDT methods. The six NDT methods commonly used in industry are visual testing (VT), penetrant testing (PT), magnetic-particle testing (MT), radiographic testing (RT), ultrasonic testing (UT), and eddy-current testing (ET). Selection of an NDT method for inspection depends on a number of variables, including the nature of the discontinuity, accessibility, joint type and geometry, material type, detectability and reliability of the inspection method, inspector qualifications, and economic considerations. A summary of NDT methods that describes advantages and disadvantages of each is provided in paragraph 4-5 and Table 4-1. The following are recommended steps for inspecting for cracks:

(1) Visual examination, particularly with the aid of a magnifying glass ($5 \times$ or higher), is the most efficient first step.

(2) If cracks are suspected and the gate component is dry, PT inspection can be used to confirm the presence of a crack. For most cases, more sophisticated methods, such as UT and MT, can also be employed but may not be needed.

(3) Record the location, orientation, and length of the cracks. Record conditions of the gate when cracks are detected.

Table 4-1
Selection Guide for Inspection Method

Method	Applications	Advantages	Disadvantages
Visual	Surface discontinuities	Economical, fast	Limited to visual acuity of the inspector
Liquid penetrant	Surface cracks and porosity	Relatively inexpensive and reasonably rapid	Cleaning is needed before and after inspection. Surface films hide defects
Magnetic particle	Surface discontinuities and large subsurface voids	Relatively economical and expedient	Applicable only to ferromagnetic materials
Radiographic	Voluminous discontinuities Surface and internal discontinuities	Provides a permanent record	Planar discontinuities must be favorably aligned with radiation beam. Cost of equipment is high
Ultrasonic	Most discontinuities	Sensitive to planar type discontinuities. High penetration capability	Small, thick parts may be difficult to inspect. Requires a skilled operator.
Eddy current discontinuities	Surface and subsurface can be inspected.	Painted or coated surfaces signal High speed	Many variables can affect the test

(4) Take photographs of all cracks showing their position relative to the components of the structure.

(5) The inspector should complete a report following the actual inspection. The report should include the identification and location of inspected structures, date and time of inspection, type of inspection, inspection procedure, inspection equipment, inspector identity and qualifications, and a record of discontinuities detected that includes the location, size, orientation, and classification of each discontinuity. Standard symbols are found in AWS (1998b).

b. Inspection for loose rivets. The inspection of riveted structures should include procedures to identify loose and/or deteriorated rivets. Loose rivets may exist where there are corrosion patterns around the rivet head (as shown in Figure 4-1) or where fretting corrosion (Chapter 2) is observed. A rivet with a deteriorated head may be loose. If loose rivets are suspected, a nonvisual means of inspection is likely required. A commonly practiced nonvisual inspection technique is to impact the rivet head transversely with a hammer. The effectiveness of the rivet may be judged by the tone of the impact. Ewins (1985) describes a method in which the rivet is impacted longitudinally with an instrumented impact hammer. A vibration signal is emitted from the tested rivet. By monitoring the vibration signal emanating from the rivet and comparing the signal to that of a sound rivet, the condition can be determined. The magnitude of the impact force must be consistent for these comparisons. Generally, the signal from a loose rivet will have a lower and broader frequency than the signal from a sound rivet. During inspection, it is not necessary to check each rivet in a structure. Detrimental situations can be identified by testing a representative sample of rivets.

c. Inspection for corrosion. Appropriate tools to assist in measuring and defining corrosion damage include a depth micrometer (for pitting), feeler gages (for crevice corrosion), an ultrasonic thickness gage (for thinning), a ball peen or instrumented hammer (for corroded or loose rivets), a camera, a tape measure, and a means to collect water samples. When corrosion is observed, the type, extent, severity, and possible cause should be reported. If the corrosion is severe, the specific locations should be noted and the severity (amount of thinning, etc.) should be quantitatively determined. Some guidelines on subjective quantification of the severity of corrosion damage are given by Greimann, Stecker, and Rens (1990). If extensive paint system failure is evident, the river water should be analyzed for corrosiveness. Weight loss (ASTM D2688) and electrochemical (ASTM G96) methods can be used to determine the corrosivity of water. Corrosivity of water can also be determined by correlation with pH and ion concentration levels (Pisigan and Singley 1985).
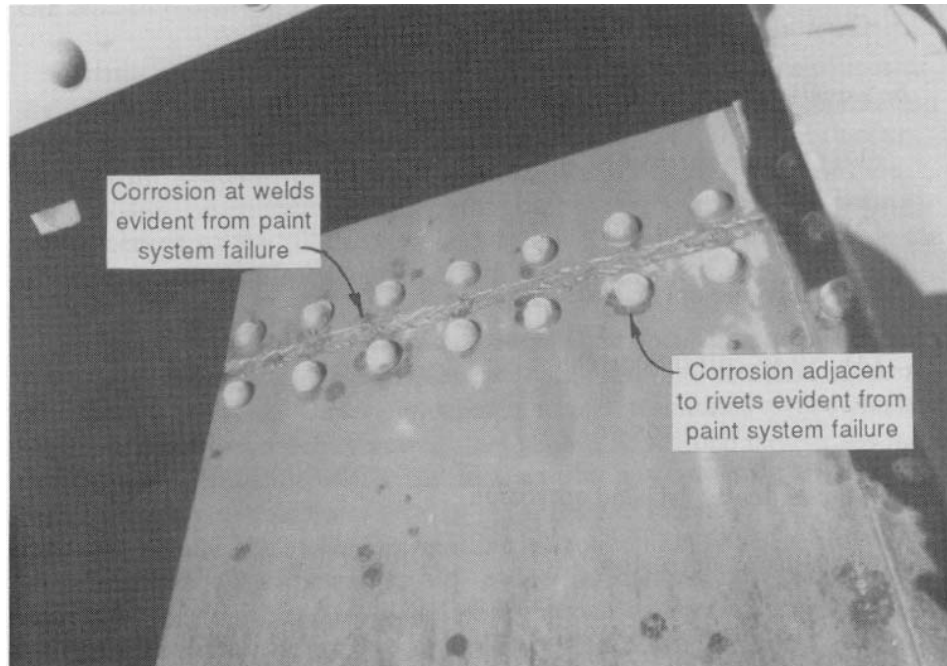
Figure 4-1. Localized corrosion

Although each of these techniques can be used, the weight loss and electrochemical methods are recommended since they provide a more direct measurement and are easier to apply. Common NDT methods that can be applied for inspecting structures for corrosion damage include VT inspection and UT inspection. Newer methods of inspecting for corrosion, such as magnetic resonance testing, are being developed, but these are not yet ready for routine implementation.

(1) Visual inspection.

(a) Visual inspection is the primary NDT technique of inspecting for corrosion. It can be done in situ, usually with only ordinary lighting. A visual inspection of all corrosion-susceptible areas (identified in Chapter 2) should be made to locate, identify, and determine the extent of corrosion. Any failure of the paint system should also be identified.

(b) The extent of corrosion at crevice sites, particularly in riveted structures, should be recorded during each inspection. A sheet feeler gauge may be used to quantify the width of a crevice exhibiting corrosion. Measuring the depth of the crevice (distance into the crevice) may be difficult due to corrosion product blocking the gauge.

(c) When corrosion exists around rivet heads, deterioration of the rivet head and rivet should be checked. A deteriorated rivet will have reduced strength and may not perform as intended. Figure 4-2 shows where rivet heads have split or have developed rosette heads. A corrosion pattern around a rivet may suggest that corrosion is occurring somewhere beneath the rivet head, or that the rivet is loose. Figure 4-1 shows such a corrosion pattern. The corrosion pattern should always be recorded in these instances.

(d) The extent of paint system failure and regions of localized discoloration of structural components should be recorded. In areas where paint failure has occurred, the surface should be visually examined for pitting. When pitting is present, it should be quantified using a probe type depth gauge following guidance specified in ASTM G46.
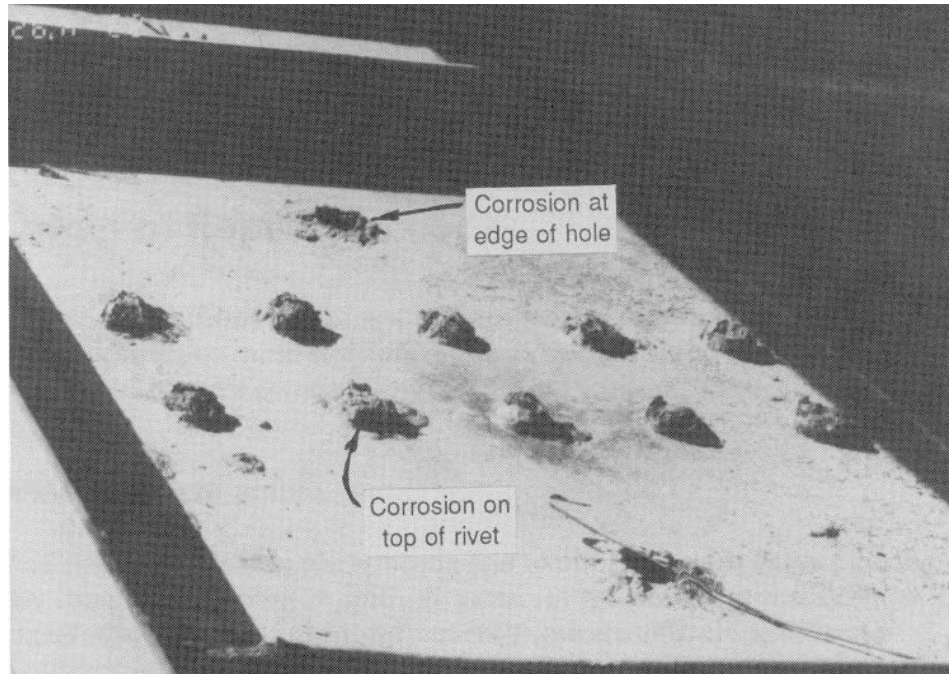
Figure 4-2. Corrosion of rivet heads

(2)   Ultrasonic inspection.

(a)   Ultrasonic inspection is useful when corrosion appears to have caused significant thickness loss in critical components and can be used to obtain a baseline reference for thickness. The thickness of a steel plate or part can be determined to an accuracy of ±0.01 cm (0.005 in.). The technique can be performed through a paint film or through surface corrosion with only a slight loss in accuracy. Ultrasonic transducers are available in a number of sizes. Thus, ultrasonic inspection is useful in determining both general and localized thickness loss due to corrosion, even on curved skin plates.

(b)   Ultrasonic inspection can be used when only one side of a component is accessible. The open surface can be scanned with the transducer to identify thickness variation over the surface and to determine where corrosion has occurred. Methods and equipment for automated scanning and mapping of thickness variation are available but are probably not economically justifiable for in situ use on hydraulic steel structures.

(c)   When ultrasonic inspection is used, the transducer must be coupled to the steel using a coupling liquid, but this is not a serious limitation. Ultrasonic inspection to determine thickness is generally not reliable when pitting corrosion is prevalent, because the size and depth of the pitting impair the output signal of the transducer.

d.   Inspection for plastically deformed members. When plastically deformed or buckled members are found during an inspection, the type and extent of the deformation must be described accurately and in detail so that an assessment of the effect of the damage can be made. The location of the damaged member should be noted as well as the type and extent of deformation (global member buckling, local buckling of a flange, or impact damage to the skin plate). The magnitude of all deformations should be measured and recorded. Sketches and photographs should be made. The condition of adjacent members, effect on structure performance or operation, and possible causes of the damage should also be noted.

4-4. Inspector Qualifications

For the results of an inspection to be worthwhile, the inspector must be qualified. Corps personnel are often not adequately trained in inspection methods; therefore, inspections are often performed via contract with inspection specialists. The following qualification requirements apply to all inspectors, whether Government or contractor employees.

a. Qualification in NDT methods.

(1) The effectiveness of NDT depends on the capabilities of the person who performs the test. Inspectors performing NDT should be qualified in accordance with the American Society for Nondestructive Testing (ASNT) Recommended Practice No. SNT-TC-1A (ASNT 1980). The SNT-TC-1A document is a guide to establish practices for training, qualification, and certification of NDT personnel. Three basic levels of qualification are defined in SNT-TC-1A as follows:

(a) NDT Level I: An NDT Level I individual shall be qualified to properly perform specific calibrations, specific NDT, and specific evaluations for acceptance or rejection determinations according to written instructions and to record results.

(b) NDT Level II: An NDT Level II individual shall be qualified to set up and calibrate equipment and to interpret and evaluate results with respect to applicable codes, standards, and specifications. The NDT Level II individual shall be able to organize and report the results of NDT.

(c) NDT Level III: An NDT Level III individual shall be capable of establishing techniques and procedures; interpreting codes, standards, and procedures; and designating the particular NDT methods, techniques, and procedures to be used.

(2) Certification of all levels of NDT personnel is the responsibility of the employer. The employer must establish a written practice for the control and administration of NDT personnel training, examination, and certification.

b. Qualification in weld inspection.

(1) Welding inspectors are responsible for judging the quality of the product in relation to some form of written specification. The following qualifications are necessary for individuals to inspect welds adequately.

(a) A welding inspector must be familiar with engineering drawings and able to interpret specifications.

(b) A welding inspector should be familiar with welding processes and welding procedures.

(c) A welding inspector should be able to maintain adequate records.

(d) A welding inspector should have passed an eye examination with or without corrective lenses to prove near-vision acuity of Snellen English, or equivalent, at 300 mm (12 in.), and far-vision acuity of 20/40, or better.

(2) In addition, one of the following three requirements is necessary to qualify an individual as a weld inspector for a hydraulic steel structure:

(a) Current or previous certification as an AWS Certified Welding Inspector (CWI) in accordance with the provisions of ANSI/AWS QC1.

(b)   Current or previous qualification by the Canadian Welding Bureau (CWB) to the requirements of the Canadian Standard Association (CSA) Standard W178.2 (CSA 1917).

(c)   An engineer or technician who, by training, experience, or both, in metals fabrication, inspection, and testing, is competent to perform inspection of the work.

4-5. Summary of NDT Methods

a.   Detailed visual testing (VT). Detailed VT inspection uses the same inspection tools and procedure as normal VT (described in Chapter 3), except that because existing discontinuities in a structural member or connection are known from periodic inspections, a more concentrated examination is performed. The type, geometry, size, location, and orientation of the discontinuities must be quantitatively determined. The entire structure may be inspected rather than just representative members or connections. VT inspection is described in ANSI/AWS B1.10.

(1)   Advantages. VT inspection is useful for checking the presence of surface discontinuities. It is simple, quick, and easy to apply. It requires no special equipment other than good eyesight, sometimes assisted by simple and inexpensive equipment.

(2)   Disadvantages and limitations. A major disadvantage of VT inspection is the need for an inspector who has considerable experience and knowledge in many different areas. Although VT inspection is an invaluable method for detecting surface discontinuities, it is less reliable in detecting and quantifying small surface discontinuities or detecting subsurface discontinuities.

b.   Penetrant testing (PT). PT inspection is also a method used to detect and locate surface discontinuities. PT is described by ASTM E165 and E1316, and ANSI/AWS B1.10. Liquid penetrants can seep into various types of minute surface openings by capillary action. Therefore, this process is well suited for detecting discontinuities such as surface cracks, overlaps, porosity, and laminations. PT inspection can be performed using visible dye or fluorescent dye visible with ultraviolet light. Three different penetrants commonly used with either dye are water washable, solvent removable, and postemulsifiable. The various penetrant inspection systems are listed in order of decreasing inspection sensitivity and operational cost as follows:

- Postemulsifiable fluorescent dye

- Solvent-removable fluorescent dye

- Water-washable fluorescent dye

- Postemulsifiable visible dye

- Solvent-removable visible dye

- Water-washable visible dye

(1)   Advantages. PT inspection is relatively inexpensive and reasonably rapid. Equipment generally is simpler and less costly than that for most other NDT methods.

(2)   Disadvantages and limitations. The major limitation of PT inspection is that it can detect only discontinuities that are open to the surface. Another disadvantage is that the surface roughness of the object being inspected may affect the PT inspection results. Extremely rough or porous surfaces may produce false

indications. Some substances in the penetrants can affect structural materials. If penetrants are corrosive to the material being inspected, they should be avoided.

c. Magnetic particle testing (MT). MT inspection is used to detect surface or near-surface discontinuities in ferromagnetic materials. ASTM E709 and E1316 and ANSI/AWS B1.10 provide information on MT. Magnetic fields can be generated by yokes, coils, central conductors, prod contacts, and induced current. When the material is magnetized, magnetic discontinuities that lie in a direction generally transverse to the direction of the magnetic field will cause a leakage field at the surface of the material. The presence of this leakage field is detected when fine ferromagnetic particles are applied over the surface. Some of the particles are gathered and held by the leakage field. This collection of particles indicates the discontinuities. Several magnetic particle materials commonly used for MT inspection are dry powders (i.e., suitable for field inspection of large object), wet magnetic particles suspended in water or light oil (i.e., suitable for very fine or shallow discontinuities), magnetic slurry suspended in heavy oil, and magnetic particles dispersed in the liquid polymers to form solid indications.

(1) Advantages. The MT inspection is a sensitive means of detecting small and shallow surface or near-surface discontinuities in ferromagnetic materials. MT inspection is considerably less expensive than radiographic or ultrasonic inspection and is generally faster and more economical than penetrant inspection. Compared to PT inspection, MT inspection has the advantage of revealing cracks filled with foreign material.

(2) Disadvantages and limitations. MT inspection is limited to ferromagnetic material. For good results, the magnetic field must be in a direction that will intercept the direction of the discontinuity. Large currents sometimes are required for very large parts. Care is necessary to avoid local heating and burning of surfaces at the points of electrical contact. Demagnetization is sometimes necessary after inspection. Discontinuities must be open to the surface or must be in the near subsurface to create flux leakage of sufficient strength to accumulate magnetic particles. If a discontinuity is oriented parallel to the lines of force, it will be essentially undetectable.

d. Radiographic testing (RT). RT inspection is based on differential absorption of penetrating radiation by the material being inspected. Radiation from the source is absorbed by the test piece as the radiation passes through it. The discontinuity and its surrounding material absorb different amounts of penetrating radiation. Thus, the amount of radiation that impinges on the film in the area beneath the discontinuity is different from the amount that impinges in the adjacent area. This produces a latent image on the film. When the film is developed, the discontinuity can be seen as a shadow of different photographic density from that of the image of the surrounding material. Evaluation of the radiograph is based on a comparison of these differences in photographic density. The dark regions represent the more easily penetrated parts (i.e., thin sections and most types of discontinuities) while the lighter regions represent the more difficult areas to penetrate (i.e., thick sections). An essential element to the radiographic process is film, a thin transparent plastic base coated with fine crystals of silver bromide (emulsion). RT inspection shall conform to ASTM E94, ASTM E142, ASTM E747, and ASTM E1032. Other applicable documents include ASTM E242, ASTM E1316, ASTM E999, ASTM E1025, ANSI/AWS B1.10, and ANSI/AWS D1.1.

(1) Advantages. RT inspection detects surface and internal discontinuities, is generally not restricted by the type of material or grain structure, and provides a permanent record for future review.

(2) Disadvantages and limitations. RT presents a potential radiation hazard to personnel, is costly (radiographic equipment, facilities, and safety programs are expensive), and is relatively time consuming. The RT method is difficult to conduct during field applications. To provide reliable detection, discontinuities must be favorably aligned with the radiation beam, and accessibility to both sides of the parts to be inspected is required.

e. Ultrasonic testing (UT). UT inspection is a nondestructive method in which high-frequency sound waves are used to detect surface and internal discontinuities. The sound waves travel through the materials to be inspected and are reflected from surfaces, refracted at interfaces between two substances, and diffracted at edges or around obstacles. The reflected sound waves are detected and analyzed to define the presence and location of discontinuities. Cracks, laminations, shrinkage cavities, pores, and other discontinuities that act as metal-gas interfaces can be easily detected. Inclusions and other nonhomogeneous defects in the metal can also be detected. UT inspection is usually performed with longitudinal waves or shear waves (i.e., angle beam). Most UT inspections for discontinuities are performed using angle-beam technique. The pulse-echo method with A-scan is most commonly used for inspection of welds. The most commonly used frequencies are between 1 and 5 MHz, with sound beams at angles of 0, 45, 60, and 70 degrees. During application of the method, all surfaces of the part to be examined should be free of weld spatter, dirt, grease, oil, paint, and loose scale. Applicable guidance documents include ASTM A435/A435M, ASTM A577/A577M, ASTM E114, ASTM E164, ASTM E214, ASTM E1316, ANSI/AWS B1.10, and ANSI/AWS D1.1.

(1) Advantages. UT provides near-instantaneous indications of discontinuities. It is not hazardous to personnel, nor does it have adverse effects on materials. The method is very accurate. It has superior penetrating power allowing the detection of discontinuities deep in the part, is highly sensitive permitting the detection of small discontinuities, and provides good accuracy in determining the size, position, and shape of discontinuities.

(2) Disadvantages and limitations. Manual operation and interpretation of results require experienced technicians. Even with experienced personnel, reference standards are needed for calibrating the equipment and for characterizing discontinuities. Parts that are rough, irregular in shape, very small, or inhomogeneous are difficult or impossible to inspect.

f. Eddy-current testing (ET). ET inspection is an electromagnetic method that is based on the principles of electromagnetic induction. When an alternating current is passed through a coil, eddy current is created in the material being tested by an alternating magnetic field. The test coil is electronically monitored to detect the changes of magnetic field caused by the interaction between the eddy currents and the initial field. Any surface or subsurface discontinuities that appreciably alter the normal flow of eddy currents can be detected by ET inspection. ASTM E1316 and ANSI/AWS B1.10 provide guidance on the use of ET.

(1) Advantages. Because ET inspection is an electromagnetic induction technique, it does not require direct contact between probe and the material being tested, so coated materials can be inspected. ET inspection is adaptable to high-speed inspection.

(2) Disadvantages and limitations. The test material must be an electrical conductor (not a concern for inspection of hydraulic steel structures). Internal discontinuities that are more than approximately 6 mm (1/4 in.) from the surface cannot be accurately detected by eddy-current inspection. The method is based on indirect measurement, and the correlation between the instrument readings and the structural characteristics of the material being inspected must be carefully established. Since many variables can affect an eddy-current signal, interpretation of results must be done by experienced personnel.

4-6. Discontinuity Acceptance Criteria for Weldments

a. Discontinuity classification. The common weld discontinuities detected from various NDT methods can be classified into planar and nonplanar types. Planar type discontinuities include cracks, delaminations or laminar tearing, and sometimes incomplete joint penetration or incomplete fusion. The nonplanar type discontinuities are volumetric weld discontinuities, which include porosity, slag or tungsten inclusions, undercut, underfill, and overlap. Figure 4-3 shows these common types of weld discontinuities (ANSI/AWS B1.10).
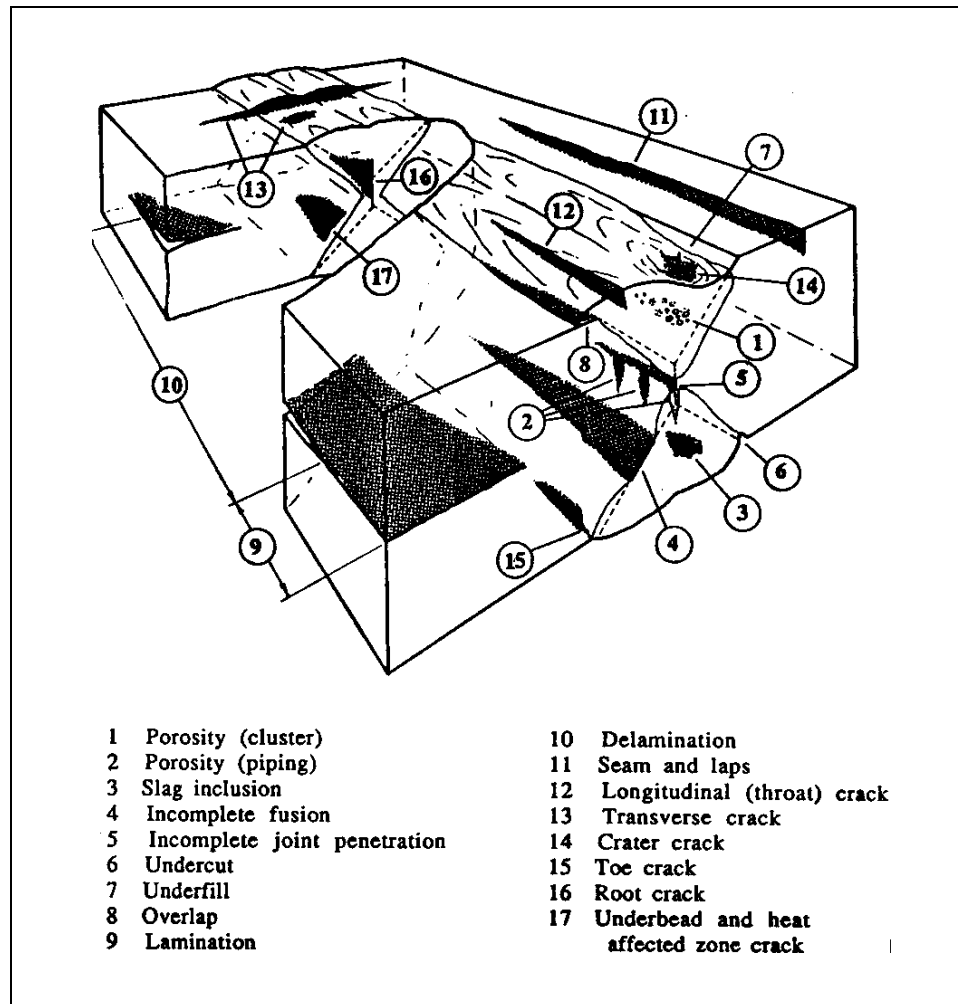
1	Porosity (cluster)	10	Delamination
2	Porosity (piping)	11	Seam and laps
3	Slag inclusion	12	Longitudinal (throat) crack
4	Incomplete fusion	13	Transverse crack
5	Incomplete joint penetration	14	Crater crack
6	Undercut	15	Toe crack
7	Underfill	16	Root crack
8	Overlap	17	Underbead and heat affected zone crack
9	Lamination		

Figure 4-3. Weld discontinuities (ANSI/AWS B1.10; copyright permission granted by American Welding Society)

b. Acceptance criteria. The results obtained from various NDT inspections for new fabrication are assessed according to the recommended acceptance criteria for weld discontinuities as presented by ANSI/ AWS D1.1. These acceptance criteria as they apply to various NDT inspection results can be summarized in three perspectives: weld profile, static loading case, and dynamic loading case. Weld profile is a code compliance for weld quality. Inspection for this code compliance is usually made by visual inspection with the aid of a weld gauge. The purpose of this code compliance is to provide information on the structural fitness of the welds. Weld profile noncompliance may be acceptable if an engineering assessment is conducted. The code acceptance criteria recognize the effect of dynamic loading on the structures as opposed to the statically loaded case. Planar type discontinuities are not acceptable in either case, and permissible conditions on nonplanar type discontinuities are specified in the code criteria with smaller allowances for the dynamically loaded structures. Repair or replacement of structural members or connections that contain unacceptable discontinuities (i.e., flaws) may be required. These acceptance criteria are obviously applicable to existing structures with discontinuities as well. To avoid unnecessary repair or replacement, fracture mechanics analysis may be conducted to reassess these unacceptable discontinuities for new fabrication or existing structural weldments. A maintenance schedule may be developed in lieu of immediate repair or replacement of the distressed members or connections using a damage-tolerance fracture control plan (Chapter 6).

Chapter 5
Material and Weld Testing

5-1. Purpose of Testing

   a.   A structural inspection may reveal that certain structural members or connections are weakened due to some form of distress, but have not failed. With strength less than the design strength, these members and connections operate with a safety factor lower than that intended in design. The structure could continue to be operated with this reduced factor of safety, or the load conditions could be adjusted to raise the actual factor of safety. To determine the appropriate decision, engineering assessments that include fracture and fatigue analysis should be conducted, as discussed in Chapter 6. Mechanical properties of the structural members and welds are usually needed in the analysis.

   b.   For hydraulic steel structures fabricated in recent years, the materials used for the structural members and welds are usually well documented and can be identified from the design drawings. For older structures, however, information on mechanical properties of the structural materials or welds may not be readily available. Mechanical tests of these materials and welds are sometimes required to determine necessary information for fracture and fatigue analyses. In addition, determination of the chemical composition of unknown materials may be required.

5-2. Selection of Samples from Existing Structure

Material information that may be required to evaluate a steel structure includes chemical composition, tensile strength, bend ductility, fillet weld shear strength, hardness, and fracture toughness. The test samples may be taken from the materials left from original fabrication, removed from existing gate members or connections, or obtained from weldments made of similar materials with welding procedures similar to those used in the original fabrication.

5-3. Chemical Analysis

When the chemical composition of an existing structural (steel) material is not available, it may be necessary to perform a chemical analysis. This is an important initial task in the overall material and weld testing program. The information from this analysis will provide a basis for characterizing the properties of the unknown materials. This information can be used to assist in selecting appropriate NDT methods, assessing corrosion problems, conducting fracture analyses, and assessing material weldability for possible repair. A chemical analysis for material compositions should be in conformance with ASTM E30 and E350.

5-4. Tension Test

   a.   Tension tests provide information on the strength and ductility of materials under uniaxial tensile stress. The pertinent data obtained from a tension test are ultimate tensile strength, yield strength, Young's modulus, percent elongation, percent reduction of cross-sectional area, and the stress-strain relationship.

   b.   Transverse tension tests are generally used to determine weld quality during the weld qualification process. Similar tests could be used for existing structures if the original fabrication practices can be replicated. The transverse rectangular tension specimens are machined from a butt-welded plate, with the weld crossing in the midsection of the specimen (AWS B4.0 (AWS 1998a), Figure C-2). Specimens are then tested to failure in tension with results reflecting the effects of nonhomogeneous weld/metal interface and other weld defects. When weldment thickness is beyond the capacity of test equipment, the weldment is divided through its

thickness into as many specimens as required to cover the full weld thickness. The results of the partial-thickness specimens are averaged to determine the properties of the full-thickness joint.

c. The base metal and weld metal tests are performed on a tensile testing machine in accordance with the requirements of ASTM E8. The machine should be calibrated in accordance with ASTM E4. The rate of straining should be between 0.05 and 0.5 units per unit of gauge length, per minute.

d. Material properties are calculated as follows:

(1) Ultimate tensile strength = maximum load/original cross-sectional area in the gauge length.

(2) Yield strength = load at 0.2 percent offset/original cross-sectional area in the gauge length.

(3) Percent elongation = (final gauge length - original gauge length)/original gauge length × 100.

(4) Reduction of area: Fit the ends of the fractured specimen together and measure the thickness and width at the minimum cross section. Calculate the reduced area.

e. At least two specimens should be tested for each sample type. The result of the tension test is the average of the results of the specimens.

5-5. Bend Test

a. In accordance with ASTM E190, bend tests are generally used in the weld qualification process for new fabrication. Similar tests, however, could be conducted for existing structures if original fabrication practices can be simulated. Guided bend tests are used to evaluate the ductility and soundness of welded joints and to detect incomplete fusion, cracking, delamination, effect of bead configuration, and macrodefects of welded joints. The quality of welds can be evaluated as a function of ductility to resist cracking during bending. The top and bottom surfaces of a welded plate are designated as the face and root surfaces, respectively. Face bends have the weld face on the tension side of the bent specimen, and the weld root is on the tension side for root bends. For thick plates, transverse slices are cut from the welded joint, and one of the cut side surfaces becomes the tension side of the bent specimen. For all types of bend tests, face, root, and side, the specimen is tested at ambient temperature, and deformation should occur between 1/2 and 2 min.

b. When the plate thickness is less than or equal to 10 mm (3/8 in.), two specimens are tested for face bend and two specimens are tested for root bend. When the thickness of the plate is greater than 10 mm (3/8 in.), four specimens are tested for side bend.

c. Transverse side bend test specimens (Figure A-5 of AWS 1998a) are used for plates that are too thick for face bend or root bend specimen. The weld is perpendicular to the longitudinal axis of the specimen. The side showing more significant discontinuities should be the tension surface of the specimen.

d. For a transverse face bend specimen (Figure A-6a of AWS 1998a), the weld is perpendicular to the longitudinal axis of the specimen. The weld face becomes the tension surface of the specimen during bending. For a transverse root bend specimen (Figure A-6b of AWS 1998a), the weld is perpendicular to the longitudinal axis of the specimen. The root surface of the weld becomes the tension surface of the specimen during bending.

e. During the test, the convex surface of the bent specimen should be examined frequently for cracks or other open defects. If a crack or open defect is present after bending, exceeding a specified size measured in any direction, the specimen is considered to be failed. Cracks occurring on the corners of the specimen during

testing are not considered to fail a specimen unless they exceed a specified size or show evidence of defects (AWS 1998a).

5-6. Fillet Weld Shear Test

a.   The fillet weld shear test is used to determine the shear strength of fillet welds. Fillet weld shear tests are generally used in the weld qualification process for new fabrication; however, similar tests could be conducted for existing structures if original fabrication practices can be simulated. The test is performed in accordance with the requirements of ASTM E8 on a tensile machine. The machine should be calibrated in accordance with ASTM E4. For longitudinal shear strength, the specimen is prepared in accordance with Figure E-1 of AWS B4 (AWS 1998a), and for transverse shear strength, the test specimen is prepared in accordance with Figure E-2 of AWS B4. The specimen is positioned in the testing machine so that the tensile load is applied parallel to the longitudinal axis of the specimen. The length, average throat dimension, and legs of each weld should be measured and reported. The welds are sheared under tensile loads and the maximum tensile loads are reported.

b.   Shear strength in pounds per square inch is calculated by dividing the maximum load by the effective weld throat area (i.e., theoretical throat thickness times total length of fillet weld sheared). At least two specimens are tested. The result of the shear test is the average of the results of the specimens. A test is considered invalid if the failure is caused by a base metal defect. The fracture location must also be included in the report.

5-7. Hardness Test

a.   Hardness tests are used to provide generic information on the material properties (primarily toughness and strength). Hardness measurements provide indications of metallurgical changes caused by welding, metallurgical variations, and abrupt microstructural discontinuities in weld joints, brittleness, and relative sensitivity to cracking under structural loads.

b.   Specimens for hardness testing include as-welded partial or complete assemblies, weldments from which the reinforcement has been removed, and weld joint cross sections. For hardness tests of existing hydraulic steel structures, the weld reinforcement may or may not be removed. When it is removed, a local area of the reinforcement is ground smooth before testing. For large assemblies, portable hardness testers are available that can be transported for use in the field. Microhardness testing of welds is usually performed on ground, polished, or polished and etched transverse cross sections of the weld joints.

c.   The most common hardness testing methods include Brinell, Rockwell, and Vickers tests. Selection of test method depends on hardness or strength of the material, the size of the welded joints, and the type of information desired. The Brinell, which is appropriate for field evaluations, produces a large indentation suited for large welds in heavy plates. The Rockwell test produces much smaller indentations than the Brinell test and is more suited for hardness traverses. The Rockwell hardness test is also suitable for field inspection if a portable tester is used (see ASTM E110). The Vickers test makes relatively small indentations and is suited for hardness measurements of the various regions in the weld heat-affected zone and for fine-scale traverses. The Brinell and Rockwell tests are generally used for hardness measurements of fusion-welded joints in laboratory or field environments. For each type of hardness test performed, at least five indentations should be made for each region. The result of the hardness test is the average of the indentations. The hardness values from different test methods can be correlated through a conversion chart provided by ASTM E140.

d.   The Brinell hardness test is performed in accordance with the requirements of ASTM E10. It is an indentation hardness test using calibrated machines to force a hard ball into the surface of the material and to

measure the diameter of the resulting impression after removal of the load. The Brinell hardness number, HB, is related to the applied load and to the surface area of the permanent impression made by a ball indenter.

e. The Rockwell hardness test is performed in accordance with the requirements of ASTM E18. This test is an indentation hardness test, in which a diamond spheroconical indenter or hard ball indenter is forced into the surface of the material in two operations. The Rockwell hardness number, HR, is a number derived from the net increase in the depth of indentation as the force is increased from a preliminary test force to a total test force and then returned to the preliminary test force. The higher the number, the harder the material.

f. The Vickers hardness test is performed in accordance with the requirements of ASTM E92. The Vickers hardness test is an indentation hardness test in which a square based pyramidal diamond indenter with specified face angles is forced into the surface of the material. The Vickers hardness number is related to the applied load and the surface area of the permanent impression.

5-8. Fracture Toughness Test

Fracture toughness testing provides a measure of resistance to fracture of a material. Test methods include Charpy V-notch test (CVN), Plane-Strain Fracture Toughness test (K_{Ic}), and Crack-Tip Opening Displacement (CTOD) test. The CVN test is used to measure the ability of a material to absorb energy. The K_{Ic} and CTOD tests are used to determine resistance to fracture given a specific crack subject to a specific stress level. As discussed in Chapter 2, the welding process and welding procedure have a significant effect on the fracture toughness of a welded joint. If possible, fracture toughness test specimens should be selected from a distressed member or connection, so that the test results are representative of the structure. As an alternative, test samples may be made using similar materials and welding procedures to those used in the original fabrication. Size and orientations of the test specimens taken from structure samples should follow the provisions specified in Figure D-3 of AWS (1998a). Test specimens should not contain metal that has been affected thermally as a result of cutting, preparation, or welding stops or starts. When an evaluation of the base metal or heat-affected zone is required, the location of the notch should be specified.

a. *Charpy V-notch test.*

(1) The CVN test provides information about behavior of metal when subjected to a single application of a load resulting in multiaxial stresses associated with a notch coupled with high rates of loading. For some materials and temperatures, impact tests on notched specimens have been found to predict the likelihood of brittle fracture better than tension tests or other tests used in material specifications.

(2) The specimen preparation and test procedure for the CVN test is described by ASTM E23. When specified, the surface finish of the V-notch of the Charpy impact specimen is 0.5 μm (20 μin.), or less. The testing machine is a pendulum type of rigid construction and of capacity more than sufficient to break the specimen in one blow. The test is performed at various specified temperatures over the range of temperatures that covers brittle to ductile behavior.

(3) Five specimens should be tested for each test condition, and the amount of energy absorbed by the specimen at fracture should be recorded. The highest and lowest values are discarded, and the result is taken as the average of the remaining three specimens tested. If any specimen fails to break, or jams in the machine, the data of that specimen are not included in the calculation of the average.

(4) In addition to the absorbed energy, other test indicators, such as lateral expansion of the fractured specimen and appearance of the fractured surfaces, can also be used to characterize the fracture toughness of the test material. The amount of expansion on each side of each half can be measured using a lateral expansion gauge. The two broken halves must be measured individually, and the larger value is used.

(5) Fracture characteristics of a material are also related to the appearance of the fractured surface. The fracture appearance can be quantified by measuring the length and width of the cleavage portion of the fracture surface or comparing the appearance of the fractured surface with a fracture appearance chart as shown in ASTM E23.

b. Plane-strain fracture toughness test. The critical stress intensity factor K_{Ic} characterizes fracture toughness of a material given the presence of a sharp crack when the state of stress at the crack tip is plane strain. K_{Ic} is a material property for a given temperature and load rate, and can be experimentally determined using compact tension test specimens or bend test specimens. The specimen preparation and test procedures must be in accordance with ASTM E399. For a result to be considered valid, it is required that both the specimen thickness and the crack length exceed 2.5 (K_{Ic}/σ_{ys}), where σ_{ys} is the 0.2 percent offset yield strength and K_{Ic} is the plane strain fracture toughness of the material at the desired test temperature and loading rate. The initial selection of a size of specimen may be based on an estimated value of K_{Ic} for the material to be tested. Due to practical considerations and cost considerations, CVN test results are easier to achieve and are more available than K_{Ic} test results. An approximation of K_{Ic} may be obtained through Barsom and Rolfe's (1987) two-stage CVN-K_{Ic} transition method as discussed in paragraph 7-1*b*.

c. Crack-tip opening displacement test. The CTOD test may be used to characterize the toughness of materials that are too ductile or lack sufficient size to be tested for K_{Ic}. CTOD is the displacement of the crack surfaces normal to the original (unloaded) crack plane at the tip of a crack. The CTOD at the fracture incipient load (critical CTOD) indicates the fracture toughness of the test material at a given temperature. The values of the critical CTOD can be used for inspection and fracture assessment criteria, when used in conjunction with fracture mechanics analyses. Preparation of the test specimen and the test procedure for CTOD testing are described in ASTM E1290.

Chapter 6
Structural Evaluation

6-1. Purpose of Evaluation

a. Structural evaluation is the process of determining the capability of a structure to perform its intended function. The evaluation includes the assessment of both the long- and short-term effects of all reported damage and unusual loading conditions. It results in recommendations that include the requirements for future inspections, any repair and maintenance procedures, and the urgency of these tasks. The engineering decision on appropriate repair or planned maintenance is based on the concept of fitness for service of the distressed structure. A structure is fit for service when it functions satisfactorily during its lifetime without reaching any serious limit state.

b. In order to perform a structural evaluation, performance criteria and analytical tools are needed. Loading and performance criteria for hydraulic steel structures are outlined in EM 1110-2-2105, EM 1110-2-2701, EM 1110-2-2702, and EM 1110-2-2703. Basic fatigue and fracture analysis concepts are presented in this chapter and in Chapter 2, and traditional structural analysis techniques can be applied for the assessment of corrosion damage and plastically deformed members. Quantitative techniques for corrosion effects on bridges and sheet piling have been developed based on reliability concepts (Kayser and Nowak 1987, 1989; Mlakar et al. 1989).

6-2. Fracture Behavior of Steel Materials

a. The operating service temperature of a steel structure has a significant effect on the fracture behavior of the steel. For low- and intermediate-strength steels, the material changes from brittle fracture behavior (i.e., critical stress intensity factor K_{Ic} applies when the state of stress at the crack tip is plane strain) to ductile fracture behavior (i.e., critical stress intensity factor K_c or crack-tip opening displacement (CTOD) applies) at a certain transition temperature. This temperature is called the nil-ductility transition (also abbreviated as NDT, which should not be confused with nondestructive testing, also NDT) temperature and is measured by the drop weight test in accordance with ASTM E208. The nil-ductility transition temperature is defined as the highest temperature at which a standard specimen breaks in a brittle manner under dynamic loading. At temperatures above the nil-ductility transition temperature, the material has sufficient ductility to deflect inelastically before total fracture. Below the nil-ductility transition temperature, the fracture toughness remains relatively constant with changing temperature. For impact loading, the nil-ductility transition temperature approximately defines the upper limit of the plane-strain condition as shown in Figure 6-1.

b. For steel, the nil-ductility transition temperature depends on material thickness and applied loading rate. The anticipated level of structural performance (i.e., brittle or ductile) can be determined from the results of the fracture toughness test performed at temperatures around the transition temperature. With an additional consideration of the geometric constraint effect due to material thickness (i.e., β_{Ic} factor, Equation 2-2), the appropriate fracture parameter K_{Ic}, K_c, or CTOD can be selected for fracture analysis. For structures subject to static or dynamic loading, the respective fracture toughness-to-temperature relations must be used to characterize the fracture behavior. Figure 6-1 shows the schematic relationships between level of structural performance and service temperature for various loading rates (Barsom and Rolfe 1987) (see also paragraph 7-1.).

6-3. Fracture Analysis

a. When inspections reveal discontinuities (i.e., cracks or flaws), it is necessary to establish acceptance levels to determine if repairs are needed to prevent fracture. Fracture mechanics may be used to establish acceptance levels for various discontinuities by comparing the discontinuity size with the critical discontinuity
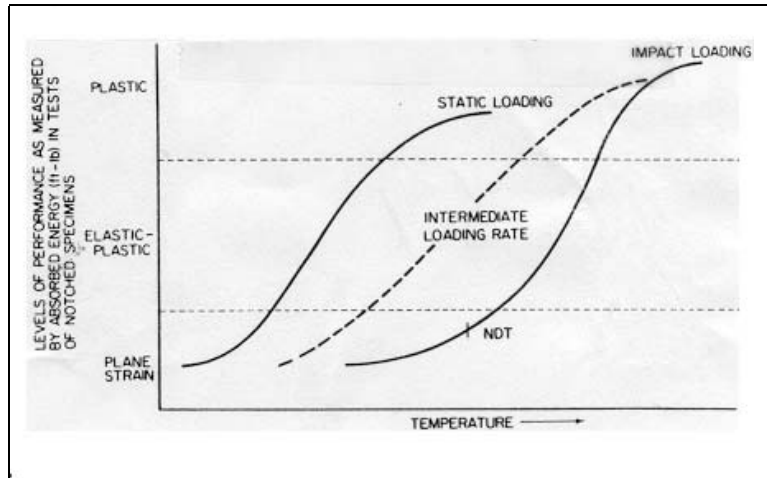
Figure 6-1. Relation between notch toughness and loading rates (Barsom and Rolfe (1987), p 110. Reprinted by permission of Prentice-Hall, Inc., Englewood Cliffs, NJ.)

size. Each case is unique depending on a given set of loads, environmental factors (e.g., temperature), geometry, and material properties. The critical discontinuity size is determined using fracture mechanics principles, which relate stress, discontinuity size, and fracture toughness to existing conditions. If the discontinuity size is less than the critical size, fracture will not likely occur and the expected remaining life may be determined by a fatigue analysis. To ensure this, the stress-intensity factor K_I must be less than the critical stress-intensity factor K_{Ic}, K_{Id}, or K_c, or CTOD must be less than the critical CTOD value δ_{crit}. K_{Id} is the critical stress-intensity factor for dynamic loading and plane-strain conditions.

b. For hydraulic steel structures operating at a minimum service temperature that is below the nil-ductility transition temperature, linear elastic fracture mechanics (LEFM) analysis is required to assess the discontinuities revealed from inspections. For structures with discontinuities operating at temperatures above the nil-ductility transition temperature, elastic-plastic fracture mechanics (EPFM) analysis needs to be conducted. In any case, LEFM may be used as an initial evaluation tool, since it is simple to apply and generally gives a conservative answer. (In nonlinear elastic cases, LEFM analysis would be applied using K_c as the critical stress intensity factor.) As discussed in Chapter 2, the three key parameters in a fracture analysis are stress level, crack geometry, and the fracture toughness. Reliable estimates of each of these parameters should be determined. The magnitude of stress used in a fracture analysis should be determined from a reasonably detailed analysis. The crack geometry should be accurately measured during the inspection process as discussed in Chapter 4. This includes the size, shape, and orientation of the crack. Determination of material toughness is discussed in Chapters 5 and 7. An example fracture evaluation is also provided in Chapter 7.

c. The procedure of fracture assessment of discontinuities may be described by the following steps. The flow chart is shown in Figure 6-2.

(1) Determine the actual shape, location, and size of the discontinuity by NDT inspection.

(2) Determine the effective discontinuity dimensions to be used for analysis (British Standards Institution 1980; Burdekin et al. 1975; and American Society of Mechanical Engineers (ASME) 1978). Discontinuities are classified as through thickness (may be detected from both surfaces), embedded (not visible from either surface), or surface (may be observed on one surface) as illustrated in Figure 6-3. To determine the effective dimensions of a discontinuity:

(a) Resolve the discontinuity into a plane normal to the principal stresses as shown in Figure 6-4. Effective dimensions for various isolated discontinuity types are shown in Figure 6-3.
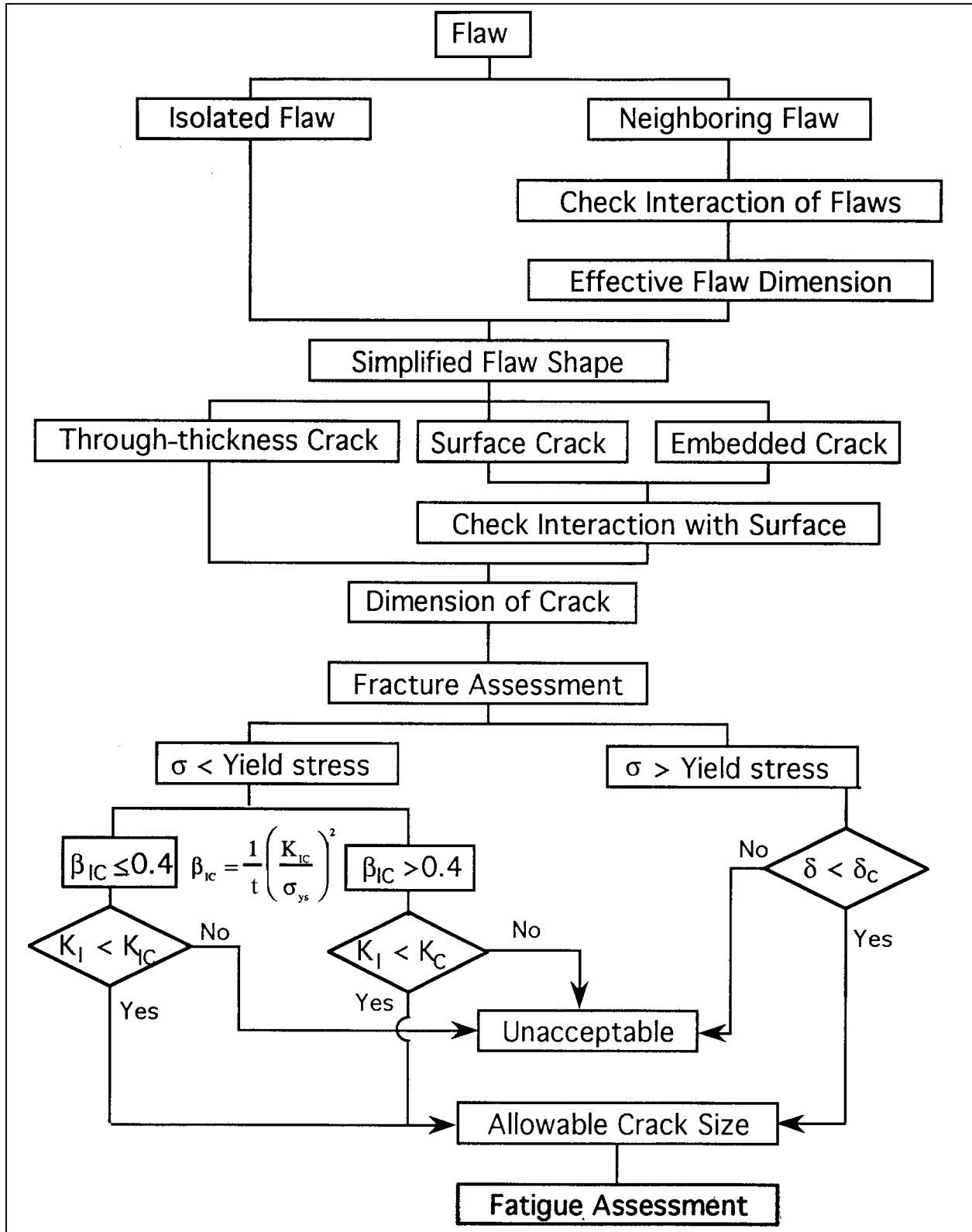
Figure 6-2. Fracture and fatigue assessment procedure where *t* = thickness of component, δ = crack tip opening displacement, δc = critical crack tip opening displacement
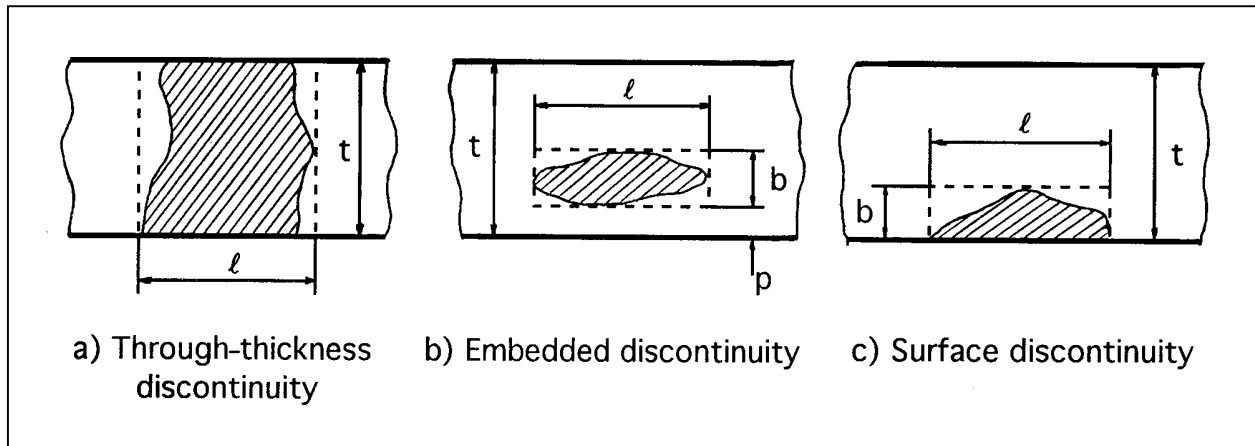
a) Through-thickness discontinuity   b) Embedded discontinuity   c) Surface discontinuity

Figure 6-3. Required dimensions of a discontinuity (after British Standards Institution 1980) where *t* = component thickness, *l* = effective crack length, (2a), *b* = effective dimension of crack in the through-thickness direction, and *P* = effective dimension of the distance between the edge of component and edge of crack in the through-thickness direction
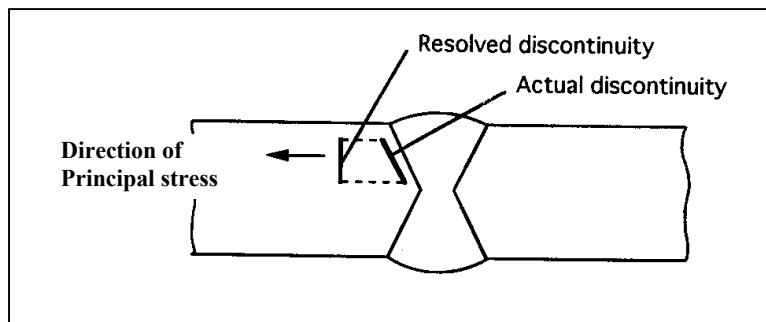

Figure 6-4. Resolution of a discontinuity (after British Standards Institution 1980)

(b)   Check interaction with neighboring discontinuities to obtain the idealized discontinuity dimensions; idealizations for interaction of discontinuities are shown in Figures 6-5 and 6-6.

(c)   Check interaction with surfaces by recategorization as shown in Figure 6-7 for surface or embedded discontinuities (idealized or actual).

(d)   Determine final idealized effective dimensions for fracture analysis.

(3)   Determine the stress level by an appropriate structural analysis, assuming no crack exists. Structural loading can be divided into primary stress σ_p and secondary stress σ_s. The primary stress consists of membrane stress σ_m and bending stress σ_b, due to imposed loading. Examples of secondary stresses include stress increase due to stress concentration imposed by geometry of the detail under consideration, thermal stress, and residual stress. For discontinuities at non-heat-treated welds, the residual tensile stress should be taken as the yield stress. An estimate of the residual stress should be used for post-heat-treated weldments. The applied stress is the sum of primary σ_p and secondary σ_s stresses. If the applied stress is greater than the yield stress, EPFM must be employed. If applied stress is less than the yield stress and the plane-strain factor $\beta_{Ic} \leq 0.4$ (Equation 2-2), LEFM should be used based on K_{Ic}. When the applied stress is less than the yield stress and $\beta_{Ic} > 0.4$, K_c (a function of plate thickness) should be used instead of K_{Ic}, if available. Otherwise, EPFM based on CTOD analysis must be employed.

Discontinuities	Criterion for interaction	Effective dimensions after interaction
1. Surface discontinuities	$s < \dfrac{\ell_1 + \ell_2}{2}$	$b = b_2$ $\ell = \ell_1 + \ell_2 + s$
2. Embedded discontinuities	$s < \dfrac{b_1 + b_2}{2}$	$b = b_1 + b_2 + s$ $\ell = \ell_2$
3. Embedded discontinuities	$s < \dfrac{\ell_1 + \ell_2}{2}$	$b = b_2$ $\ell = \ell_1 + \ell_2 + s$
4. Surface and embedded discontinuities	$s < \dfrac{b_1}{2} + b_2$	$b = b_1 + b_2 + s$ $\ell = \ell_1$
5. Embedded discontinuities	$s_1 < \dfrac{\ell_1 + \ell_2}{2}$ and $s_2 < \dfrac{b_1 + b_2}{2}$	$b = b_1 + b_2 + s_2$ $\ell = \ell_1 + \ell_2 + s_1$
6. Surface and embedded discontinuities	$s_1 < \dfrac{\ell_1 + \ell_2}{2}$ and $s_2 < b_1 + \dfrac{b_2}{2}$	$b = b_1 + b_2 + s_2$ $\ell = \ell_1 + \ell_2 + s_1$

Figure 6-5. Interaction of coplanar discontinuities (Extracts from British Standards Institution 1980. Complete copies of the standard can be obtained by post from BSI Publications, Linford Wood, Milton Keynes, MK14 6LE)

(4)   Determine material properties including yield strength σ_{ys}, modulus of elasticity E, K_{Ic} (based on the level of applied stress and the value of β_{Ic}), K_c, or CTOD. K_{Ic} may be estimated from Charpy V-Notch (CVN) test values by the transition method (paragraph 5-8) if direct K_{Ic} test data are not available.

(5)   Perform fracture assessment to determine the critical discontinuity size.

(6)   If the discontinuity is noncritical, determine the remaining life using a fatigue analysis as described in paragraphs 6-7 and 6-8.

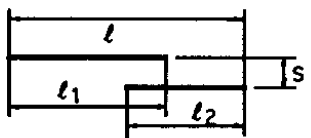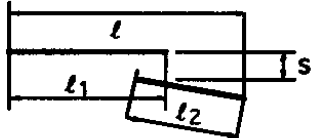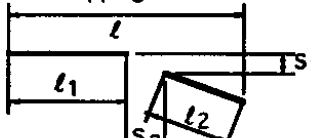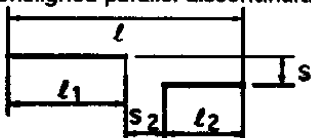These steps are further discussed in the following paragraphs.

Discontinuities	Criterion for interaction	Effective dimensions after interaction
1. Overlapping parallel discontinuities	$s < \dfrac{\ell_1 + \ell_2}{2}$	Length = ℓ
2. Overlapping discontinuities	$s < \dfrac{\ell_1 + \ell_2}{2}$	Length = ℓ
3. Nonoverlapping discontinuities	$s_1 < \dfrac{\ell_1 + \ell_2}{2}$ and $s_2 < \dfrac{\ell_1 + \ell_2}{2}$	Length = ℓ
4. Nonaligned parallel discontinuities	$s_1 < \dfrac{\ell_1 + \ell_2}{2}$ and $s_2 < \dfrac{\ell_1 + \ell_2}{2}$	Length = ℓ

Figure 6-6. Interaction of noncoplanar discontinuities (Extracts from British Standards Institution 1980. Complete copies of the standard can be obtained by post from BSI Publications, Linford Wood, Milton Keynes, MK14 6LE)
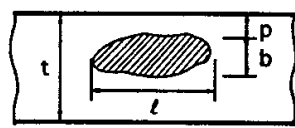
Discontinuities	Criterion for interaction	Effective dimensions after interaction
1. Embedded discontinuities	$\dfrac{p}{b} < 0.5$	Length = ℓ Height = b + p
2. Surface discontinuities	$\dfrac{b}{t} > 0.5$	Through thickness crack : length = ℓ

Figure 6-7. Interaction of discontinuities with surfaces (Extracts from British Standards Institution 1980. Complete copies of the standard can be obtained by post from BSI Publications, Linford Wood, Milton Keynes, MK14 6LE)
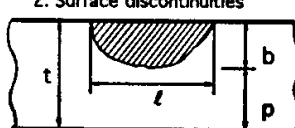
6-4. Linear-Elastic Fracture Mechanics

a.   Fundamental concepts of LEFM are described by Barsom and Rolfe (1987). LEFM is valid only under plane-strain conditions, when $\beta_{Ic} \leq 0.4$. The basic principle of LEFM is that incipient crack growth will occur when the stress-intensity factor K_I (the driving force) equals or exceeds the critical stress-intensity factor K_{Ic} (or K_{Id} for dynamic loading) (the resistance). For nonplane-strain cases, an initial evaluation based on an approximate analysis using LEFM with K_c taken as the resistance could be carried out.

b. K_I characterizes the stress field in front of the crack and is related to the nominal stress σ and crack dimension *a* for a given load rate and temperature by

$$K_I = C\sigma\sqrt{a} \tag{6-1}$$

where *C* is the dimensionless correction factor for a given geometry and loading type. If *C* is known, K_I can be computed for any combination of σ and *a*. Stress-intensity factors for various types of geometries can be calculated using the information included in Figures 6-8 through 6-16 (Barsom and Rolfe 1987). Barsom and Rolfe and Tada, Paris, and Irwin (1985) contain compilations of solutions for a wide variety of configurations.

c.   After the stress-intensity factor is determined by Equation 6-1, it should be compared to the critical stress-intensity factor K_{Ic} (or K_{Id} for dynamic loading, or K_c for approximated nonplane-strain cases). A factor of safety (FS) = 2.0 applied to crack length is considered appropriate to prevent fracture. Therefore, the crack is considered to be acceptable if $K_I < K_{ic}/\sqrt{2}$.

d. To determine the allowable maximum crack size or nominal stress for a given K_{Ic} (or K_{Id} or K_c), substitute K_{Ic} for K_I and solve for *a* or σ using Equation 6-1. The critical discontinuity size a_{cr} a structural member can tolerate at a given nominal stress σ and K_{Ic} with a factor of safety applied to the crack size is given by Equation 6-2:

$$a_{cr} = \frac{1}{FS}\left(\frac{K_{Ic}}{C\sigma}\right)^2 \tag{6-2}$$

e.   In determining the nominal stress when stress gradients are present, an approximate method is to linearize the stress distribution, and divide it into membrane stress σ_m and bending stress σ_b. The stress-intensity factor for each component of stress can be calculated separately and then added together. The total applied stress (σ_p and σ_s) can be linearized and resolved into σ_m and σ_b as shown in Figure 6-17.

6-5. Elastic-Plastic Fracture Assessment

Rearranging Equation 2-2, the upper limit of plane-strain behavior may be determined as

$$\frac{K_{Ic}}{\sigma_{ys}} = \sqrt{\frac{t}{2.5}} \tag{6-3}$$

When this upper limit is exceeded, extensive plastic deformation occurs at the crack tip (crack tip blunting) and a nonlinear EPFM model must be used for analysis. (LEFM analysis using K_c may be used if the applied stress is less than yield stress.) Crack growth criteria for nonlinear fractures can be modeled by an R-curve, J-integral, or CTOD analysis (Barsom and Rolfe 1987). The CTOD method is the recommended method of EPFM analysis for evaluating hydraulic steel structures. The recommended procedure for cases where the applied stress ($\sigma_p + \sigma_s$) is greater than the yield stress is as follows (British Standards Institution 1980).
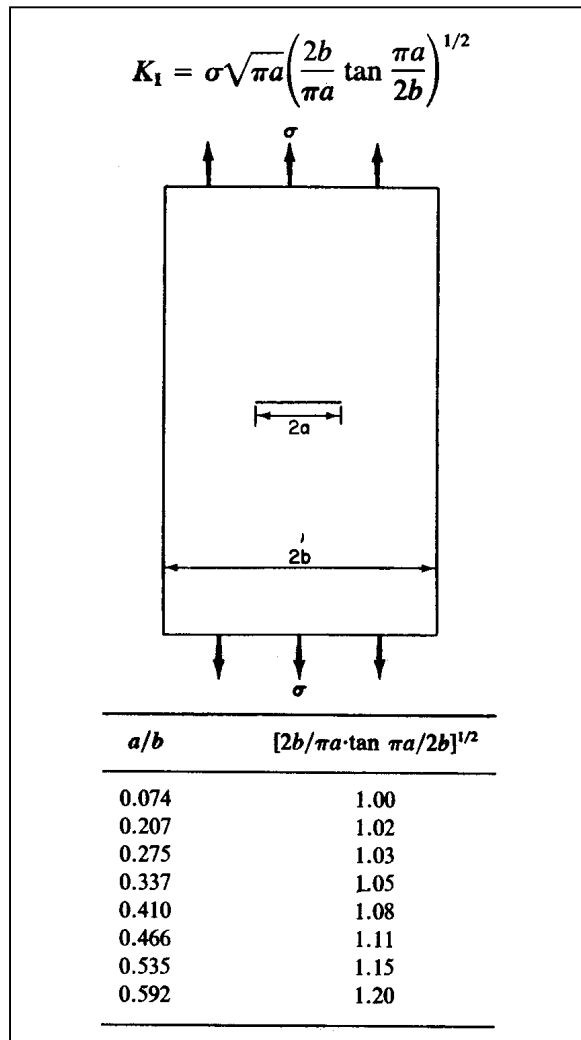
$$K_I = \sigma \sqrt{\pi a} \left(\frac{2b}{\pi a} \tan \frac{\pi a}{2b} \right)^{1/2}$$

a/b	$[2b/\pi a \cdot \tan \pi a/2b]^{1/2}$
0.074	1.00
0.207	1.02
0.275	1.03
0.337	1.05
0.410	1.08
0.466	1.11
0.535	1.15
0.592	1.20

Figure 6-8. Through-thickness crack (Barsom and Rolfe 1987, p 39. Reprinted by permission of Prentice-Hall, Inc., Englewood Cliffs, NJ.)

$$K_I = 1.12\sigma \sqrt{\pi a} \left(\frac{2b}{\pi a} \tan \frac{\pi a}{2b} \right)^{1/2}$$
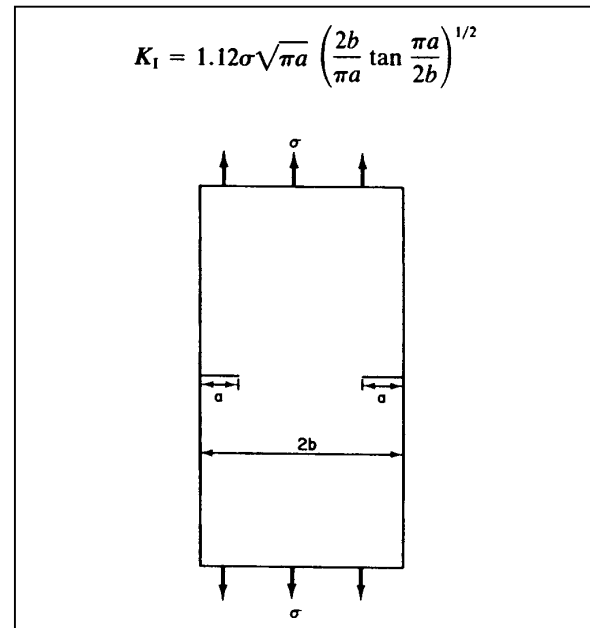
Figure 6-9. Double-edge crack (Barsom and Rolfe 1987, p 40. Reprinted by permission of Prentice-Hall, Inc., Englewood Cliffs, NJ.)

a. Determine the effective discontinuity parameter $\bar{a}$. This is the equivalent through-thickness dimension that would yield the same stress intensity as the actual discontinuities under the same load.

(1) For through-thickness discontinuities, $\bar{a} = \ell/2$, where ℓ is the measured crack length.

(2) For surface discontinuities, $\bar{a}$ is determined by Figure 6-18.

(3) For embedded discontinuities, $\bar{a}$ is determined by Figure 6-19.

b. Determine allowable discontinuity parameter $\bar{a}_m$ that is calculated by

$$\bar{a}_m = C \left[\frac{\delta_{crit}}{\varepsilon_y} \right] \tag{6-4}$$
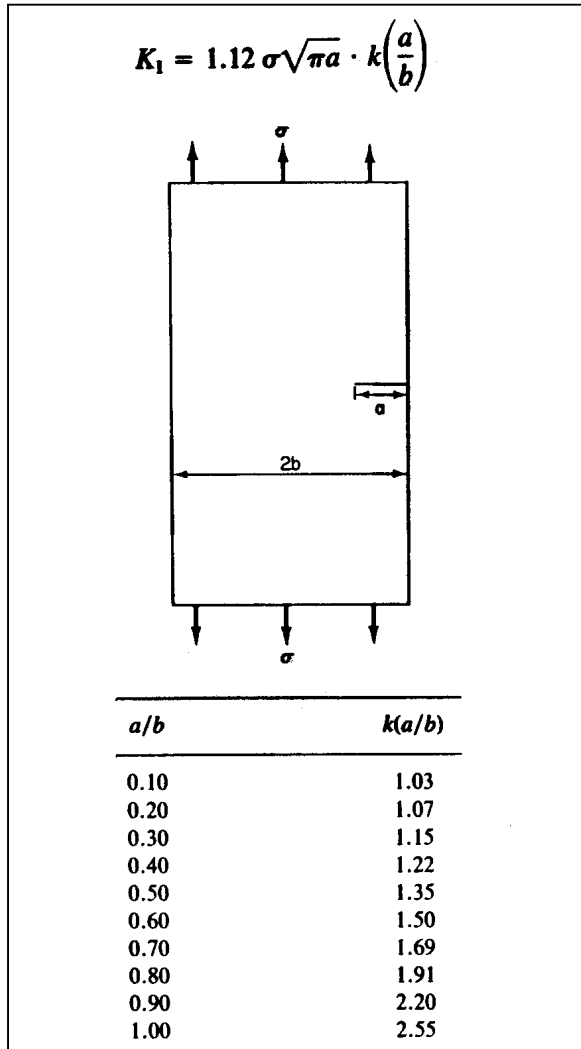
$$K_I = 1.12\,\sigma\sqrt{\pi a}\cdot k\!\left(\frac{a}{b}\right)$$

a/b	k(a/b)
0.10	1.03
0.20	1.07
0.30	1.15
0.40	1.22
0.50	1.35
0.60	1.50
0.70	1.69
0.80	1.91
0.90	2.20
1.00	2.55

Figure 6-10. Single-edge crack (Barsom and Rolfe 1987, p 40. Reprinted by permission of Prentice-Hall, Inc., Englewood Cliffs, NJ.)

$$K_I = \sigma\sqrt{\pi a}\cdot f\!\left(\frac{a}{r}\right)$$

$$K_I = f(a/r)\cdot\sigma\sqrt{\pi a}$$

a/r	f(a/r), ONE CRACK	f(a/r), TWO CRACKS
0.00	3.39	3.39
0.10	2.73	2.73
0.20	2.30	2.41
0.30	2.04	2.15
0.40	1.86	1.96
0.50	1.73	1.83
0.60	1.64	1.71
0.80	1.47	1.58
1.0	1.37	1.45
1.5	1.18	1.29
2.0	1.06	1.21
3.0	0.94	1.14
5.0	0.81	1.07
10.0	0.75	1.03
∞	0.707	1.00

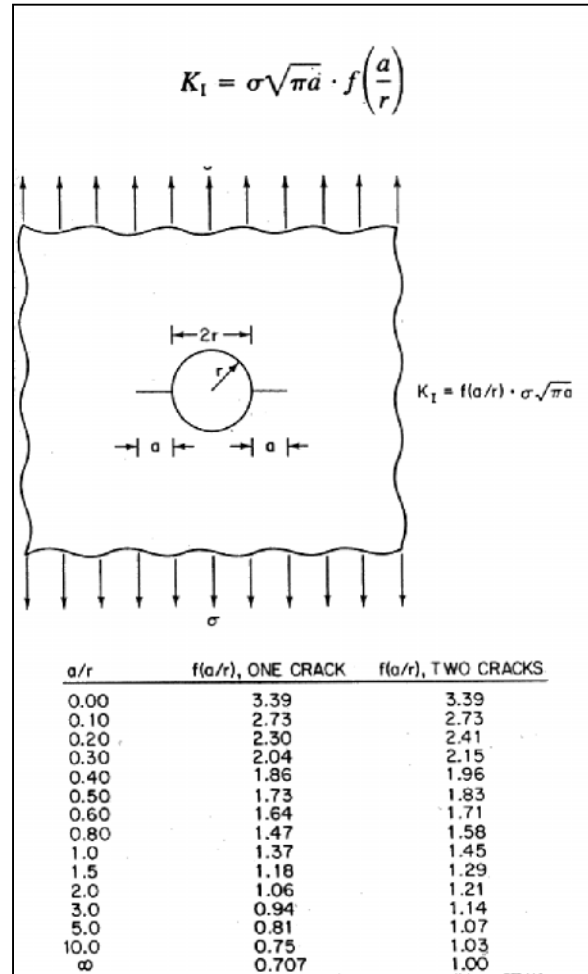**Figure 6-11. Cracks growing from round holes (Barsom and Rolfe 1987, p 42. Reprinted by permission of Prentice-Hall, Inc., Englewood Cliffs, NJ.)**

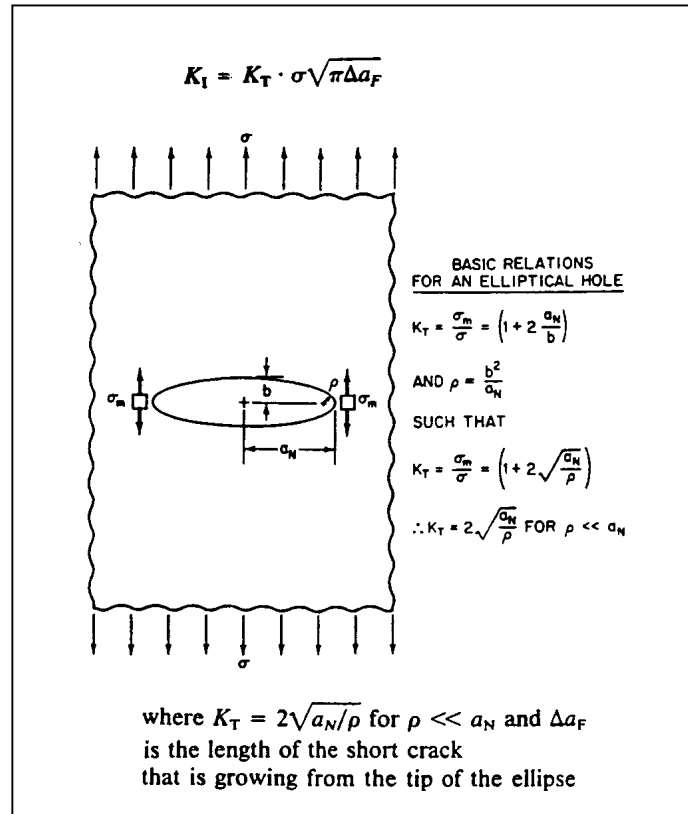where

C = values determined by Figure 6-20

δ_{crit} = critical CTOD (paragraph 5-8c)

ε_y = yield strain of the material

In determination of C, if the sum of primary and secondary stresses, excluding residual stress, is less than $2\sigma_{ys}$, the total stress ratio $(\sigma_p + \sigma_s)/\sigma_{ys}$ (including residual stress) is used as the abscissa in Figure 6-20. If this sum exceeds $2\sigma_{ys}$, an elastic-plastic stress analysis should be carried out to determine the maximum equivalent plastic strain that would occur in the region containing the discontinuity if the discontinuity were not present. The value of C may then be determined using the strain ratio $\varepsilon/\varepsilon_y$ as the abscissa in Figure 6-20.

$$K_I = K_T \cdot \sigma\sqrt{\pi\Delta a_F}$$

BASIC RELATIONS
FOR AN ELLIPTICAL HOLE

$$K_T = \frac{\sigma_m}{\sigma} = \left(1 + 2\frac{a_N}{b}\right)$$

$$\text{AND } \rho = \frac{b^2}{a_N}$$

SUCH THAT

$$K_T = \frac{\sigma_m}{\sigma} = \left(1 + 2\sqrt{\frac{a_N}{\rho}}\right)$$

$$\therefore K_T = 2\sqrt{\frac{a_N}{\rho}} \text{ FOR } \rho \ll a_N$$

where $K_T = 2\sqrt{a_N/\rho}$ for $\rho \ll a_N$ and Δa_F
is the length of the short crack
that is growing from the tip of the ellipse

Figure 6-12. Cracks growing from elliptical holes (Barsom
and Rolfe 1987, p 43. Reprinted by permission of Prentice-
Hall, Inc., Englewood Cliffs, NJ) where K_T = theoretical stress
concentration factor, a_N = half of the long dimension of the
ellipse, b = half of the short dimension of the ellipse, and
f = radius at the narrow end of the ellipse

$$K_I = \frac{6M}{B(W-a)^{3/2}} \cdot g\left(\frac{a}{W}\right)$$

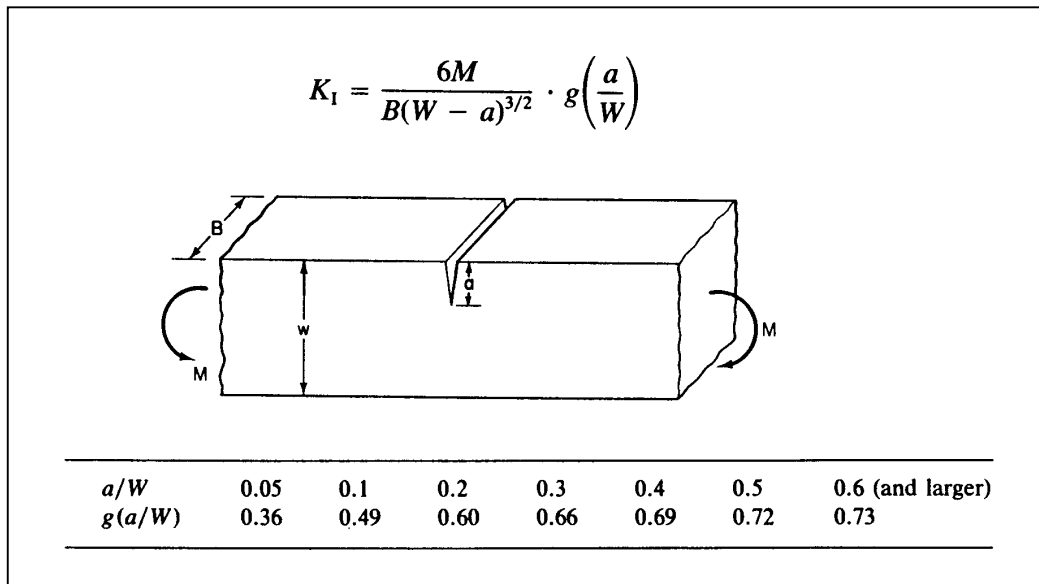| a/W	0.05	0.1	0.2	0.3	0.4	0.5	0.6 (and larger)
$g(a/W)$	0.36	0.49	0.60	0.66	0.69	0.72	0.73

Figure 6-13. Edge-notched beam in bending (Barsom and Rolfe 1987, p 45. Reprinted by
permission of Prentice-Hall, Inc., Englewood Cliffs, NJ) where M = bending moment per unit
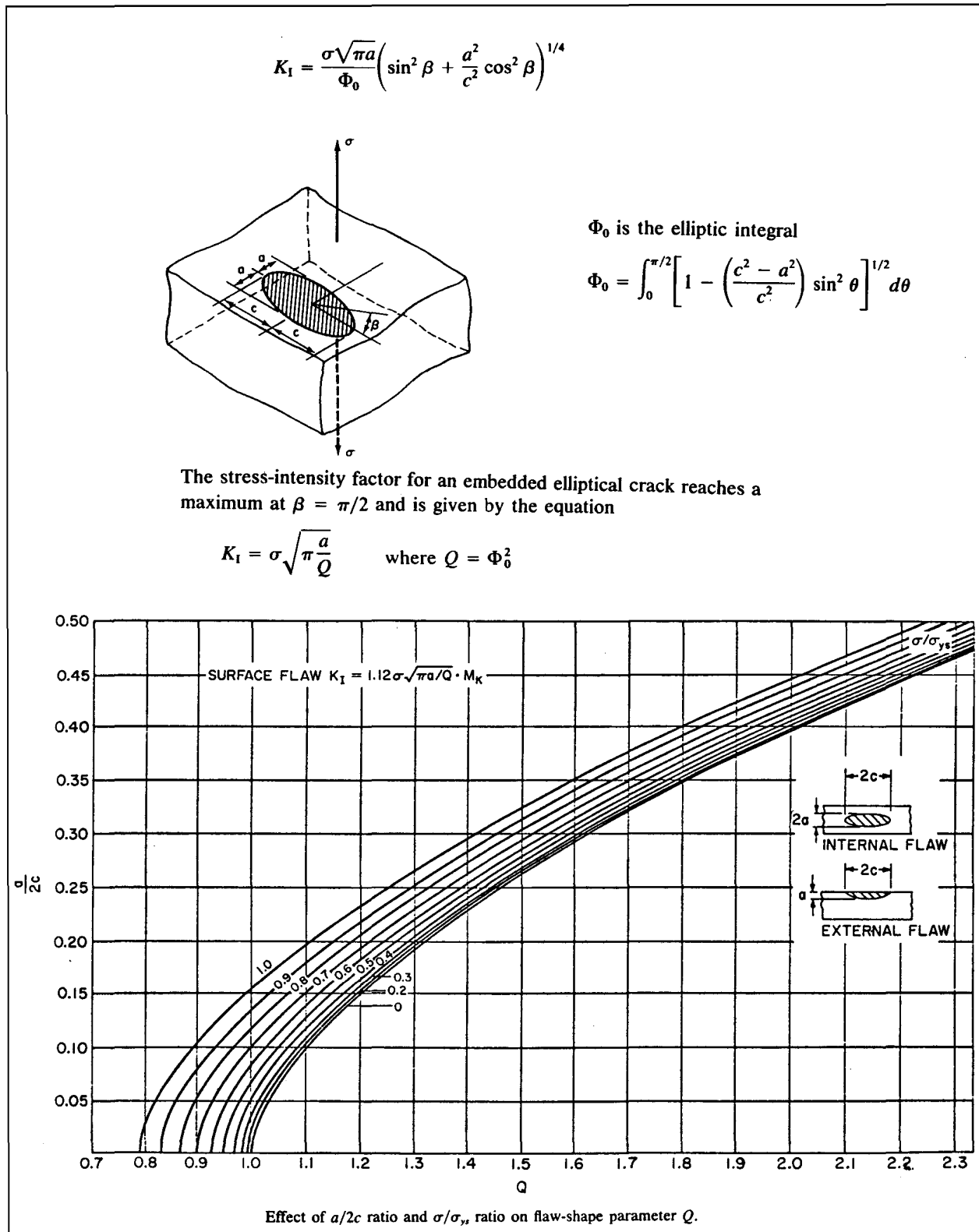thickness, B = beam width, W = beam depth, and g = function that describes effect of a/w on K_I

$$K_I = \frac{\sigma\sqrt{\pi a}}{\Phi_0}\left(\sin^2\beta + \frac{a^2}{c^2}\cos^2\beta\right)^{1/4}$$

Φ_0 is the elliptic integral

$$\Phi_0 = \int_0^{\pi/2}\left[1 - \left(\frac{c^2 - a^2}{c^2}\right)\sin^2\theta\right]^{1/2}d\theta$$

The stress-intensity factor for an embedded elliptical crack reaches a maximum at $\beta = \pi/2$ and is given by the equation

$$K_I = \sigma\sqrt{\pi\frac{a}{Q}} \qquad \text{where } Q = \Phi_0^2$$

SURFACE FLAW $K_I = 1.12\sigma\sqrt{\pi a/Q}\cdot M_K$

INTERNAL FLAW

EXTERNAL FLAW

Effect of $a/2c$ ratio and σ/σ_{ys} ratio on flaw-shape parameter Q.

Figure 6-14. Embedded elliptical or circular crack (Barsom and Rolfe 1987, p 47. Reprinted by permission of Prentice-Hall, Inc., Englewood Cliffs, NJ.)

$$K_1 = 1.12 \frac{\sigma\sqrt{\pi a}}{\Phi_0}\left(\sin^2\beta + \frac{a^2}{c^2}\cos^2\beta\right)^{1/4}$$

Φ_0 is the elliptic integral

$$\Phi_0 = \int_0^{\pi/2}\left[1 - \left(\frac{c^2 - a^2}{c^2}\right)\sin^2\theta\right]^{1/2}d\theta$$

The stress-intensity factor for $\beta = \pi/2$ (which is the location of maximum stress intensity) is given by

$$K_1 = 1.12\sigma\sqrt{\pi\frac{a}{Q}}\cdot M_K \qquad M_K = 1.0 + 1.2\left(\frac{a}{t} - 0.5\right) \qquad M_K = 1.0 \quad \text{if a/t} < 0.5$$

where $Q = \Phi_0^2$ and is presented graphically in Figure 6.14.

Figure 6-15. Surface crack (Barsom and Rolfe 1987, p 48. Reprinted by permission of Prentice-Hall, Inc., Englewood Cliffs, NJ.)

The stress-intensity factor for a crack that is subjected to eccentric line forces, P, per unit thickness, on its surfaces is given by

$$K_{I@1} = \frac{P}{\sqrt{\pi a}}\left(\frac{a + x}{a - x}\right)^{1/2}$$

$$K_{I@2} = \frac{P}{\sqrt{\pi a}}\left(\frac{a - x}{a + x}\right)^{1/2}$$

For centrally applied point forces, namely, $x = 0$,

$$K_{I@1} = K_{I@2} = \frac{P}{\sqrt{\pi a}}$$

Figure 6-16. Cracks with wedge forces (Barsom and Rolfe 1987, p 52. Reprinted by permission of Prentice-Hall, Inc., Englewood Cliffs, NJ.)

a) Surface defects   b) Embedded defects

Membrane stress : $\sigma_m = \dfrac{\sigma_1 + \sigma_2}{2}$ Bending stress : $\sigma_b = \dfrac{\sigma_1 - \sigma_2}{2}$

Figure 6-17. Linearization of stresses (Extracts from British Standards Institution 1980. Complete copies of the standard can be obtained by post from BSI Publications, Linford Wood, Milton Keynes, MK14 6LE)

c. If the effective discontinuity parameter $\bar{a}$ is smaller than the allowable discontinuity parameter $\bar{a}_m$, then the discontinuity is acceptable. Using the procedure described in *b* above results in a factor of safety equal to approximately 2.0 in the determination of $\bar{a}_m$; Figure 6-20 was developed as a design curve. Therefore, the calculated critical crack size would be equal to 2.0 $\bar{a}_m$ (British Standards Institution 1980).

6-6. Fatigue Analysis

a. For most lock gates and spillway gates that have vibration problems, fatigue loading is a real concern and a fatigue evaluation may be required. Fatigue analysis is used to predict when the cyclic loading will cause a crack to propagate to critical size resulting in fracture. A fatigue analysis can also provide crack growth rates that are useful in determining inspection intervals.

b. The total fatigue life is the sum of the fatigue crack-initiation life and the fatigue crack-propagation life to a critical size (Barsom and Rolfe 1987).

$$N_T = N_i + N_p \tag{6-5}$$

where

N_T = total fatigue life

N_I = initiation life

N_p = propagation life

Figure 6-18. Relation between dimensions of a discontinuity and the parameter $\bar{a}$ for surface discontinuities. (Extracts from British Standards Institution 1980. Complete copies of the standard can be obtained by post from BSI Publications, Linford Wood, Milton Keynes, MK14 6LE)

c. All steels have microscopic discontinuities, and welded structures always contain larger discontinuities due to the welding process. Thus, the main concern in fatigue assessment of welded structures is to determine the crack-propagation life before the critical crack size is reached that results in brittle fracture. The life of a structural component that contains a crack is governed by the rate of subcritical crack propagation.

d. Fatigue analysis methods described in paragraphs 6-7 and 6-8 are based on extensive analyses of test results from numerous specimens. Variation in test data is large, and inherent uncertainty exists in defining load and strength parameters. Therefore, fatigue life predictions should be used as a means to evaluate a reliable service life, not to actually predict when a structure will fail. Fatigue analysis is needed when the remaining structure life and the crack growth rate are necessary for developing the inspection and maintenance scheduling for a distressed structure as discussed in paragraph 6-11. An example of the estimation of fatigue life from S_r-N curves for a gate with a vibration problem is given in Chapter 7.

6-7. Fatigue Crack-Propagation

The fatigue crack-propagation behavior for metals is shown in Figure 6-21. Figure 6-21 is a plot ($\log_{10}$ scale) of the rate of fatigue crack growth per cycle of load da/dN versus the variation of the stress-intensity factor ΔK_I. The parameter a denotes crack length, N the number of cycles, and ΔK_I the stress-intensity factor range, $K_{I\max}$ to $K_{I\min}$. Based on Figure 6-21, fatigue-crack behavior for steel can be characterized by three regions. Barsom and Rolfe (1987) describe these regions in more detail.
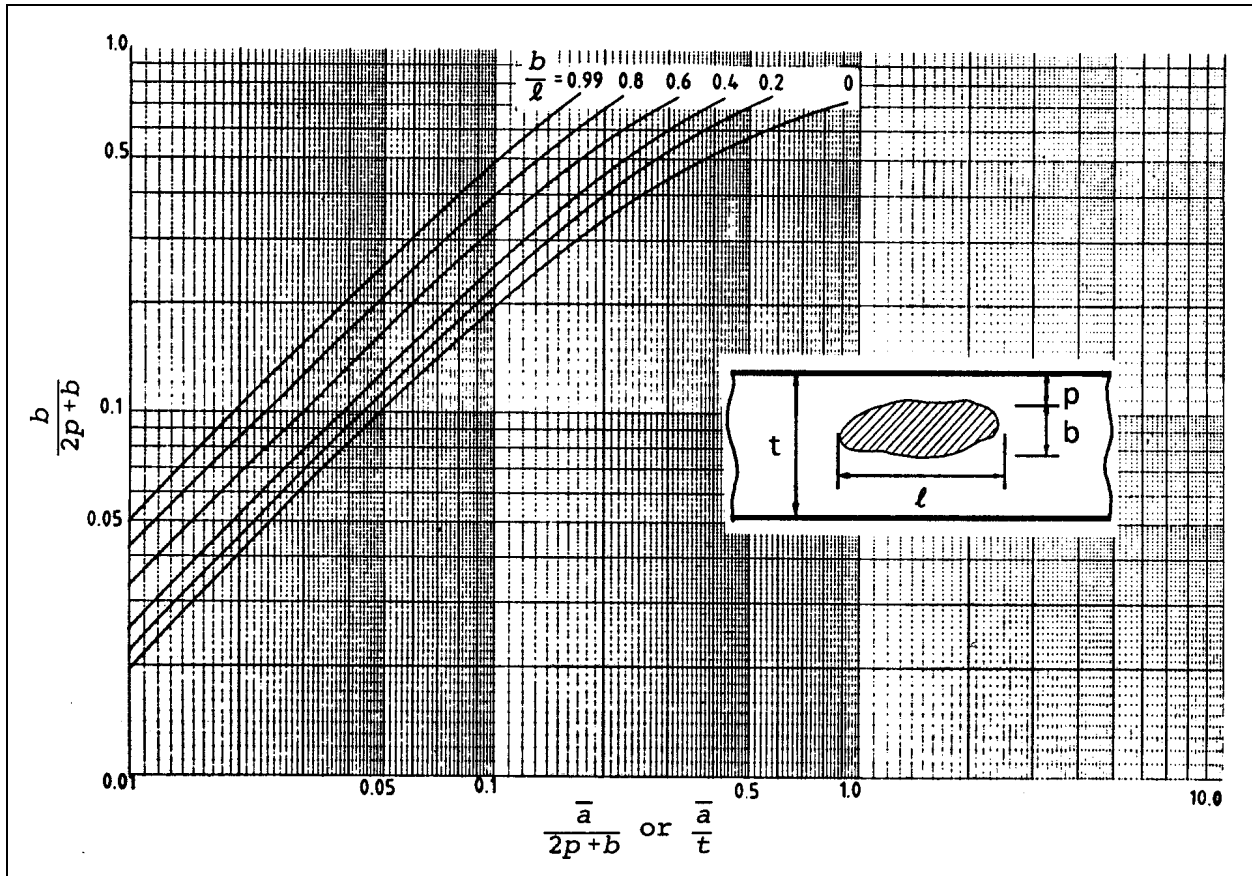
Figure 6-19. Relation between dimensions of a discontinuity and the parameter $\bar{a}$ for embedded discontinuities (Extracts from British Standards Institution 1980. Complete copies of the standard can be obtained by post from BSI Publications, Linford Wood, Milton Keynes, MK14 6LE)

a.   *Region I.* In Region I, for levels of ΔK_I below a certain threshold, cracks do not propagate under cyclic stress fluctuations. Conservative estimates of fatigue threshold, ΔK_{th}, can be determined by

$$\Delta K_{th} = 7 \, (1 - 0.85R) \text{ MPa-}\sqrt{m} \quad (6.4 \, (1 - 0.85R) \text{ ksi-}\sqrt{\text{in.}} \,) \text{ for } R > 0.1$$
$$\Delta K_{th} = 6 \text{ MPa-}\sqrt{m} \quad (5.5 \text{ ksi-}\sqrt{\text{in.}} \,) \text{ for } R < 0.1 \tag{6-6}$$

where R is the stress ratio (i.e., fatigue ratio) expressed as

$$R = \sigma_{min} / \sigma_{max} \tag{6-7}$$

Residual stress should be considered for a crack near a weld area. If ΔK_I is less than ΔK_{th}, cracks do not propagate.

b.   *Region II.* The fatigue crack-propagation behavior for $\Delta K_I > \Delta K_{th}$ in Region II (i.e., linear portion of the plot in Figure 6-21) may be represented by Equations 6-8 and 6-9. These equations were based on analyses in air at room temperature. Extensive fatigue-crack growth rate data for weld metals and heat-affected zones show that the fatigue rate in weld metals and heat-affected zones is equal to or less than that in the base metals. Thus, Equations 6-8 and 6-9 can also be used for conservative estimates of fatigue-crack growth rates in base metals, weld metals, and heat-affected zones.
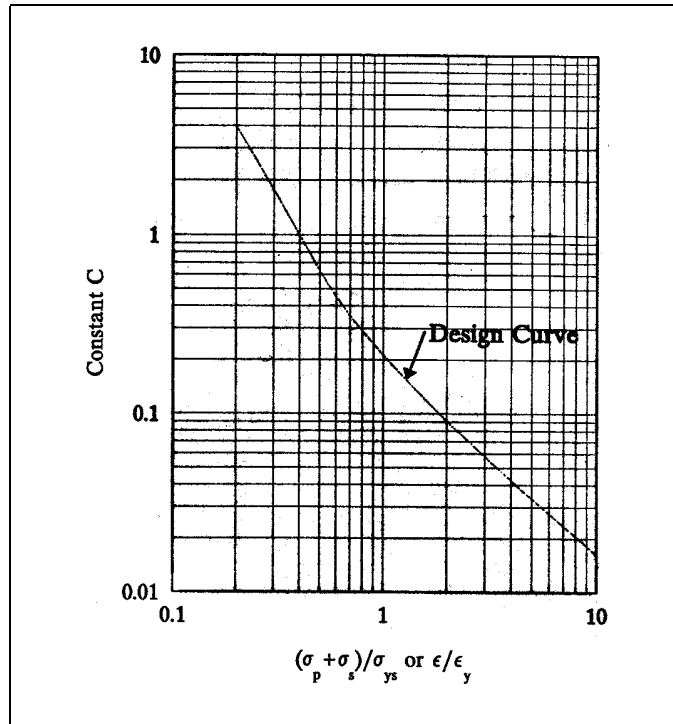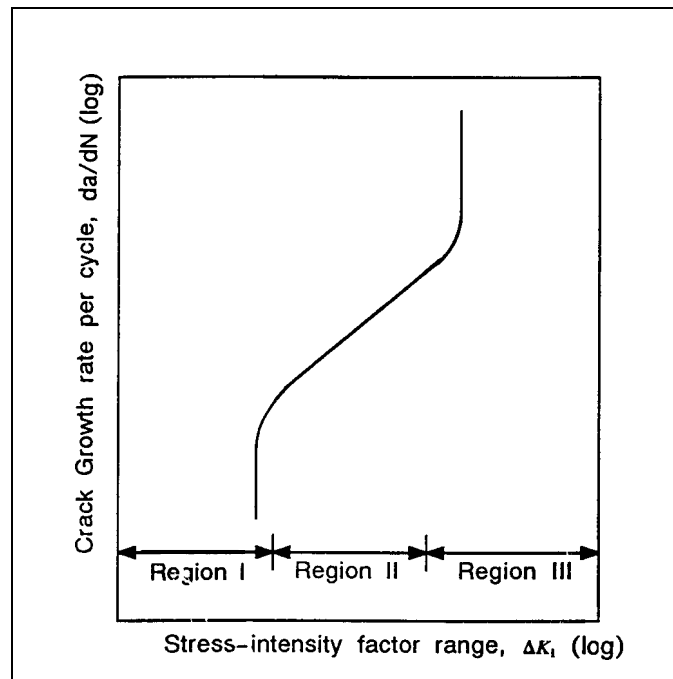
Figure 6-20. Values of constant *C* for different loading conditions (Extracts from British Standards Institution 1980. Complete copies of the standard can be obtained by post from BSI Publications, Linford Wood, Milton Keynes, MK14 6LE)

Figure 6-21. Fatigue-crack growth in steel

(1) Ferrite-pearlite steels. ASTM A36M-97 and ASTM A572/572M Grade 50 steels are classified as ferrite-pearlite steels:

$$da/dN = 6.9 \times 10^{-9} (\Delta K_I)^3 \tag{6-8}$$

where

a = mm
ΔK_I = MPa-$\sqrt{m}$

(For non-SI units, $da/dN = 3.6 \times 10^{-10} (\Delta K_I)^3$ where a = in. and ΔK_I = ksi-$\sqrt{in.}$)

(2) Martensitic steels. ASTM A514/A514M and ASTM A517/517M steels are martensitic steels:

$$da/dN = 1.35 \times 10^{-7} (\Delta K_I)^{2.25} \tag{6-9}$$

where

a = mm
ΔK_I = MPa-$\sqrt{m}$

(For non-SI units, $da/dN = 0.66 \times 10^{-8} (\Delta K_I)^{2.25}$ where a = in. and ΔK_I = ksi-$\sqrt{in.}$)

c. Region III. Region III is characterized by a significant increase in the fatigue-crack growth rate per cycle over that predicted for Region II. At a certain value of ΔK_I, the crack growth rate accelerates dramatically. For materials of high fracture toughness, the stress-intensity factor range value corresponding to acceleration in the fatigue-crack growth rate (i.e., transition from Region II to Region III) for zero to tension loading can be determined by Equation 6-10:

$$K_T = 0.0063 (E \sigma_{ys})^{1/2} \tag{6-10}$$

where

K_T = MPa-$\sqrt{m}$
E, σ_{ys} = MPa

(For non-SI units, $K_T = 0.04 (E \sigma_{ys})^{1/2}$ where K_T = ksi-$\sqrt{in.}$, and E and σ_{ys} = ksi.)

When the K_{Ic} of the material is less than K_T, acceleration in the fatigue rate occurs at a stress-intensity factor value slightly below K_{Ic}. Due to the acceleration in crack growth rate, a significant increase in fracture toughness of a steel above K_T may have a negligible effect on total fatigue life. Additionally, extrapolation of Region II behavior to Region III may overestimate the total fatigue life significantly.

6-8. Fatigue Assessment Procedures

a. Region II fatigue analysis with known discontinuities. The procedure to analyze Region II crack growth behavior in steels and weld metals using fracture mechanics concepts as recommended by Barsom and Rolfe (1987) is as follows.

(1) On the basis of the inspection data, determine the maximum initial discontinuity size a_o present in the member being analyzed and the associated K_I.

(2) Knowing K_{Ic} and the nominal maximum design stress, calculate the critical discontinuity size a_{cr} (Equation 6-2) that would cause failure by brittle fracture.

(3) Determine fatigue crack growth rate for type of steel (Equations 6-8 and 6-9 for ferrite-pearlite or martensitic steel, respectively).

(4) Determine ΔK_I using the appropriate expression for K_I, the estimated initial discontinuity size a_o, and the range of live load stress S_r (i.e., cyclic stress range). For cases of variable amplitude loading, an equivalent constant amplitude stress range, S_{re} should be computed as described in paragraph 2-3e. A live load stress range S_r, which is due to cyclic compression stresses, may be detrimental in regions where tensile residual stress exists. In these regions, cracks may propagate, since the addition of tensile residual stresses will result in an applied stress range of tension and compression. The stress range, S_r, used to determine fatigue life should be calculated from the algebraic difference of the maximum and minimum stresses even when the minimum stress is compression and has a negative value, since any tensile residual stresses will be superimposed on the applied cyclic stress (American Association of State Highway and Transportation Officials 1996; American Institute of Steel Construction 1994; EM 1110-2-2105).

(5) Integrate the crack growth rate expression (i.e., Equations 6-8 and 6-9) between the limits of a_o (at the initial K_I) and a_{cr} (at K_{Ic}) to obtain the life of the structure prior to failure. To identify inspection intervals, integration may be applied with the upper limit being tolerable discontinuity size a_t. An arbitrary safety factor based on analysis uncertainties may be applied to a_{cr} to obtain a_t (a factor of safety of 2.0 is recommended). Another consideration for specifying a tolerable discontinuity size is crack growth rate. The a_t should be chosen so that da/dN is relatively small and a reasonable length of time remains before the critical size is reached.

(6) For a determination of a_o:

(a) See Figure 6-3a for through-thickness discontinuities.

(b) For embedded discontinuities (Figure 6-3b), assume that the discontinuity grows until it reaches a circular shape (b = ℓ/2). Subsequently, it grows radially and eventually protrudes through a surface at which time it should be treated as a surface discontinuity of length ℓ.

(c) See Figure 6-3c for surface discontinuities. Initial propagation will result in a semicircular shape. Further propagation will result in the discontinuity reaching the other surface at which time it should be treated as a through-thickness discontinuity.

b. Fatigue strength evaluation without known discontinuities.

(1) Welded details. The fatigue life of welded details that do not include known discontinuities shall be determined as described in Chapters 2 and 3.

(2) Riveted details. The following fatigue strength criteria for undamaged and noncorroded riveted details are recommended:

(a) When $S_{rm} \leq 41.4$ MPa (6 ksi), where S_{rm} is the maximum stress range, the possibility of fatigue damage can be ignored.

(b) When $S_{re} < 68.9$ MPa (10 ksi), where S_{re} is the equivalent constant-amplitude stress range, use Category C and S_{re} to characterize the fatigue strength and life of the riveted member detail.

(c) When $S_{re} \geq 68.9$ MPa (10 ksi), use Category D and S_{re} to characterize the fatigue strength and life of the riveted member detail. For constant-amplitude loading, both S_{rm} and S_{re} are equivalent to S_r. This recommended S_r-N curve is illustrated in Figure 6-22.
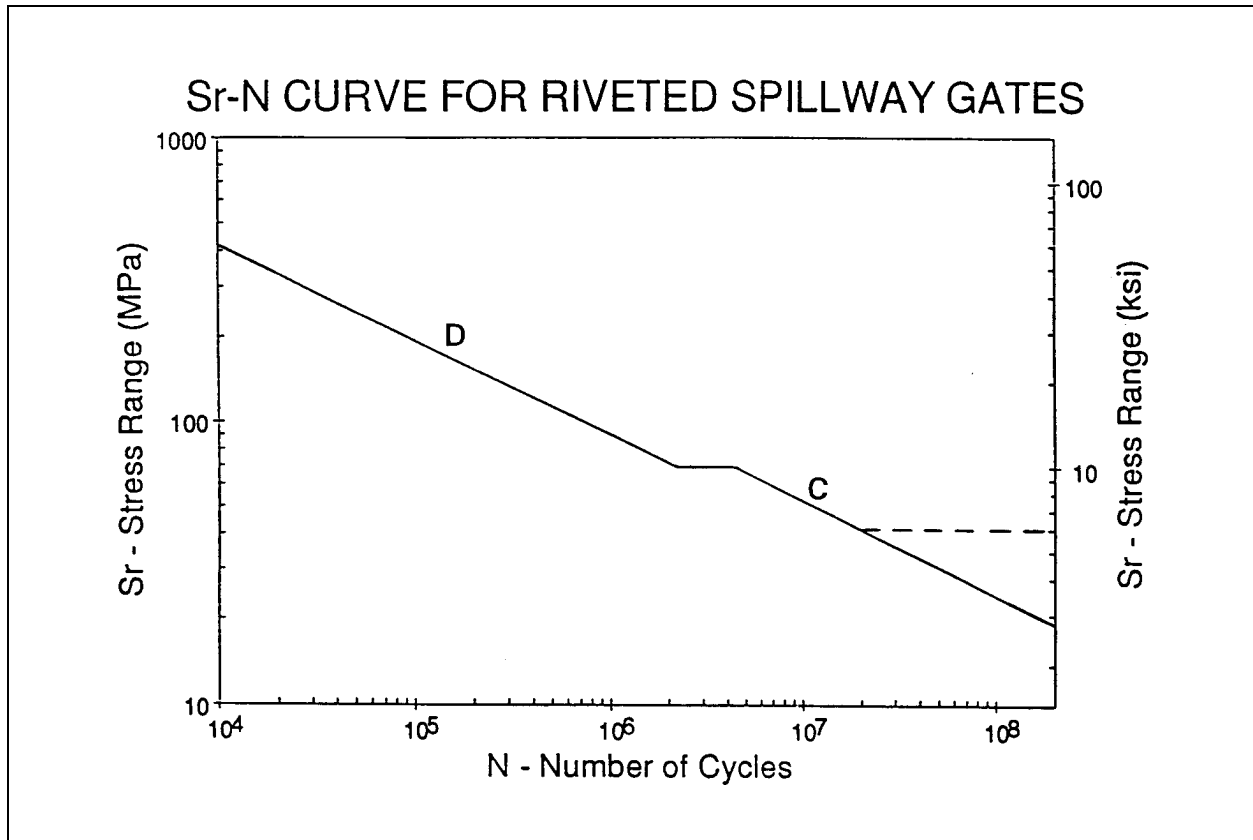

Figure 6-22. Recommended *S_r-N* curve for riveted gates

For severely corroded members or members with corroded, loose, or missing rivets where the clamping force is reduced or lost, lower fatigue strength curves may be more appropriate. Specifically, it is suggested that the Category E or E' curves and the corresponding fatigue limits should be used if corrosion notches are present (Chapter 2). As shown by Figure 2-5, fatigue cracks may initiate at corrosion notches instead of from rivet holes.

6-9. Evaluation of Corrosion Damage

Traditional member/frame structural analysis or even finite element methods can be used to evaluate the effect of reduction in sections from corrosion damage. To perform such an analysis, the extent of corrosion damage must be defined by reduction of appropriate section properties or thicknesses in the affected members. This should include consideration of the reduced thicknesses and change in relative proportions of the member. For example, depending on the location of the corrosion, the shear strength of a flexural member may be more affected than the flexural strength. Analysis of the complete structure incorporating the reduced sections may be warranted if the corrosion is severe and/or widespread.

6-10. Evaluation of Plastically Deformed Members

The effect of buckled or plastically deformed members can be characterized by a reduction in strength and stiffness. To assess the damage, an analysis should be performed that models the damage condition. This may simply be a frame analysis that incorporates the out-of-straightness of a crooked member or a local reduction of cross-sectional properties to model a locally buckled flange. In more significant cases of damage, a two- or three-dimensional model with the damaged locations represented as a hinge or with a damaged member being considered removed may be more appropriate.

6-11. Development of Inspection Schedules

Inspection schedules can be developed from crack length versus fatigue life curves. Figure 6-23 shows a typical crack length-fatigue life (a-N) curve, which can be obtained from Equation 6-8 or 6-9. Critical crack length is determined based on K_{Ic} and maximum design stress as discussed in paragraph 6-8. The time when repair is needed can be determined considering an appropriate factor of safety (2.0 is recommended), i.e., $a_r = a_{cr}/(FS)$. Remaining loading cycles before repair are then determined from a_i and a_r using an a-N curve as shown in Figure 6-23. Inspection intervals for a structure can be determined from the remaining fatigue life of the members (Pennsylvania Department of Transportation 1988).
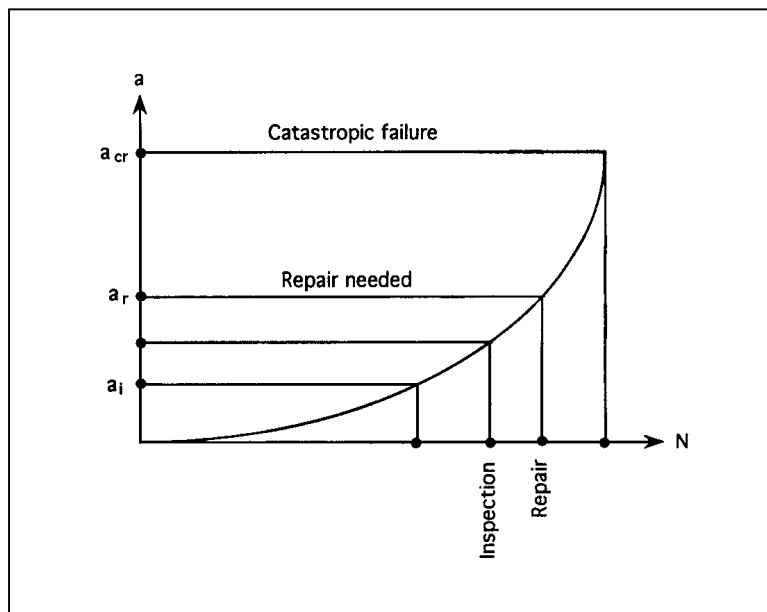

Figure 6-23. Development of maintenance schedule

6-12. Recommended Solutions for Distressed Structures

a.   If a thorough evaluation of the hydraulic steel structure reveals no evidence of distress, damage, or potential failure, it should be reinspected in accordance with the inspection intervals specified in ER 1110-2-100. However, if significant deficient conditions exist (e.g., heavy corrosion, fatigue cracks, or deformations) or severe operations occur (e.g., persistent vibrations), it may be appropriate to repair and/or recommend a shorter inspection interval to ensure the structural and operational integrity of the structure. Solutions to the cracking problems can be addressed in short-term or long-term solutions. A quick solution might involve repair of fractured members using qualified welding procedures and improved fatigue details or bolted cover plates. A long-term solution would involve detailed inspection and evaluation of the critical members and connections

using procedures discussed in this EM to assist in determining a more permanent solution. Repair procedures are discussed in Chapter 8, and recommended inspection intervals may be computed using fatigue principles as described in paragraph 6-11. The inspection intervals shall correspond to a crack size less than one-half of the critical crack length (i.e., employ a factor of safety equal to at least 2.0).

b.   In determining the recommended action for a distressed hydraulic steel structure, the redundancy of the damaged members or connections should be considered. Obviously cracks or severe corrosion in nonredundant components should be more carefully considered. Because the conditions at each site are unique, proposing a general guideline for selecting shorter inspection intervals would be difficult. Detrimental conditions should be evaluated on a case-by-case basis using appropriate analytical tools.

c.   A comprehensive maintenance and inspection program can reduce the occurrence of significant structural distress. Through a regularly scheduled cleaning and painting program, the effects of corrosion can be controlled, and by removing debris and lubricating all mechanical components, the potential overloads from lifting operations can be minimized.

Chapter 7
Examples and Material Standards

7-1. Determination of Fracture Toughness

a. General.

(1) In any linear-elastic fracture mechanics analysis, the fracture toughness, either the critical plane stress intensity factor K_{Ic} or the critical stress intensity factor K_c of the structural component must be determined. For most component geometries (thicknesses), the fracture toughness will be defined by the critical plane-stress stress intensity factor K_c. However, the critical plane-strain stress intensity factor K_{Ic} is a material property and is a lower bound for K_c.

(2) The fracture toughness (K_{Ic} or K_c) of steel increases with increasing temperature and decreasing load rate. Mild structural steels typically exhibit a relatively large increase in toughness over a certain temperature range as shown in Figure 7-1. The fracture toughness versus temperature relationship can be divided into three regions: the lower shelf region, which is characterized by relatively low toughness and small variation in toughness with temperature; the transition region, which is characterized by rapid increase of toughness with increasing temperature; and the upper shelf region, where the variation in toughness with temperature is again relatively low.
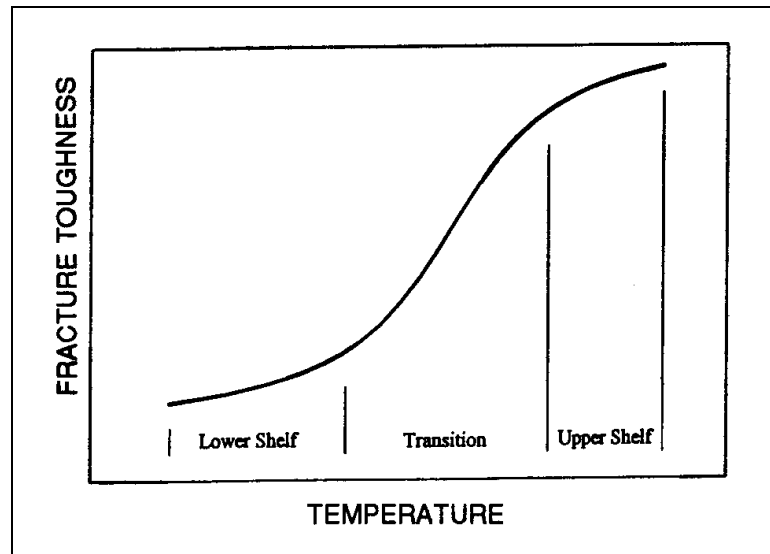

Figure 7-1. Temperature effects on fracture toughness

(3) The effect of load rate on fracture toughness is shown in Figure 7-2, which illustrates the nature of the fracture toughness versus temperature relationship for static and dynamic loading. The general shape of the temperature versus fracture toughness relationship is maintained for various loading rates. For increasing load rates, the transition region occurs at higher temperatures. (Intermediate load rate curves would lie between the static and dynamic curves shown in Figure 7-2.) For a given magnitude of fracture toughness, a temperature shift exists between fracture toughness for dynamic loading, K_{Id}, and that for slow loading rate, K_{Ic}. This empirically derived temperature shift T_s is given by Equation 7-1 (Barsom and Rolfe 1987):

$$T_s = 102 - 0.12 \, \sigma_y \, °C, \text{ for } 250 \text{ MPa} < \sigma_y < 965 \text{ MPa}$$
$$T_s = 0, \qquad \text{for } \sigma_y > 965 \text{ MPa} \tag{7-1}$$

where σ_y is the yield stress.

(For non-SI units $T_s = 215 - 1.5\ \sigma_y$ °F, for 36 ksi $< \sigma_y <$ 140 ksi, and $T_s = 0$ for $\sigma_y >$ 140 ksi.)
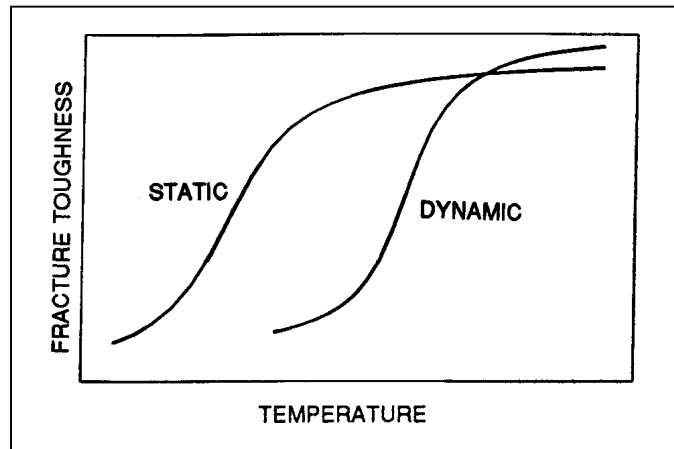

Figure 7-2. Load rate effect on toughness

  b.   Plane-strain fracture toughness.

   (1)   As described in Chapter 5, the plane-strain fracture toughness K_{Ic} is defined by ASTM E399. Unfortunately, for almost all low- to medium-strength structural steels, it is impractical if not impossible to directly determine K_{Ic} at reasonable service temperatures. One of the more common approaches to this problem has been to correlate K_{Ic} with results from other mechanical tests, most notably Charpy V-Notch (CVN).   One of the commonly used correlations between CVN and K_{Ic} is the two-stage CVN-K_{Id}-K_{Ic} correlation (Barsom and Rolfe 1987). The procedure for this is as follows:

   (a)   Determine standard impact CVN test results in the transition temperature region. (It is desirable to test at temperatures approximately T_s above the expected minimum service temperature T_o.)

   (b)   Convert CVN data to K_{Id} values based on the empirical relationship

$$K_{Id} = \sqrt{0.64 \bullet \mathrm{CVN} \bullet E} \quad \mathrm{kPa} - \sqrt{\mathrm{m}} \tag{7-2}$$

where

   CVN = Charpy V-Notch value at the given temperature, joules
      E = modulus of elasticity, kPa

(For non-SI units $K_{Id} = \sqrt{5 \bullet \mathrm{CVN} \bullet E}$ psi $- \sqrt{\mathrm{in.}}$, where CVN = ft-lb and E = psi.)

   (c)   Shift the K_{Id} values at each temperature by T_s (Equation 7-1) to determine the K_{Ic} values as a function of desired minimum service temperature: $K_{Ic}(T_o) = K_{Id}(T_o + T_s)$.

   (2)   The procedure for the CVN-K_{Id}-K_{Ic} correlation is illustrated in Figure 7-3. This correlation is valid only for the lower shelf region and the lower end of the transition region of the CVN curve, which limits its use for structural steels at practical service temperatures. Barsom and Rolfe (1987) have suggested that this correlation is valid for CVN values in foot-pounds that are less than one-half the yield strength in ksi.
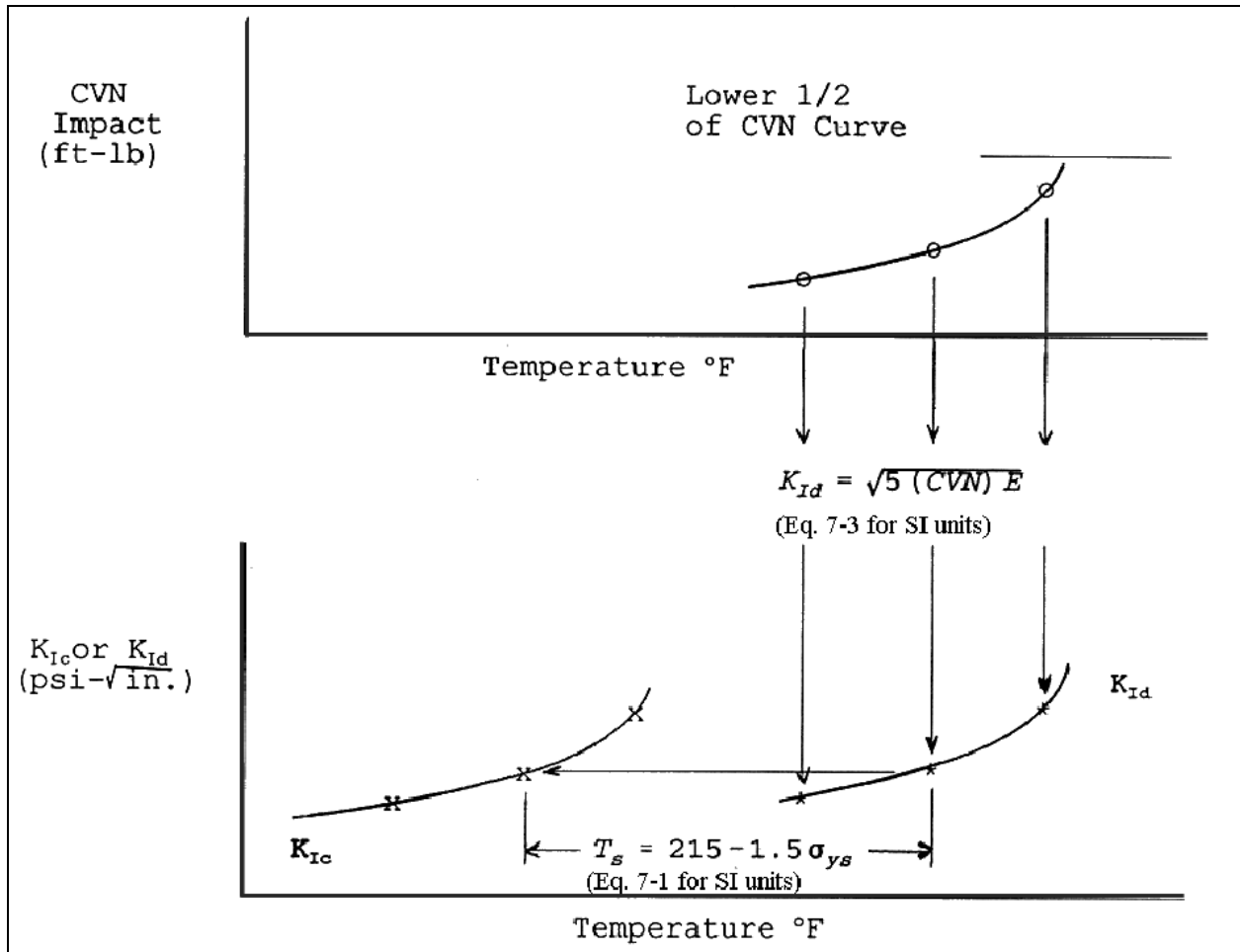
Figure 7-3. Two-stage CVN-K_{Id}-K_{Ic} correlation (°C = 5/9 (°F − 32); 1 psi-$\sqrt{\text{in.}}$ = 1.099 kPa-$\sqrt{\text{m}}$; 1 ft-lb = 1.36 J)

(3)   A CVN-K_{Ic} correlation that is valid at higher temperatures in the upper shelf region is given by

$$\left(\frac{K_{Ic}}{\sigma_y}\right)^2 = 0.646 \left(\frac{\text{CVN}}{\sigma_y} - 0.0098\right) \tag{7-3}$$

where

$K_{Ic} = \text{MPa} - \sqrt{\text{m}}$

σ_y = static yield stress in MPa

CVN = joules

(For non-SI units,

$$\left(\frac{K_{Ic}}{\sigma_y}\right)^2 = 5 \left(\frac{\text{CVN}}{\sigma_y} - 0.05\right)$$

where K_{Ic} = ksi - $\sqrt{in}$., σ_y = ksi, and CVN = ft-lb.)

(4) These two correlations provide estimates for the upper and lower shelf regions (Figure 7-1). K_{Ic} in the transition region can be estimated by interpolation.

c. Plane-stress fracture toughness. In most applications, the component or member will have insufficient thickness for plane-strain behavior. While this is generally a positive consequence since deviation from plane-strain conditions provides increasing resistance to fracture, the fracture toughness is no longer represented by K_{Ic} (except as a lower bound). The thickness required for plane-strain conditions is indicated by rearrangement of Equation 2-2:

$$t \geq 2.5 \left(\frac{K_{Ic}}{\sigma_y} \right)^2 \tag{7-4}$$

If this thickness requirement is not met, then the fracture toughness is represented by the plane-stress fracture toughness K_c, which can be estimated by various methods such as correlations with R-curve or crack tip opening displacement (CTOD) test data (Barsom and Rolfe 1987). The correlation between CTOD test data and K_c is given by

$$K_c = \sqrt{1.4\,E\,\frac{\sigma_y + \sigma_{ult}}{2}\,\delta_c} \tag{7-5}$$

where

σ_{ult} = yield and ultimate stress

δ_c = critical crack tip opening displacement as determined in accordance with ASTM E1290.

Alternatively, if the thickness is such that the plane-strain condition is nearly satisfied, K_c can be estimated by

$$K_{Ic}^2 = K_{Ic}^2 \left(1 + 1.4\,\beta_{Ic}^2 \right) \tag{7-6}$$

where β_{Ic} is given by Equation 2-2.

7-2. Example Fracture Analysis

This paragraph includes three example problems. The example in *a* below demonstrates the proposed guidelines for conducting an overall structural evaluation of a spillway gate. The example given in *c* below specifically illustrates the evaluation of a cracked member. The example in *d* below pertains to a fracture analysis on two tension members of a lock gate.

a. Spillway gate evaluation example. This case study is based on the results of an inspection of the riveted tainter gates at Lock and Dam 5 on the upper Mississippi River near Winona, MN. A supplemental example in *b* below is also included to illustrate a fatigue evaluation and is based on a hypothetical inspection report that indicates significant cyclic stresses have been measured in the gate. Although this example is based on a riveted spillway gate, the process illustrated is applicable to welded and riveted hydraulic steel structures.

(1) Preinspection assessment. The design documents and previous inspection reports were reviewed, critical areas were identified, and previously reported conditions noted. The tainter gates are 10.7 m (35 ft) wide, 4.57 m (15 ft) high, and 7.62 m (25 ft) in radius from the trunnion pin to the face of the skin plate. The

structure is framed similar to the standard tainter gate geometry as described by EM 1110-2-2702 with a 0.95-cm (3/8-in.) skin plate, C12 × 25 vertical ribs, two W30 × 118 horizontal girders, and W18 × 80 strut arm frames. All connections are riveted except for the use of bolts at the strut arm-trunnion block detail. The gates have Type J side seals and steel bottom seal details. The gates have a history of structural problems including significant gate vibrations and buckled web and flange plates on the strut arm. No extreme loads or unusual events had been reported since the last inspection. A change in operational practice was instituted to avoid gate opening settings that cause structural vibration. Because of the history of problems at this site, a thorough visual inspection was made previously on several gates.

(2) Inspection. An in-depth inspection was made of the gate with particular attention to the critical areas. Weather conditions at the dam site during the inspection were sunny and warm. The examination was conducted while water was being released from the gates. The following conditions were noted:

(a) Member or component deformation. Local web and flange plate buckling on the strut arms adjacent to the knee brace intersection from the upper horizontal girder was visible on several gates and is most severe on Gate 24. The condition has not deteriorated since the last inspection and was most likely caused by excessive ice loads on the structure.

(b) Seal problems. Water was observed flowing through the side seals.

(c) Rivet deterioration. Corrosion and a small amount of section loss were visible on some rivet heads.

(d) Mechanical/electrical problems. At Gate 25, one chain hoist was out of its guide on the skin plate. This hoist was toward the Minnesota side of the gate.

(e) Fabrication defects. There was no previous indication that fabrication defects existed in the structural members, and none were observed during this inspection.

(f) Corrosion. Paint loss and blistering were visible along the top surface of the web on the upper horizontal girder under the diversion plate. Blistered paint was left intact during the inspection.

(g) Fatigue cracking. No fatigue cracks were observed.

(h) Vibration or other unusual behavior. To check for vibration, the gate was fully closed and then reopened approximately 3.0 cm (0.1 ft) when vibration began. By rough measurement, the vibration frequency was estimated at 5-10 Hz. The amplitude of vibration was maximum at midspan of the gate and was sufficient to create an audible noise and make ripples in the backwater. The vibration ceased when the gate was opened further.

(i) Application of unusual loads. Except for the noted vibration, no unusual or extreme loads were reported. There was, however, an extensive accumulation of debris on the structural members in back of the skin plate, primarily large timber pieces.

(3) Evaluation. Because several detrimental conditions were detected during the inspection, the structural integrity of the spillway gate must be evaluated.

(a) Since an evaluation of the local buckling of the strut arms was conducted when it was first observed and the amount of buckling on the strut arms had not increased since the last inspection, it is believed that the structural capacity of the buckled members or of the gate is not in jeopardy at this time.

(b)   The amount of water leakage from the side seals is considered tolerable and will have no effect on normal gate operations.

(c)   Misalignment of the chain hoist is not severe enough to jeopardize operation of the gate but should be corrected.

(d)   Deterioration due to corrosion and rivet head loss are considered minor and will have no effect on normal gate operations or gate strength.

(e)   Flow-induced structural vibrations can cause serious damage to the spillway gate. In previous studies, stress ranges of approximately 27.6 MPa (4 ksi) have been calculated. Although this stress range is below the 41.4-MPa (6-ksi) threshold for fatigue crack growth at riveted details, the presence of groove welds to water-seal gaps between adjacent skin plates and tack welds to attach the diversion plate to the gate ribs may reduce this threshold stress range. However, since no fatigue cracks were detected and it is known how to control the gate vibrations, the structural capacity is not in jeopardy.

(f)   Although the accumulation of debris on the gate structure has not caused any structural or corrosion problems, it should be removed.

(4)   Recommendations. Based on the evaluation of conditions for the riveted tainter gates, the following recommendations are provided as steps that should be taken to ensure structural integrity for normal operations until the next regular inspection:

(a)   Continue operation of the spillway gates outside the range that causes vibration.

(b)   Schedule maintenance at Gate 25 to make repairs or adjustments to reinstall the chain hoist in the guide on the skin plate.

(c)   Schedule maintenance to remove large debris from all gate structures.

(d)   The buckled strut arm members should be occasionally monitored by lock personnel to detect any increases in deformation or distress to adjacent components.

(e)   Gate vibrations should be monitored by lock personnel to detect any changes. The inspection interval should be reduced to 2 to 3 years to monitor the buckled members and any future effects of the noted vibration problem more closely.

   b.   Fatigue evaluation.

(1)   To illustrate fatigue strength considerations, let it be assumed that during the inspection of tainter gates a more significant mode of vibration had recently been observed. Because of this new information, a thorough inspection was made at all fatigue-sensitive details on several gates where this vibration was observed. However, no fatigue cracks were visible.

(2)   Based on the inspection findings in this assumed example, a field study was recommended to deter-mine the significance of these new vibrations. The results of the field study revealed that vibrations of approximately five cycles per second or Hertz (Hz) were producing cyclic stresses of up to 55.2 MPa (8 ksi) at several details on the riveted structure.

(3)   The integrity of the riveted gate structure must be assessed by determining the fatigue strength of the details that are subjected to these cyclic loads. Since the measured maximum stress range is less than

68.9 MPa (10 ksi), the Category C curve will be used to determine the approximate number of cycles to failure at the detail (this does not imply that the entire structure will fail). By projecting lines on the S_r-N curve shown in Figure 6-22, it can be determined that the number of cycles to failure is approximately 12.5 million. With the measured frequency of vibration equal to 5 Hz, it would take approximately 694 hours (29 days) of vibration at this stress range to exceed the fatigue strength of the riveted connection. But because this new mode of vibration has only recently been observed, it is probable that not many cycles have accumulated to date. In fact, unless the gates in this assumed example are allowed to vibrate for extended periods, it may take up to 3-1/2 years before fatigue cracks develop if vibrations are limited to 1/2 hour per day while the gates are being adjusted.

(4) The recommended action to address this assumed condition would consist of three steps:

- Minimize the occurrence of gate vibrations by operating outside the range causing vibration.

- Reduce the inspection interval to approximately 1 year and inspect a greater number of gates to ensure that similar vibration is not occurring.

- Begin engineering studies to determine solutions to reduce the stresses caused by these vibrations.

c. Fracture evaluation example.

(1) During an inspection, a 9-cm (3.5-in.) crack was found on the downstream flange of a horizontal girder on a tainter gate. The crack is an edge crack similar to that shown in Figure 6-10. Prior to the inspection, no indication of damage had been reported. Since the cracked girder is a main framing element of the tainter gate, an immediate assessment of its critical nature is required. The crack is near the midlength of the girder. The girder flange is 35.6 cm (14 in.) wide and 3.8 cm (1.5 in.) thick.

(2) To evaluate this crack, a fracture analysis must be conducted. For this example, a linear-elastic fracture mechanics (LEFM) analysis will be used. The first step in performing the analysis is to obtain data on the three key parameters necessary for any fracture analysis: the crack size and geometry, the nominal stress in the member or component σ, and the critical stress intensity factor, K_{Ic} or K_c.

(3) The crack size and the geometry have already been determined from the inspection. For an LEFM analysis, the nominal member stress is required. For this case, the nominal girder flange stress can be determined from a plane frame analysis similar to that used in the design of tainter gate girders. An analysis showed that the nominal girder flange stress in the vicinity of the crack was 117.2 MPa (17 ksi) in tension.

(4) The next step in the analysis is to determine the fracture toughness. A review of the hypothetical design documents indicated that the gate had been fabricated from A36 steel. Since K_{Ic} testing (ASTM E399) of mild steels at reasonable service temperatures is impractical if not impossible, the fracture toughness will be determined from correlations with CVN data. As a first estimate, published CVN data for A36 steel will be used. This can be only an estimate, since K_{Ic} values can vary significantly for the same type of steel. K_{Ic} is also very dependent on temperature, so a minimum operating temperature for the structure must be established. Based on A36 steel CVN data (Barsom and Rolfe 1987), Figure 7-4 shows the approximation of K_{Ic} as a function of temperature. The curve on the left is calculated from the two-stage CVN-K_{Id}-K_{Ic} correlation (valid for the lower shelf and the lower end of the transition region; see paragraph 7-1*b*), and the curve on the right is from the upper shelf CVN-K_{Ic} correlation (Equation 7-3). The heavy line of each curve indicates the range in which the correlations are valid, as discussed in paragraph 7-1. The minimum service temperature for this example is -31.6 °C (-25 °F). Since neither curve is valid at this temperature, an estimate for K_{Ic} is determined by linear interpolation between the two correlations as indicated by the dashed line in Figure 7-4. This interpolation indicates that K_{Ic} is approximately 62.6 Mpa-$\sqrt{m}$ (57 ksi-$\sqrt{in.}$) at -31.6 °C (-25 °F). Conservatively, an estimate of K_{Ic} of 55 MPa-$\sqrt{m}$ (50 ksi-$\sqrt{in.}$) is selected for use in the analysis.

**Figure 7-4. CVN-K_{Ic} correlations (°C = 5/9 (°F − 32);
1 ksi-$\sqrt{in.}$ = 1.099 MPa-$\sqrt{m}$)**

(5) Since the crack size and geometry of detail are known and the stress level and material fracture toughness have been estimated, the crack can be evaluated for fracture by calculating the stress intensity factor and comparing to the fracture toughness. For a single-edge crack perpendicular to the stress field in a finite-width plate, the stress intensity factor incorporating a factor of safety (FS), K_{If}, is given by

$$K_{If} = 1.12\sigma \sqrt{\pi\, a\, FS} \bullet k \left(\frac{a\ FS}{b} \right) \tag{7-7}$$

where

a = crack size

k = function of a and b

b = half-width of the plate

(Tabulated values for k and stress intensity factor formulas for other crack geometries are given in Chapter 6.) For a factored crack length-to-plate half-width ratio of $(a \times FS)/b = (3.5 \times 2)/7 = 1.0$, $k = 2.55$, then

$$K_{If} = 1.12\,(117.2) \sqrt{\pi\ (0.09)\,(2)} \bullet 2.55 = 250\,\text{MPa} \text{ - } \sqrt{m} = 288\,\text{ksi} \text{ - } \sqrt{in.} \tag{7-8}$$

Since K_{If} is greater than $K_{Ic} = 54.95$ MPa-$\sqrt{m}$ (50 ksi-$\sqrt{in.}$), an unsafe condition exists for plane-strain conditions. Checking the plane strain assumption with Irwin's β factor from Equation 2-2:

$$\beta_{Ic} = \frac{1}{0.038} \left(\frac{55}{248} \right)^{2} = 1.3 > 0.4 \tag{7-9}$$

Since $\beta_{Ic} > 0.4$, the plane-strain condition assumption is not valid and the fracture toughness is represented by the critical stress intensity factor K_c. Using Equation 7-6 to estimate K_c (even though there is considerable deviation from plane strain condition) gives

$$K_c^2 = K_{Ic}^2 \left(1 + 1.4\ \beta_{Ic}^2\right) = 55^2 \left(1 + 1.4 \cdot 1.29^2\right) = 10{,}072 \left(\text{MPa-}\sqrt{\text{m}}\ \right)^2 \left[8{,}324 \left(\text{ksi-}\sqrt{\text{in.}}\ \right)^2\right]$$

$$K_c = 100\ \text{MPa-}\sqrt{\text{m}}\ \left(91\ \text{ksi-}\sqrt{\text{in.}}\ \right) \tag{7-10}$$

$$K_c < K_{If} = 250\ \text{MPa-}\sqrt{\text{m}}\ \left(228\ \text{ksi-}\sqrt{\text{in.}}\ \right)$$

(6)   Since K_c is less than K_{If}, an unsafe condition exists. This indicates that an immediate repair plan should be developed and implemented. If the repair will be costly and/or substantially affect the function of the project, a more accurate analysis should be made. The analysis was based on an estimation of K_{Ic} that may not accurately reflect the plane-strain fracture toughness of the material, and the approximation of K_c from K_{Ic} introduces more uncertainty in the estimation of the fracture toughness of the girder flange. A more exact analysis would require having tests conducted on the girder material so that a more accurate value of K_c may be obtained. A CTOD test, which can be used to estimate K_c (Equation 7-5), would likely be most appropriate because of the uncertainty in correlating CVN data at the service temperature. Alternatively, an elastic-plastic fracture assessment can be performed as outlined in Chapter 6.

d.   Lock gate fracture example. Cracks of various shapes were revealed on two tension members on a lock gate by nondestructive testing inspection. One member has the cross-sectional dimensions of 10 cm (4 in.) thick by 30.5 cm (12 in.) wide. The other member is 2.5 cm (1 in.) thick by 30.5 cm (12 in.) wide. The crack types and shapes include single-edge crack; through-thickness center crack; surface crack along the 0.3-m (12-in.) side ($a/2c = 0.1$ and 0.2), and embedded circular cracks.   The material properties at the minimum service temperature of -1.1 °C (30 °F) were determined by material testing and are summarized as follows:

σ_{ys} = offset yield strength of 345 MPa (50 ksi)

σ_{ult} = 552 MPa (80 ksi)

 E = 206,840 MPa (30,000 ksi)

K_{Ic} = 66 MPa-$\sqrt{\text{m}}$ (60 ksi-$\sqrt{\text{in.}}$)

 K_{Id} = 44 MPa-$\sqrt{\text{m}}$ (40 ksi-$\sqrt{\text{in.}}$)

δ_{crit} = critical CTOD value of 0.0052 cm (0.002 in.) (static)

δ_{crit} = 0.0025 cm (0.001 in.) (dynamic)

From structural analysis, the maximum applied tensile stress is 207 MPa (30 ksi). For each cracked member, the critical crack size will be determined for each cracking condition under static loading and dynamic loading, respectively:

(1)   Example for 10-cm (4-in.) by 30-cm (12-in.) plate:

$$\beta_{Ic} = \frac{1}{t}\left(\frac{K_{Ic}}{\sigma_{ys}}\right)^2 = \frac{1}{10}\left(\frac{66}{345}\right)^2 = 0.36$$

$\beta_{Ic} < 0.4$; therefore, LEFM is applicable.

(a) Single-edge crack (see Figure 6-10):

$$K_I = 1.12\,\sigma\sqrt{\pi a}\ \ k\left(\frac{a}{b}\right)$$

where σ is the nominal stress.

$$C = 1.12\ \sqrt{\pi}\ \ k\left(\frac{a}{b}\right) \text{ in Equation 6-1}$$

Assume $k\,(a/b) = 1.0$. The critical discontinuity size is calculated as

$$a_{cr} = \frac{1}{\pi}\left(\frac{K_{Ic}}{1.12\,\sigma}\right)^2 = 2.59 \text{ cm (1.02 in.)}\ \ \text{(Equation 6-2 with no factor of safety)}$$

$(a/b) = 0.17$ and $k(a/b) = 1.06$; therefore, iteration is needed for a_{cr} and $k(a/b)$. After iteration, $a_{cr} = 2.34$ cm (0.92 in.) $(k(a/b) = 1.05)$. With $FS = 2.0$, $a_{cr} = 0.5\,(2.34) = 1.17$ cm (0.46 in.) for dynamic loading:

$$a_{cr} = \frac{0.5}{\pi}\left(\frac{K_{Id}}{1.12\,\sigma}\right)^2 = 0.58 \text{ cm (0.23 in.)}$$

(b) Through-thickness center crack (Figure 6-8). Calculate the stress intensity factor:

$$K_I = \sigma\ \sqrt{\pi a}\ \sqrt{\frac{2b}{\pi a}\ \tan\left(\frac{\pi a}{2b}\right)}$$

Assume

$$\sqrt{\frac{2b}{\pi a}\ \tan\left(\frac{\pi a}{2b}\right)} = 1.0$$

$$a_{cr} = \frac{1}{\pi}\left(\frac{K_{Ic}}{\sigma}\right)^2 = 3.23 \text{ cm (1.27 in.)}$$

$$\sqrt{\frac{2b}{\pi a}\ \tan\left(\frac{\pi a}{2b}\right)} = 1.02$$

After iteration, $a_{cr} = 3.1$ cm (1.22 in.). With FS = 2.0, $a_{cr} = 3.1/2 = 1.55$ cm (0.61 in.) and for dynamic loading,

$$a_{cr} = \frac{0.5}{\pi}\left(\frac{K_{Id}}{\sigma}\right)^2 = 0.71 \text{ cm (0.28 in.)}$$

(c)   Surface crack along the 30.5-cm (12-in.) side ($2c$ is the length of the surface crack along the slope of the component; see Figure 6-15):

- $a/2c = 0.1$

$$K_I = 1.12 \; \sigma \; \sqrt{\pi \frac{a}{Q}} \; M_K$$

$$\frac{\sigma}{\sigma_{ys}} = \frac{207}{345} = 0.6$$

where Q is the flow shape parameter defined by Figure 6-14 and M_k is a variable that describes the effect of a/t on K_I.

From Figure 6-14, $Q = 1.02$, assume $M_k = 1.0$

$$a_{cr} = \frac{Q}{\pi} \left(\frac{K_{Ic}}{1.12 \, \sigma} \right)^2 = 2.64 \, \text{cm} \, (1.04 \, \text{in.}) \; (a/t = 0.26; \, M_k = 1.0)$$

With $FS = 2.0$, $a_{cr} = 2.64/2 = 1.32$ cm (0.52 in.), and for dynamic loading,

$$a_{cr} = \frac{0.5 \; Q}{\pi} \left(\frac{K_{Ic}}{1.12 \, \sigma} \right)^2 = 0.58 \, \text{cm} \, (0.23 \, \text{in.})$$

- $a/2c = 0.2$

From Figure 6-14, $Q = 1.24$, assume $M_k = 1.0$

$$a_{cr} = \frac{Q}{\pi} \left(\frac{K_{Ic}}{1.12 \, \sigma} \right)^2 = 3.2 \, \text{cm} \; (1.23 \, \text{in.}) \; (a/t = 0.32; \, M_k = 1.0)$$

With $FS = 2.0$, $a_{cr} = 3.2/2 = 1.6$ cm (0.63 in.), and for dynamic loading,

$$a_{cr} = \frac{0.5 \, Q}{\pi} \left(\frac{K_{Ic}}{1.12 \, \sigma} \right)^2 = 0.71 \, \text{cm} \, (0.28 \; \text{in.})$$

(d)   Embedded circular crack (see Figure 6-14).

$$K_I = \sigma \; \sqrt{\pi \frac{a}{Q}}$$

$a/2c = 0.5$; from Figure 6-14, $Q = 2.4$

with $FS = 2.0$,

$$a_{cr} = \frac{0.5 \, Q}{\pi} \left(\frac{K_{Ic}}{\sigma} \right)^2 = 3.89 \, \text{cm} \, (1.53 \, \text{in.})$$

and for dynamic loading:

$$a_{cr} = \frac{0.5\,Q}{\pi}\left(\frac{K_{Ic}}{\sigma}\right)^2 = 1.73 \text{ cm (0.68 in.).}$$

(2) Example for 2.5-cm (1-in.) by 30-cm (12-in.) plate:

$$\beta_{Ic} = \frac{1}{t}\left(\frac{K_{Ic}}{\sigma_{ys}}\right)^2 = \frac{1}{0.025}\left(\frac{66}{345}\right)^2 = 1.46.$$

$\beta_{Ic} > 0.4$; therefore, elastic-plastic fracture mechanics is applicable.

Determine the allowable discontinuity parameter $\bar{a}_m$ (paragraph 6-5b).

$$\bar{a}_m = C\left[\frac{\delta_{crit}}{\varepsilon_y}\right] \quad \text{(Equation 6-4)}$$

where ε_y is the yield strain of the material

$$\varepsilon_y = \frac{\sigma_{ys}}{E} = \frac{345}{206,843} = 0.0017$$

$$\frac{\sigma}{\sigma_{ys}} = \frac{207}{345} = 0.6$$

From Figure 6-20, $C = 0.44$

For static loading

$$\bar{a}_m = 0.44\left(\frac{0.0052}{0.0017}\right) = 1.32 \text{ cm (0.52 in.)}$$

For dynamic loading

$$\bar{a}_m = 0.44\left(\frac{0.0025}{0.0017}\right) = 0.65 \text{ cm (0.26 in.)}$$

Critical crack lengths can be determined for various crack shapes from the allowable discontinuity parameter $\bar{a}_m$ (paragraph 6-5b).

7-3. Example Fatigue Analysis

This example shows how to apply fatigue analysis to determine expected life given an initial flaw size a_i. For this case, consider an initial surface flaw of the type shown in Figure 6-15 with $a/2c = 0.25$. The member is a 10-cm- (4-in.-) thick plate of ASTM A572/572M Grade 345 (50) steel. The critical stress intensity factor (fracture toughness) K_{Ic} of this steel is 66 MPa-$\sqrt{m}$ (60 ksi-$\sqrt{in.}$) at the minimum service temperature.

    a. The maximum stress level is 207 MPa (30 ksi) and the minimum stress is zero. A curve relating the initial surface flaw size a_i to number of cycles to failure N_p will be developed. From Figure 6-15

$$K_I = 1.12\,\sigma\sqrt{\pi\frac{a}{Q}}\ M_K$$

$$\frac{\sigma}{\sigma_{ys}} = \frac{207}{345} = 0.6 \text{ and } Q = 1.39 \text{ (Figure 6-14)}.$$

Assume $M_k = 1.0$.

With $FS = 2.0$,

$$a_{cr} = \frac{0.5\,Q}{\pi}\left(\frac{K_{Ic}}{1.12\,\sigma}\right)^2 = 1.8 \text{ cm (0.71 in.)}$$

(for crack sizes up to $a = 1.8$ cm (0.71 in.), $M_k = 1.0$) and for ferrite-pearlite steel, $da/dN = 6.9\times10^{-9}\,(\Delta K_I)^3$ (Equation 6-8):

$$\Delta K_I = 1.12\Delta\sigma\ \sqrt{\pi\frac{a}{Q}} = 348.5\sqrt{a}\ \text{ MPa}\sqrt{\text{m}}\ \left(50.5\ \sqrt{a}\ \text{ ksi}\sqrt{\text{in.}}\right)$$

   b.   Fatigue life can be determined as:

$$N = \int_{a_i}^{a_{cr}} \frac{da}{(6.9\times10^{-9})(\Delta K_I)^3}$$

$$N = \frac{1}{(6.9\times10^{-9})(348.5)^3} \int_{a_i}^{a_{cr}} a^{-3/2}\ da$$

$$N = (6.9)\left(\frac{1}{\sqrt{a_i}} - \frac{1}{\sqrt{a_{cr}}}\right)$$

   c.   The curve for fatigue life N as a function of initial crack length a_i for this example is shown in Figure 7-5.
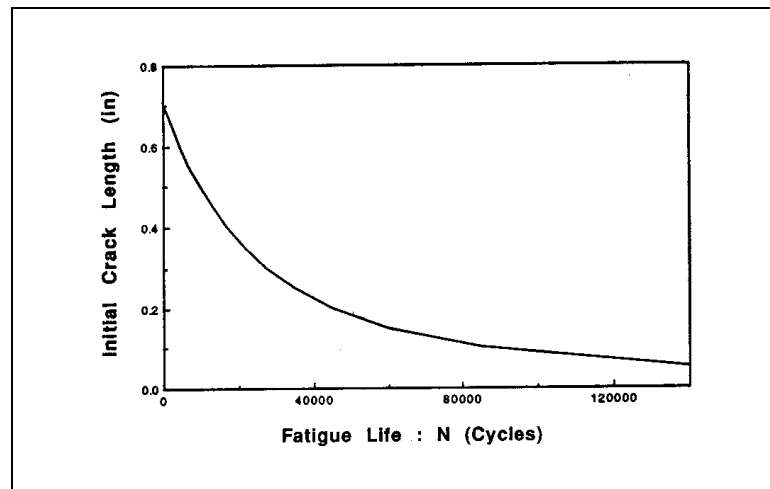

Figure 7-5. Fatigue life *N* versus initial crack-length *a_i* curve (1 in. = 2.4 cm)

7-4. Example of Fracture and Fatigue Evaluation

   a. Single-edge crack.

   (1) Figure 7-6 shows a horizontal girder with a single-edge crack. The initial crack length is assumed to be 3 mm (1/8 in.). The flange plate containing the edge crack is assumed to be under a cyclic load from zero to maximum tension (i.e., fatigue ratio $R = 0$). The stress ranges vary from 124 MPa (18 ksi) to 186 MPa (27 ksi). The fatigue life can be calculated using the following crack growth equation (Equation 6-8):

$$\frac{da}{dN} = 6.9 \times 10^{-9} \ (\Delta K_I)^3$$

where

$$K_I = 1.12 \ \sigma \ \sqrt{\pi a} \ k \ (a/b)$$

By integrating the crack growth equation, the life of the propagating crack can be determined for any crack length:

$$N = \int_{a_i}^{a_{cr}} \frac{da}{(6.9 \times 10^{-9}) \ (\Delta K_I)^3}$$

where K_I is a function of crack length

and from Equation 6-2:

$$a_{cr} = \frac{1}{\pi} \left(\frac{K_{Ic}}{1.12 \ \sigma \ k \left(\dfrac{a}{b} \right)} \right)^2$$

With K_{Ic} assumed to be 38.4 MPa-$\sqrt{m}$ (35 ksi-$\sqrt{in.}$) and a maximum stress of 124 MPa (18 ksi), $a_{cr} = 2.3$ cm (0.89 in.) using the procedure described in paragraph 7-2d(1)(a).

   (2) Figure 7-7a shows the calculated crack growth versus life cycle for a stress range of 124 MPa (18 ksi) (1/2 σ_{ys}). The remaining life N, calculated by the equation for the life of the propagating crack in (1) above, is 207,700 cycles. If the structure operates 10,000 times per year, then the remaining life of the girder is:

$$\frac{207,700}{10,000} = 20.8 \ \text{years}$$

Critical crack length (determined by Equation 6-2) is a function of external loading as shown in Figure 7-7b. Figure 7-7c shows the fatigue life for stress ranges varying from 124 MPa (18 ksi) to 186 MPa (27 ksi) calculated using the crack growth equation with variable stress and a_{cr}. The remaining life of the girder flange containing a 3-mm (1/8-in.) initial crack is shown in the figure as a function of stress.

   b. Double-edge crack. A girder flange containing double-edge cracks is shown in Figure 7-8. The crack growth curves were calculated for stress ranges varying from 69 to 138 MPa (10 to 20 ksi). The same integration procedure as used for the single-edge crack case is employed for calculating the fatigue life. A 3-mm
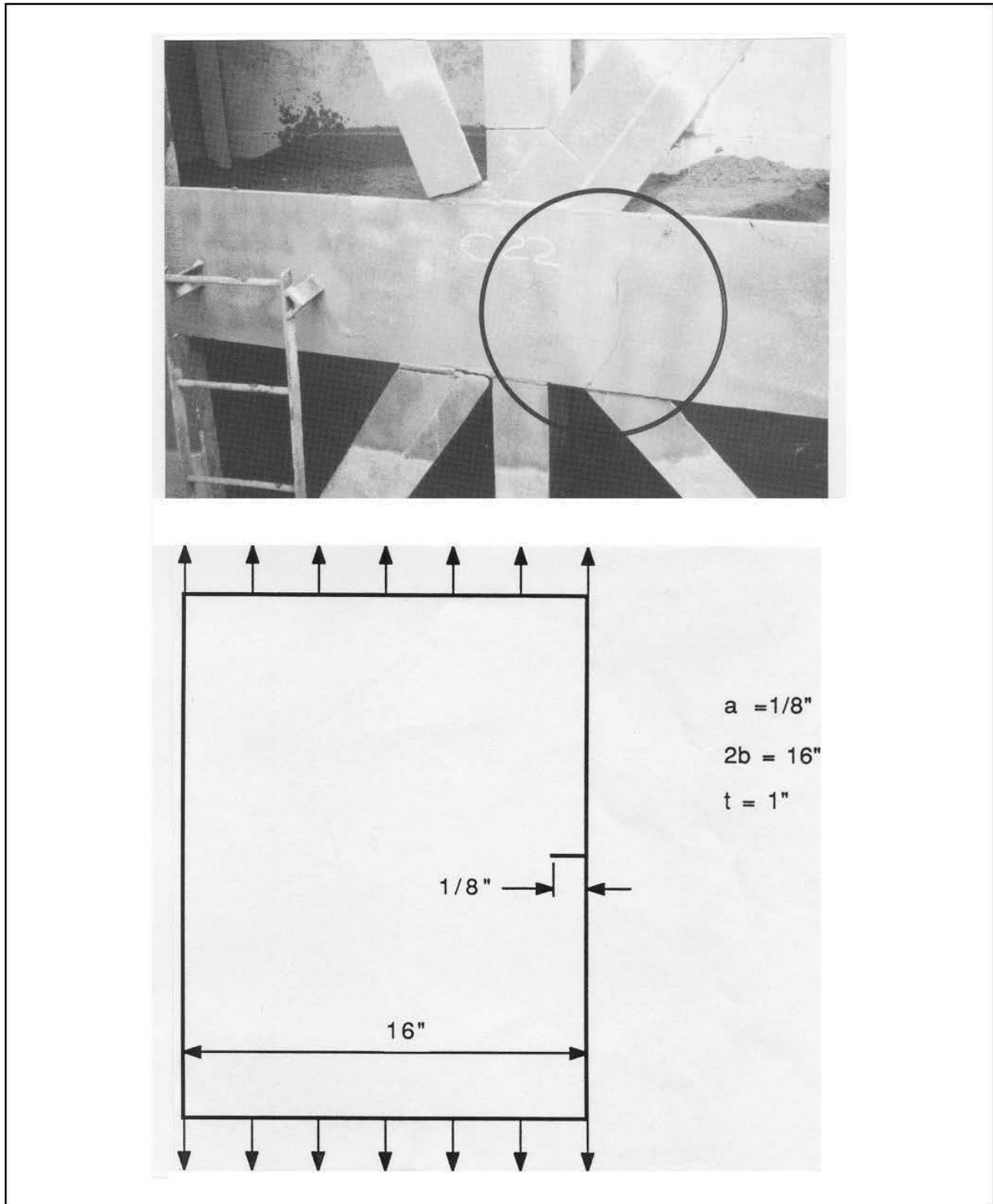
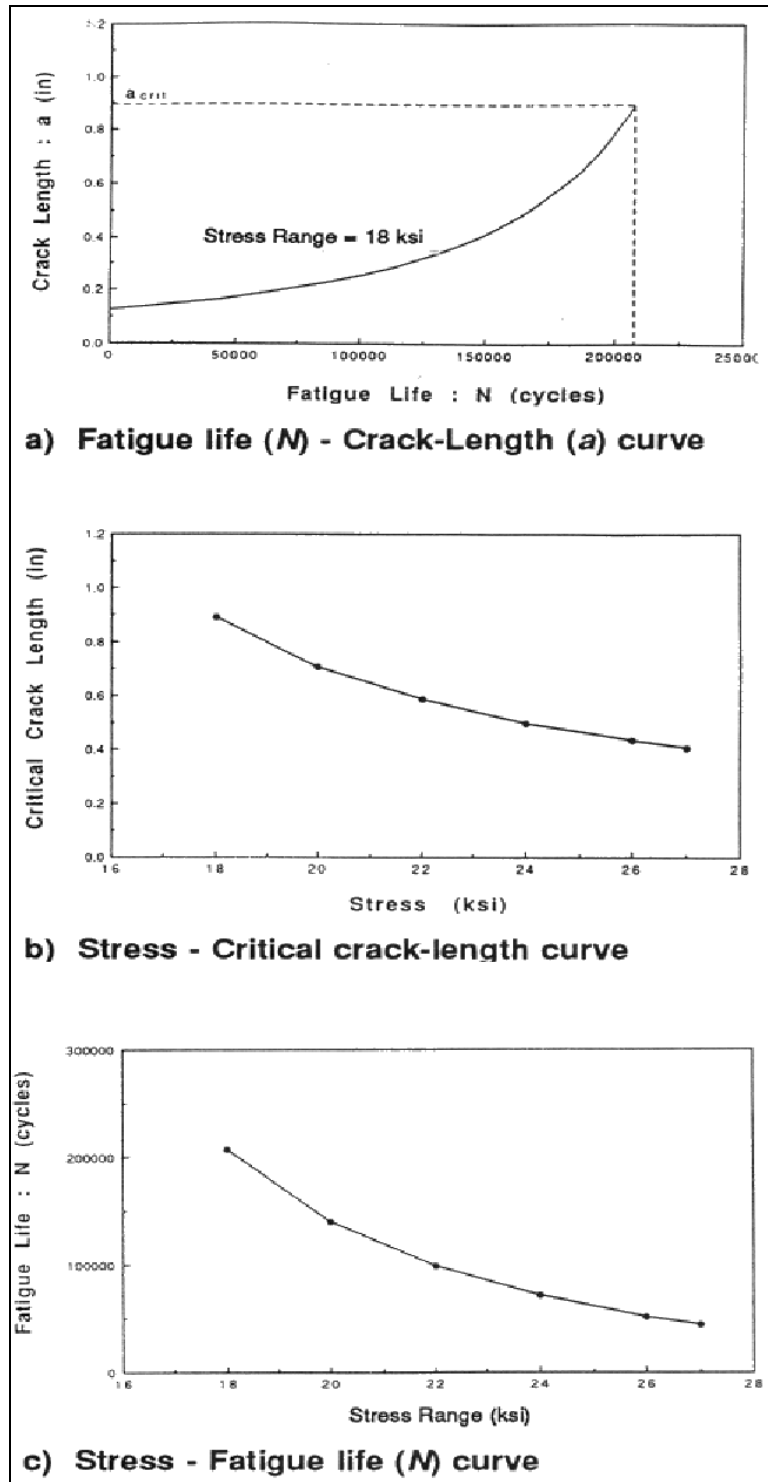**Figure 7-6. A single-edge cracked girder (1 in. = 2.54 cm)**

**Figure 7-7. Curves for fatigue life of a flange with a single-edge crack
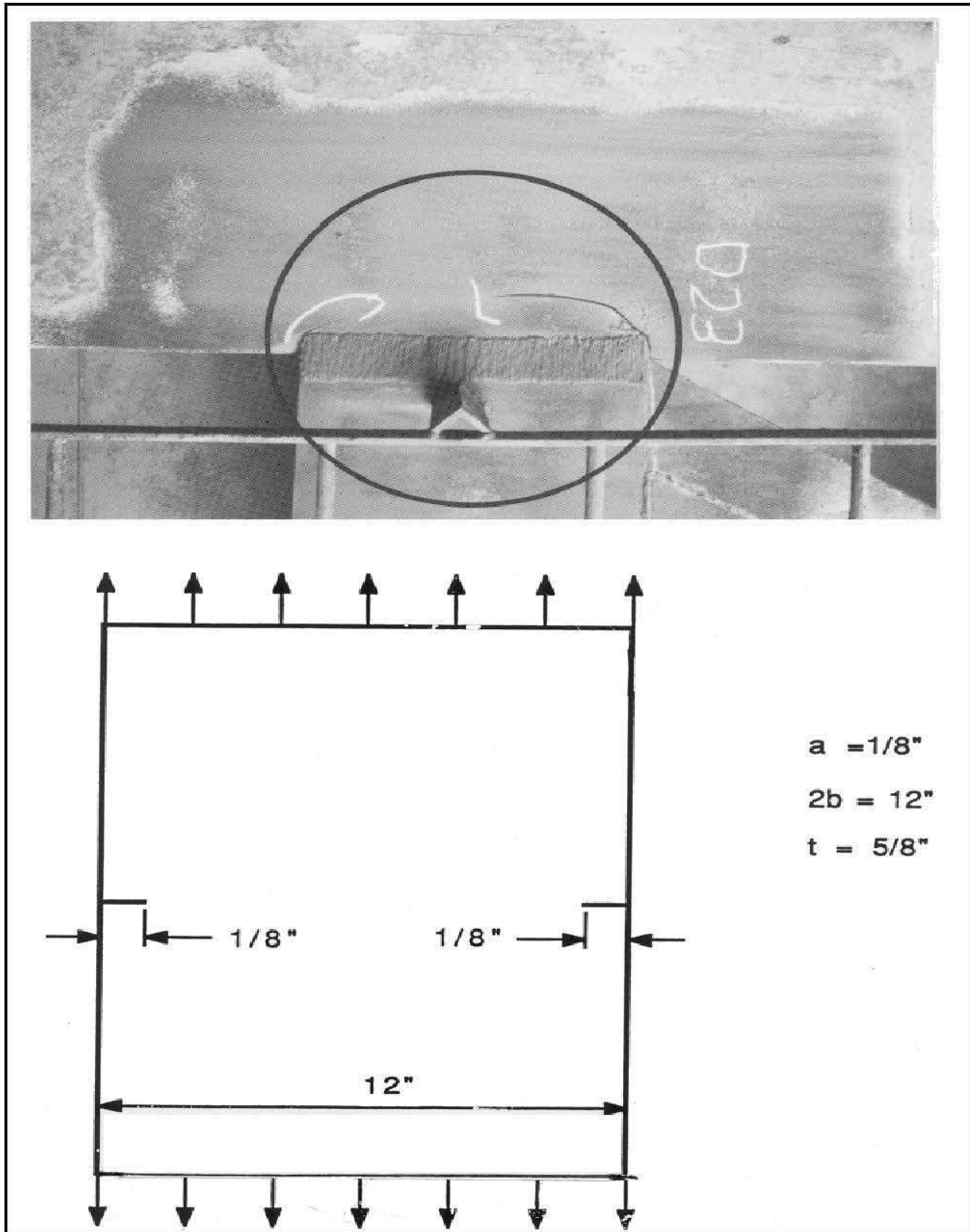(1 in. = 2.54 cm; 1 ksi = 6.89 MPa)**

Figure 7-8. A double-edge cracked flange (1 in. = 2.54 cm)

(1/8-in.) initial crack length is also assumed in this case. The predicted crack growth curve for stress range of 124 MPa (18 ksi) is shown in Figure 7-9a. Figure 7-9b shows the relationship between stress and critical crack length. The remaining life of the girder flange plate for various stress ranges is also shown in Figure 7-9c.

c. Surface crack. Figure 7-10 shows a crack assumed to have initiated in the diagonal bracing member from a surface crack at the corner of the bracket. It is assumed that the crack propagated through the thickness of the bracing member and then grew toward the edge of the flange plate. A single-edge crack condition similar to the first example case was developed. The fracture and fatigue analysis of this example consists of three propagation steps.

(1) The first step is to analyze the crack propagation of a hemispheric surface crack having an initial radius of 1.6 mm (1/16 in.). When the surface crack breaks through the surface on the other side of the plate (i.e., the radius of hemispheric crack becomes the same as the plate thickness of 9.5 mm (3/8 in.)), a through-thickness crack condition is reached.

(2) The second step is to analyze crack growth of a plate containing a through-thickness crack. Once the through-thickness crack reaches the edge of the plate, the single-edge crack condition is developed.

(3) The third step is to analyze crack growth of the edge crack. The total remaining life of the diagonal bracing member from the initial hemispheric surface crack can be determined by adding the three propagation lives. The calculated crack growth curve for a stress range of 124 MPa (18 ksi) is shown in Figure 7-11a. The total remaining life and critical crack length are also shown in Figure 7-11b and c for stress ranges varying from 69 to 138 MPa (10 to 20 ksi).

d. Inspection schedule. The inspection schedule can be determined from the fatigue life curve of the single-edge crack in the primary member. The maximum stress range is assumed as 124 MPa (18 ksi). The procedure is shown in the following steps.

(1) Determine critical crack length:

a_{cr} = 2.26 cm (0.89 in.) (paragraph 7-4a)

(2) Determine crack length when repair is needed (Figure 6-23):

a_r = 2.26/2 = 1.13 cm (0.45 in.) (FS = 2.0)

(3) Determine fatigue life from fatigue life *N* versus crack length *a* curve:

N = 160,000 cycles; 160,000/10,000 = 16 years (10,000 cycles/year)

Therefore, the girder should be inspected within 16 years after the initial crack (a_i = 3 mm (1/8 in.)) was found.

7-5. Structural Steels Used on Older Hydraulic Steel Structures

Steel standards for the period when many hydraulic steel structures were constructed are of interest from both a structural evaluation and a repair and maintenance standpoint. In a structural evaluation, the characteristics of corrosion resistance, fracture resistance, crack propagation rate, and stability of properties with seasonal temperature changes are considered important parameters. The weldability of steels is also of interest since welding will likely be considered for repair and maintenance procedures even for riveted structures. However, at the time the gates were constructed, these properties probably were not determined or even much considered.
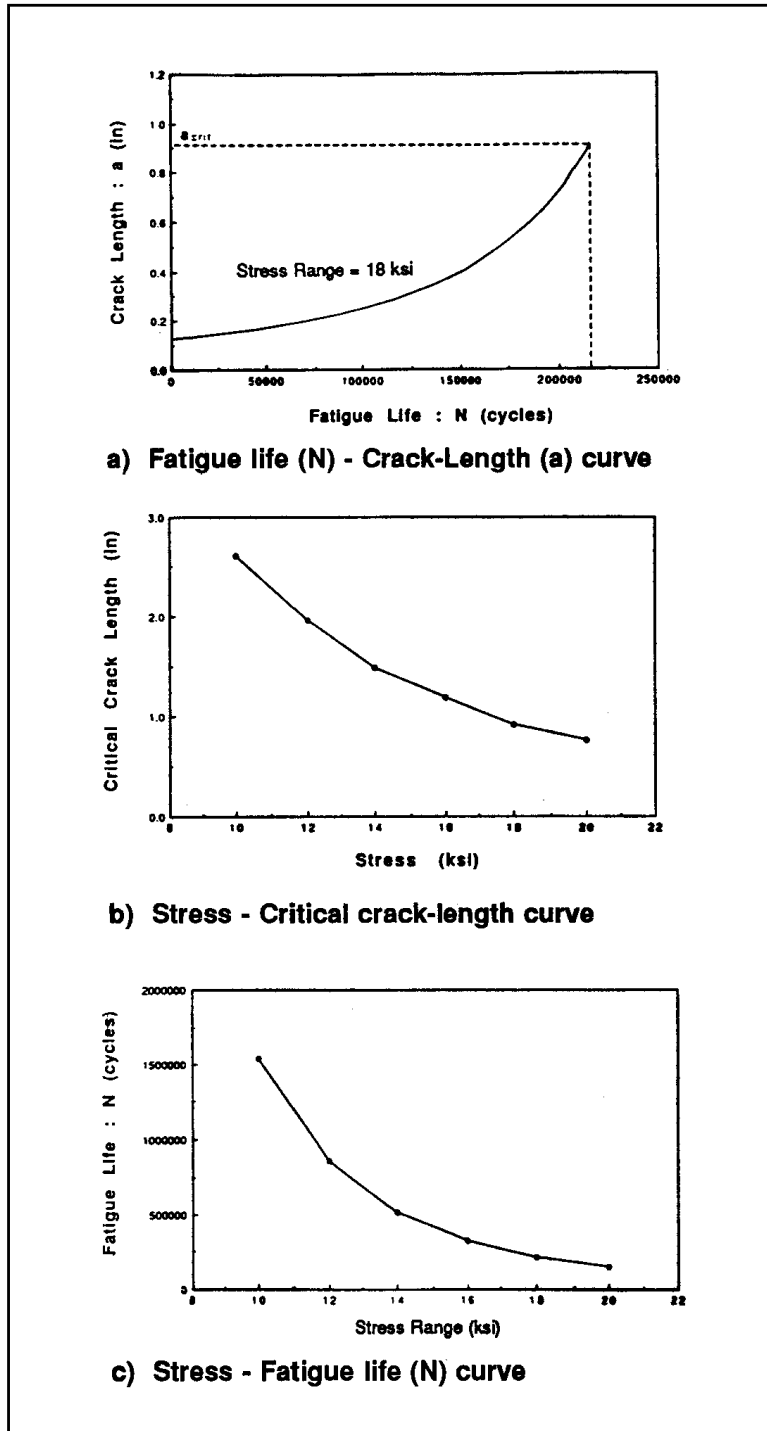
a) Fatigue life (N) - Crack-Length (a) curve

b) Stress - Critical crack-length curve

c) Stress - Fatigue life (N) curve

Figure 7-9. Curves for fatigue life of a flange with a double-edge crack (1 in. = 2.54 cm; 1 ksi = 6.89 MPa)

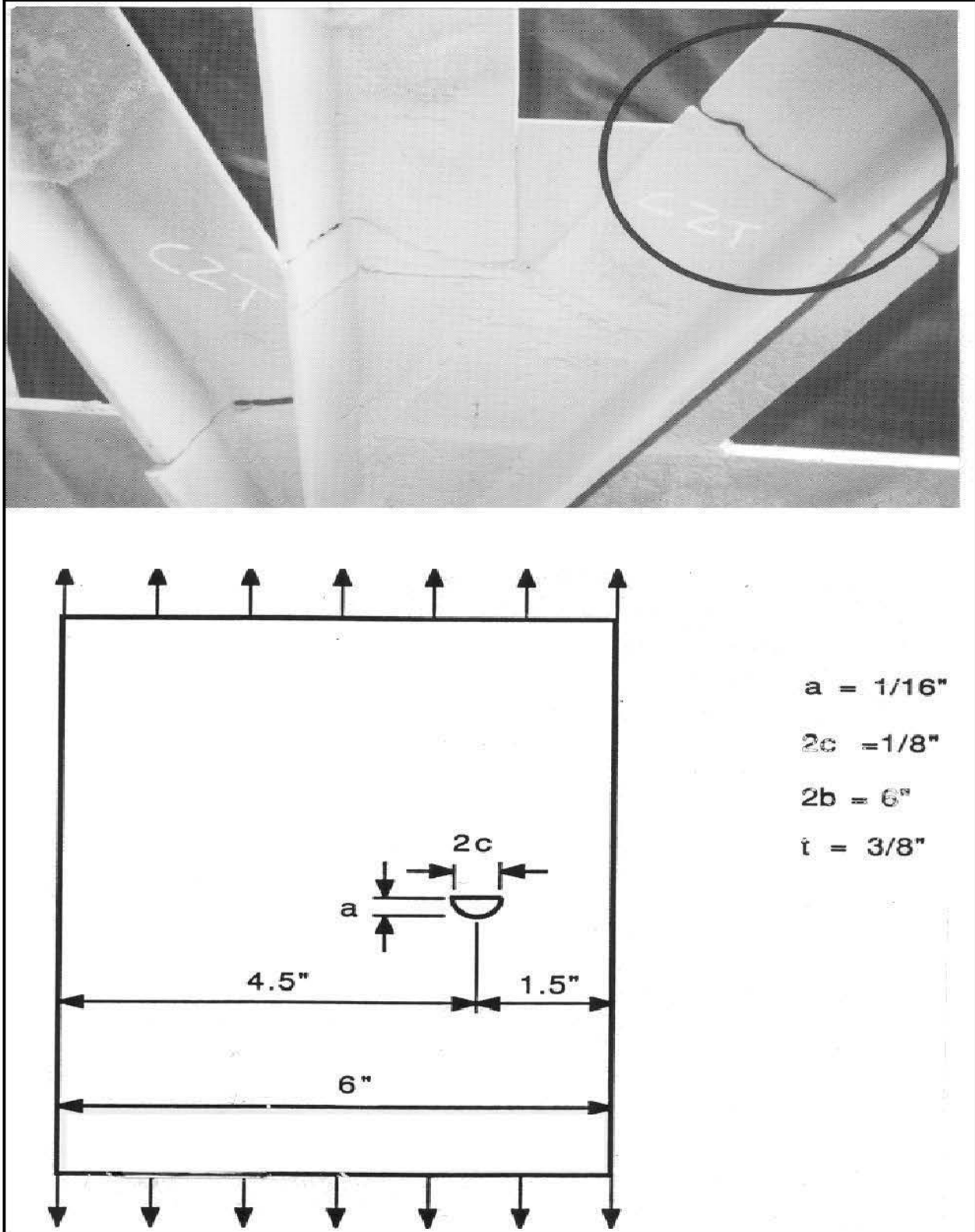**Figure 7-10. A stiffening member with a crack (1 in. = 2.54 cm)**

a) Fatigue life (N) - Crack-Length (a) curve

b) Stress - Critical crack-length curve

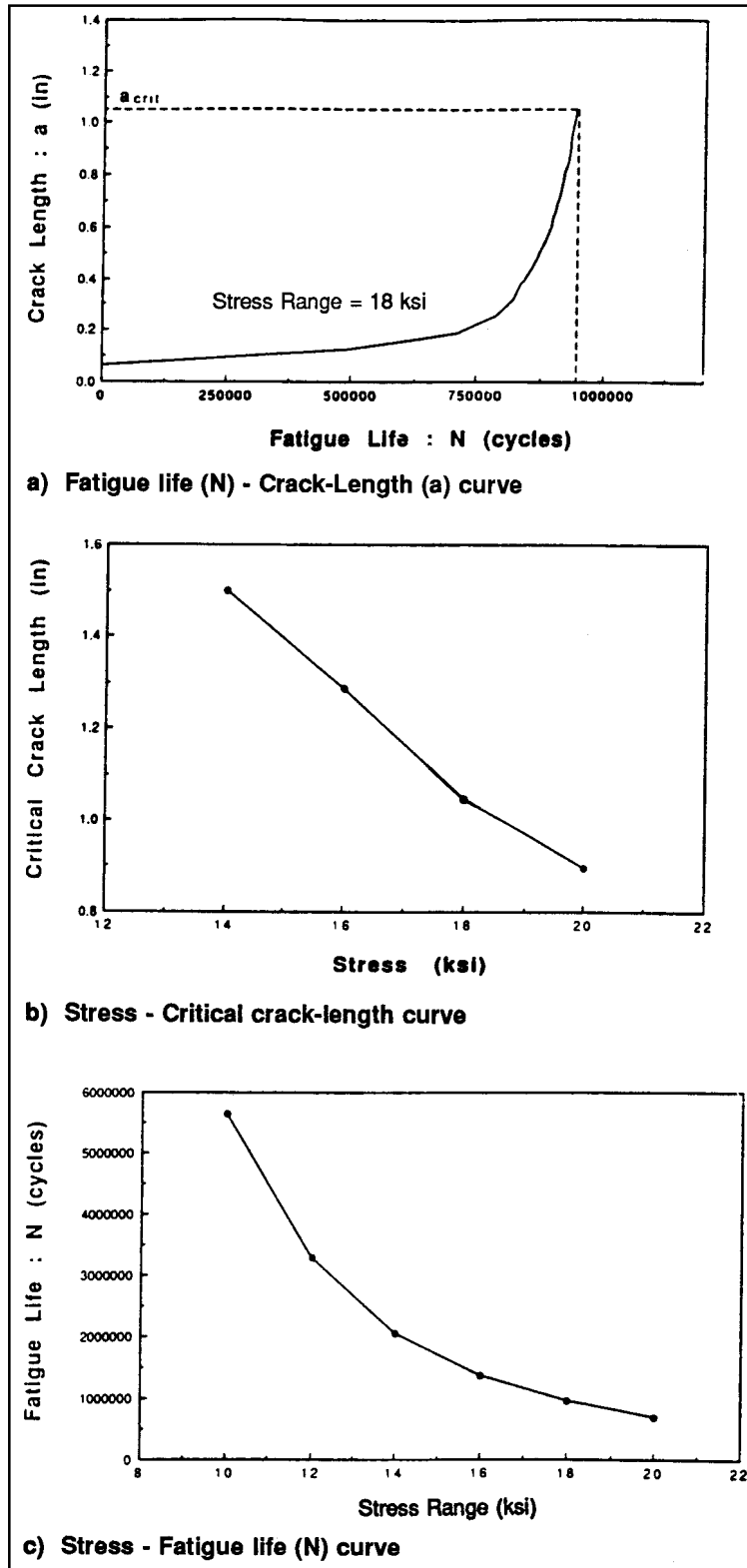c) Stress - Fatigue life (N) curve

Figure 7-11. Curves for fatigue life of a stiffening member with a
surface crack (1 in. = 2.54 cm; 1 ksi = 6.89 MPa)

   a.   Structural steel standards.

   (1)   In the 1930's when many hydraulic steel structures were designed and built, several structural steels were commonly in use. In the mid-1930's, structural steel could have been either ASTM A7-33T or ASTM A9-33T steel (Ferris 1953). A7 steel was generally regarded at the time as a steel for bridges, whereas A9 steel was a steel for buildings. The primary differences between the two were that A7 steel had a lower maximum allowable phosphorus content and had a limit on sulfur content compared with A9 steel. A7 steel also was restricted to open-hearth or electric-furnace production and excluded the older acid-bessemer production. These compositional and production restrictions suggest that A7 bridge steel was recognized as the premium steel of the two. For a brief period (1932-33), structural steel also could have been supplied as ASTM A140 steel, which was a tentative replacement for both A7 and A9 steels (Ferris 1953).

   (2)   Steel identified as silicon steel on design drawings is mostly likely ASTM A94-25T structural silicon steel. This was a high-strength steel with a specified minimum silicon content that attained its high strength (minimum yield point of 310 MPa (45 ksi) and tensile strength of 552 to 655 MPa (80 to 95 ksi)) through a high level of carbon (0.44 percent maximum). It also had limits on its phosphorus and sulfur contents.

   (3)   An important characteristic of the early steels, regardless of whether they were A7, A9, A140, or A94 silicon steel, is that they had either no specified level or a high level of carbon in their composition. Consequently, the carbon level was either not rigorously controlled or was moderately high, with the result that the steels probably had and have only poor to fair weldability. The specification for A94 structural silicon steel specifically limits welding and specifies a preheat condition when welding must be done. Of course, the steels were being used for riveted structures, so weldability was not then a concern to designers. But it needs to be considered for weld repairs or maintenance contemplated today.

   (4)   In 1939, A7 and A9 were consolidated into a single specification, A7 steel (ASTM A7-39) for bridges and buildings, which then became the single specification for structural steel. In 1954 a new structural steel for welding, A373 steel, was introduced (ASTM A373-58T). Both A7 and A373 steels were consolidated in 1965 into one specification, A36 steel (ASTM A36-60T), which is the basic structural steel today and is used for both welded and bolted applications.

   b.   Rivet steel standards.

   (1)   Rivet steel was not typically specified by steel grade, but only as structural steel, carbon steel, or as rivets. However, the allowable shear stress for power-driven rivets was occasionally identified as 82.7 MPa (12 ksi), and the allowable bearing stress as 165.4 MPa (24 ksi). Until 1932, rivet steel was included in the ASTM A7 and A9 specifications, but with lower yield and tensile strengths than structural steel (Ferris 1953). However, in 1932, ASTM A141 was issued as a tentative specification for structural rivet steel, with somewhat more enhanced strength requirements than earlier. More restrictive diameter tolerances were included in a 1936 tentative revision. Until 1949, rivet yield strength was specified as one-half times the tensile strength or not less than 193 MPa (28 ksi). In 1949, the yield strength for A141 rivet steel was changed to 193 MPa (28 ksi) minimum (Ferris 1953). In 1960, A141 rivet steel was incorporated into the new tentative A36 steel specification (ASTM A36-60T).

   (2)   In 1936, a new tentative specification, ASTM A195, was issued for high-strength structural rivet steel, for rivets produced from structural silicon steel (ASTM A195-36T). As opposed to A141 rivet steel, A195 rivet steel had carbon, manganese, silicon, and copper requirements. In addition, A195 rivet steel yield strength was specified as one-half times the tensile strength or not less than 262 MPa (38 ksi). A195 steel rivets were to be used with A94 structural silicon steel, although the use of A141 steel rivets may have continued.

(3) In 1964, a new specification, ASTM A502, was published for steel structural rivets, and superseded ASTM A141 and A195. The later version of this specification (ASTM A502) covers three grades of steel rivets: general-purpose carbon steel rivets, carbon-manganese steel rivets for use with high-strength carbon and high-strength low-alloy steels, and rivets comparable to ASTM A588 weathering steel. The later specification includes hardness requirements but not tensile and yield strength requirements.

c. Allowable and yield stresses. During the same period that A7 steel was evolving, the American Institute of Steel Construction (AISC) changed their basic allowable working stress for structural steel only once, raising it in 1936 from 124 to 138 MPa (18 to 20 ksi) (Ferris 1953). The ASTM requirement for minimum yield point during this period was generally one-half times the tensile strength, or not less than 207 MPa (30 ksi); in 1933, the minimum of 207 MPa (30 ksi) was raised to 227.5 MPa (33 ksi) for plate and shape products. When A373 steel was introduced, that steel had a minimum yield point of 220.6 MPa (32 ksi), suggesting that to improve weldability at that time, some sacrifice in strength was necessary. Only when A36 steel was introduced in 1960 in a tentative specification (ASTM A36-60T) did the minimum yield point for structural steel plates and shapes increase to 248 MPa (36 ksi). By that time, weldability and welding practices for structural steel had markedly improved and standardized.

d. Weldability of earlier steels.

(1) A very good reference that discusses the weldability of steels, including steels that have limited weldability, is the monograph "Weldability of Steels" published by the Welding Research Council (Stout et al. 1987). Now in its fourth edition, the monograph has chapters on the properties of steel related to weldability, factors affecting weldability in fabrication, and the weldability of different steels.

(2) For early steels, reference can be made to the first edition of the monograph (Stout and Doty 1953) which includes suggested (as of 1953) welding practices for A7 steel meeting the tentative specification ASTM A7-50T. However, even the first edition does not include data for A9 or A94 steels. A copy of the suggested (1953) practices for A7 steel is listed in Table 7-1. For thicknesses up to 1 in. (the normal case for hydraulic steel structures), a comparison of the recommended practices in Table 7-1 suggests that for carbon levels of 0.25 percent or less, no special welding requirements are needed for A7 steel. However, as the carbon level increases, more stringent practices are needed. Because A7 steel did not have a specified carbon level, repair and maintenance welding should be conducted favoring the more stringent practices. For other early steels or for steels of unknown specification, ANSI/AWS D1.1 provides optional methods for determining welding requirements based on the chemical composition of the steel.

(3) A generally conservative practice for repair and maintenance welding on riveted spillway gates is to use the practices for A7 steel in Table 7-1, with the assumption that the carbon level is between 0.26 and 0.30 percent.

Table 7-1
Suggested Practices for Sound Welding with A7 Steel (After Stout and Doty 1953)

A7 Steel

	CONDITIONS REQUIRING NO PREHEATING, POSTHEATING, OR SPECIAL ELECTRODES													
Steel Specification	Conditions for Which No Special Precautions Are Required		Remarks	Grade or Quality	Specification Requirements (Abridged)									
					Composition								Tensile Properties	
	Carbon Range, %	Thickness Range, in.			C	Mn	Si	Ni	Cr	Mo	Other	Yield Point psi	Tensile Strength psi	Elongation %
ASTM A7-50T Steel for bridges and buildings	Up to 0.25, Incl.	Up to 1, Incl.	Over 1 in., see Table II	...	(Not speci-fied)	(Not speci-fied)	(Not speci-fied)	...	...	...	0.20 min. Cu when specified	33,000 min.	60,000-72,000	21 in 8 inches (min.)
	0.26 - 0.30, Incl.	Up to 1/2, Incl	Over 1/2 in., see Table II											
			Over 0.30 carbon see Table II											

TABLE II. CONDITIONS REQUIRING SOME CONTROL OVER HEAT INPUT AND REQUIRING LOW HYDROGEN ELECTRODES OR PREHEAT AND GENERALLY POSTHEATING			
Conditions for Which Precautions Are Required			
Carbon Range %	Thickness Range In.	Recommended Arc Welding Conditions General Notes: Electrodes should be of suitable composition when alloy steels are welded. Welding conditions are not given for materials over 4 inches thick.	
Up to 0.25 Incl.	Over 1-2, Incl.	Condition A or B	
	Over 2-4, Incl.	Condition C	
0.26-0.30 Incl.	Over 1/2-1, Incl.	Condition A or B	Condition A = 100°F minimum preheat and interpass temperature, 1100-1250°F stress relief optional.
	Over 1-2, Incl.	Condition B or C	Condition B = No welding below 10°F, EXX15 or EXX16 electrode, 1100-1250°F stress relief optional.
	Over 2-4, Incl.	See Table III	Condition C = 200°F minimum preheat and interpass temperature, 1100-1250°F stress relief optional.
0.31-0.35 Incl.	Up to 1/2, Incl.	Condition A or B	
	Over 1/2-1, Incl.	Condition B or C	
	Over 1-4, Incl.	See Table III	

TABLE III. CONDITIONS REQUIRING PREHEAT, SPECIAL WELDING TECHNIQUES, AND POSTHEATING AND/OR PEENING			
Conditions for Which Precautions Are Required			
Carbon Range %	Thickness Range In.	Recommended Arc Welding Conditions General Notes: Electrodes should be of suitable composition when alloy steels are welded. Welding conditions are not given for materials over 4 inches thick.	
0.26-0.30 Incl.	Over 2-4, Incl.	Condition J	Condition J = 100°F minimum preheat and interpass temperature with EXX15 or EXX16 electrode or 300°F preheat with other than EXX16 electrode, 1100-1250°F stress relief optional, peening may be necessary for thicknesses over 1 inch.
0.31-0.35 Incl.	Over 1-2, Incl.	Condition J	Condition K = 200°F minimum preheat and interpass temperature with EXX15 or EXX16 electrode or 300°F preheat with other than EXX15 or EXX16, 1100-1250°F stress relief optional, peening may be necessary for thicknesses over 1 inch.
	Over 2-4, Incl	Condition K	

Chapter 8
Repair Considerations

8-1. General

Most damage to hydraulic structures is due to impact of barges and debris, corrosion, or cracking. Many hydraulic structures are riveted and may include damaged or loose rivets that must be replaced. Repairs to hydraulic steel structures must maintain the required structural integrity and should be designed, if possible, to avoid recurrence of the original damage. In all cases, repairs should be designed using industry-approved detailing and fabrication procedures and should be detailed to avoid future corrosion or cracking problems (see paragraph 8-2*a* and paragraph 8-3). Repair of corroded areas is discussed in paragraph 8-2*b*, repair of cracks is discussed in paragraph 8-4, and rivet replacement is discussed in paragraph 8-5. Paragraph 8-6 discusses several repair examples. The type of repair details selected will be determined considering the following factors:

a. Cause of damage. If the cause of original damage is not accounted for, it is likely that the damage will reoccur. If possible, the cause of damage should be eliminated or minimized.

b. Remaining service life of the structure. A repair of a structure that is intended to be in service for only a short time might obviously be less extensive than for a structure intended for longer service.

c. Frequency and type of future inspections. Due to cost or construction constraints, it may be prohibitive to provide an ideal repair. In such cases, a less than ideal repair might be adequate provided a strict inspection plan is developed. Development of inspection schedules for fatigue cracking is discussed in paragraph 6-11.

d. Construction constraints. In general, repairs must be completed in a field environment that will include less than ideal conditions. For example, access to the repaired area may be restricted. Conditions may not be appropriate for welding (i.e., temperature, water, or access may inhibit proper welding). Certain situations might involve decrease in structural strength resulting from temporary removal of rivets, cover plates, or other parts. Distribution of dead and live load stresses must be considered. Repair components are generally effective only in resisting live load unless dead load is removed during repair. Each of these conditions will influence the design of the repair detail.

8-2. Corrosion Considerations

a. New repair details. The primary means to avoid corrosion is by providing a protective coating system. The coating system applied to repair plates or components must be compatible with the protective system of adjacent steel. EM 1110-2-3400, CWGS 09940 and CWGS 05036 provide detailed information on selection, application, and specifications of coating systems. Structural detailing also has a significant impact on susceptibility to corrosion. Repairs should be detailed as much as possible to compensate for conditions that contribute to corrosion (paragraph 3-3*b*). The following items should be considered in the design process:

(1) Detail components such that all exposed portions of the repair detail can be painted properly. Break sharp corners or edges to allow paint to adhere properly.

(2) Where repair plates or components are horizontal, provide drain holes to prevent entrapment of water. Drain holes should be located at the lowest position with the size generally ranging from 25 mm (1 in.) to 75 mm (3 in.) in diameter. The cut edges of holes should be smooth and free of notches especially in areas subject to tensile forces.

(3) Grind weld ends, slag, weld splatter, or any other deposits off the steel. These are areas that form crevices that can trap water. Use continuous welds.

(4) Where dissimilar metals are in contact (generally carbon steel and either stainless steel or bronze), provide an electric insulator between the two metals and avoid large ratios of cathode (stainless steel) to anode (carbon steel) area. Surfaces of both metals should be painted.

(5) Welded connections are generally more resistant to corrosion than bolted connections. In bolted connections, small volumes of water can be trapped under fasteners and between plies that are not sealed. Where possible, use welds in lieu of bolts considering the effect on fracture resistance.

b. Existing corroded components. Where significant corrosion exists but strengthening is not required, the area should be cleaned appropriately and a new protective coating system applied. This will inhibit further corrosion, and future repairs might be avoided. In many cases, gate components such as skin plates include pitting corrosion that reduces component thickness where pitting exists. In certain cases, pits may be repaired by filling with weld metal. If this is done, strict weld procedures must be specified so the process is compatible with the existing base metal. This method is not recommended for fracture-critical components.

8-3. Detailing to Avoid Fracture

a. General considerations. Regarding fracture resistance and fatigue strength, bolted repairs are often preferable to welded repairs. However, bolted repairs typically are more expensive and require more time to design and install. Dimensional constraints can also restrict the use of bolted splice plates. Sound welding, particularly under field conditions encountered during repair operations, can be difficult, increasing the possibility of poor quality welds. Moisture, paint, and other foreign material that can produce weld defects and cracking are often present. Welding residual stresses and degradation of material toughness in the heat-affected zone can also contribute to cracking of the repair. Weld intersections, intermittent welds, and tack welds on tension members should be avoided.

b. Distortion. Most of the fatigue damage detected in U.S. bridges is due to distortion, mainly at unstiffened web gaps at the ends of diaphragms or floor beam connection plates (Keating 1994: Fisher 1984). An excellent summary of case studies on bridge failures due to distortion is presented by Fisher (1984). Out-of-plane behavior has been measured in field testing of lift gates (Commander et al. 1994). Unintended distortion can result from unanticipated forces such as those occurring at a semirigid connection designed to be a simple connection. Unintended distortion is generally due to out-of-plane displacement of structural components that is not accounted for in design. Details that are known to be predisposed to distortion damage should be avoided.

c. Better details.

(1) Most fractures of structural elements are attributed to adverse stress concentration conditions, unintended distortion, and inferior fabrication. Regardless of the primary contributing factor, cracking is generally associated with or assisted by conditions of adverse stress concentration. Therefore, detailing to minimize the effect of stress concentrations will prevent most fractures or at least will provide a more durable condition. If fracture is a concern, the detail that provides the least critical stress concentration condition should be used. In the design of structural details for new or repair applications, utilization of fatigue design criteria is a very simple means to ensure high fracture resistance. Even without fatigue loading, susceptibility to fracture is reflected by the level of stress and the stress concentration condition as discussed in paragraph 3-3*a*.

(2) Fatigue strength relationships (S_r-N curves) for welded details are described in paragraph 2-3b. All bolted details provide a lower bound strength equivalent to a Category B detail. Due to a lower clamping force in rivets, riveted details have lower fatigue strength compatible with Category C or Category D as described in paragraph 2-3c.

(3) A designer has some flexibility in selecting a detail to minimize likelihood of cracking. For a given condition, various details would serve the same purpose but have different fatigue strength. If budget and other constraints permit, a designer should generally choose the detail with the highest fatigue strength (the least likely to have cracking problems) regardless of loading. In cases of repair, the goal should be to provide a condition with an improved fatigue resistance compared to the original condition. Figure 8-1 shows several situations where a detail can be improved.

(4) If possible, all Category E details should be avoided. Figures 8-1a and 8-1b demonstrate that other details with higher fatigue strength may be substituted for Category E details. The gusset plate attachments on the left sketch in each figure produce a Category E in the girder flange at the termination of the longitudinal welds or where there is a transverse weld. The Category E situation can be avoided by using a bolted connection (category B) or a gusset plate with a full-penetration weld ground smooth and a generous radius. In both cases, the stress concentration condition has been improved dramatically. Another way to avoid the adverse effects of Category E details is to locate the detail in a region of low stress. Cover plates can be extended to a region of low flexure, and attachments to flanges can be moved to the web where the flexural stress is low.

(5) Fatigue strength can be improved significantly by providing a smooth transition between connected elements as shown in Figures 8-1b and 8-1c. A flange attachment can be improved from a Category E to a Category B detail by providing a radius transition and grinding the weld smooth (Figure 8-1b). The fatigue strength of a transverse groove weld is improved from a Category C to a Category B by removing the weld reinforcement and grinding the weld smooth (Figure 8-1c) (see groove welded connections of Table 2-1). Other important considerations are to avoid intermittent welds on backup bars and discontinuous backup bars. A category E situation exists at the termination of each intermittent weld, and a built-in crack exists where a backup bar is discontinuous.

8-4. Repair of Cracks

Effective methods for repairing cracks or improving a detail include weld-toe grinding, peening, remelting, and hole drilling. The appropriate repair method for a given situation is dependent on the size and location of the crack and the type of detail at which the cracking occurred. Small through-thickness cracks subject to low stress range can be arrested by drilling a hole at the crack tip. For large cracks and/or higher stress range, repair can be accomplished by removing the crack tip by drilling a hole and repairing the remaining length of the crack by welding or with bolted splice plates. Simply welding the crack closed, even with a full penetration weld, should never be done without removing the crack tip with a hole. Such a repair generally worsens the condition due to the added residual stresses and deleterious thermal effects of welding (see paragraph 2-2c). Shallow surface cracks that typically occur at the toe of fillet welds can be repaired by grinding, air hammer peening, or gas tungsten arc (GTA) remelting. Surface cracks with depths that exceed the penetration capability of GTA remelting and the effectiveness of peening cannot be repaired by these procedures. Such cracks can be repaired by installing bolted splice plates that transfer the stress around the crack.

a. *Hole drilling.* Hole drilling is the most commonly applied means of arresting fatigue cracks. A hole drilled at the tip of a crack essentially blunts the crack tip and the local stress concentration is greatly reduced compared to that for a sharp crack. It has been successfully applied to various types of structures, including navigation lock gates and several bridges (Fisher 1984). Hole drilling is effective for through-thickness cracks in plates or plate components of structural members.
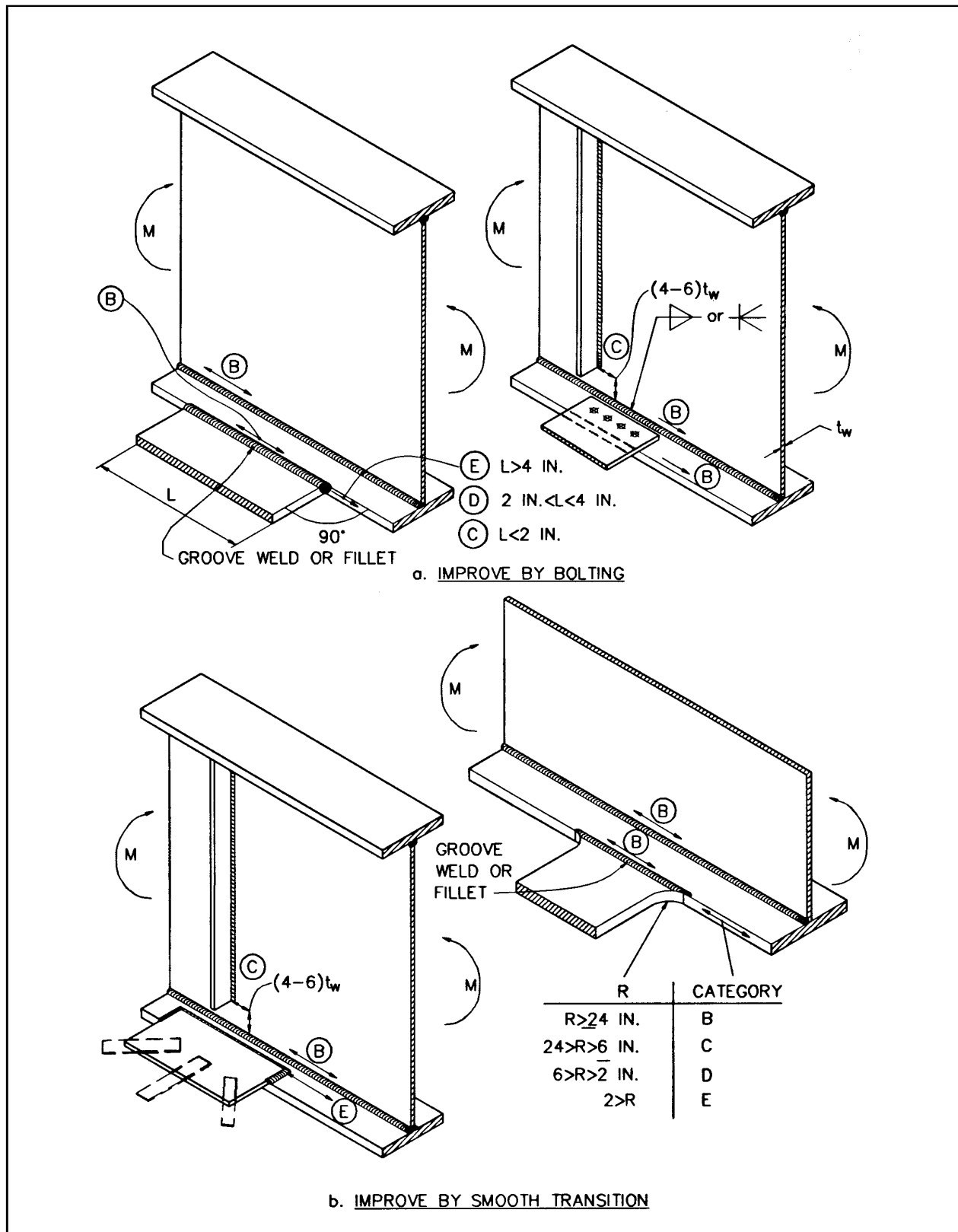
Figure 8-1. Better fatigue details (1 in. = 2.54 cm) (after Fisher 1977) where t_w is the web thickness, M is the bending moment, L is the length of weld considered, and R is the radius on attached component (Continued)
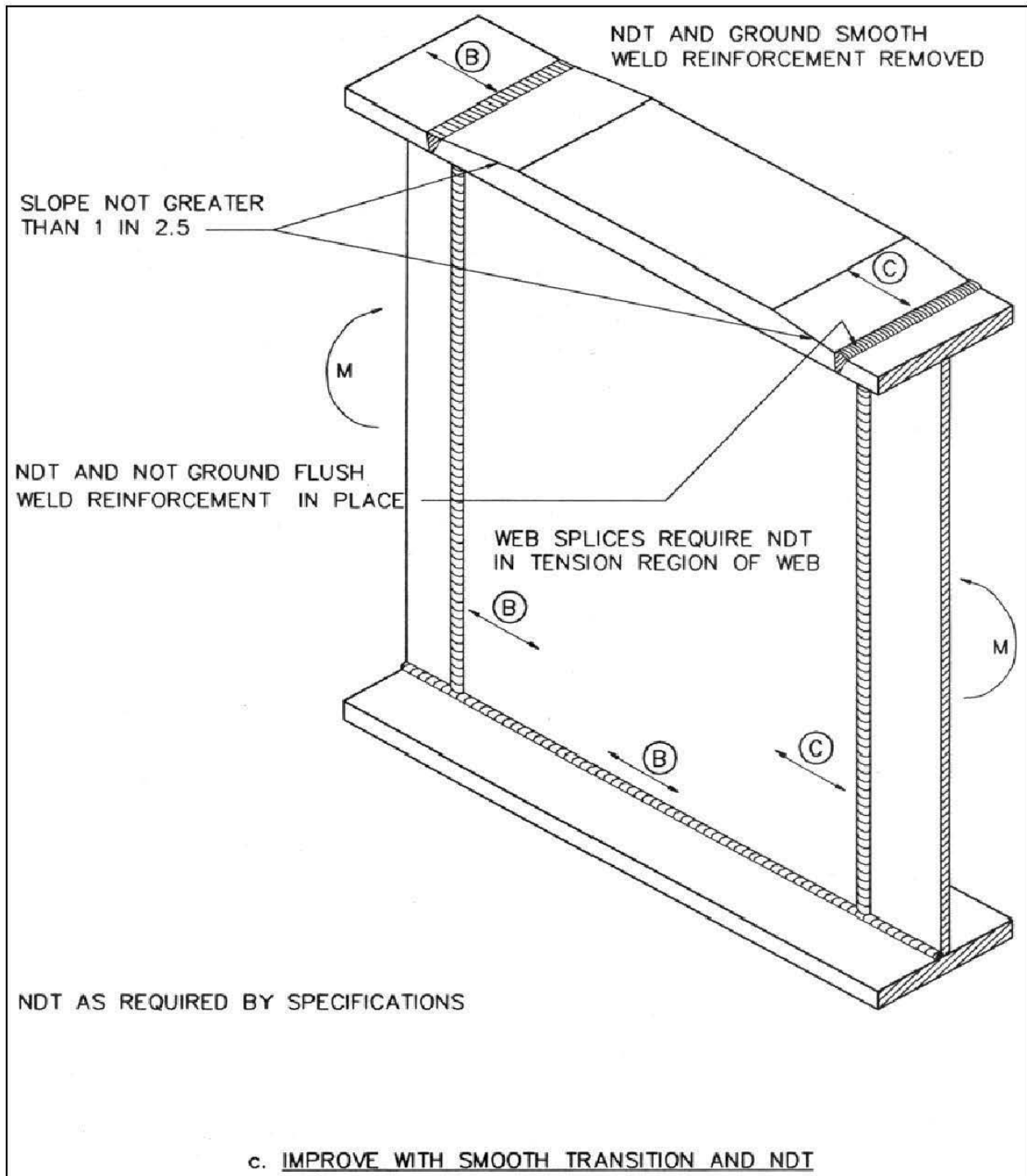
NDT AND GROUND SMOOTH
WELD REINFORCEMENT REMOVED

SLOPE NOT GREATER
THAN 1 IN 2.5

NDT AND NOT GROUND FLUSH
WELD REINFORCEMENT IN PLACE

WEB SPLICES REQUIRE NDT
IN TENSION REGION OF WEB

NDT AS REQUIRED BY SPECIFICATIONS

c. IMPROVE WITH SMOOTH TRANSITION AND NDT

Figure 8-1. (Concluded)

(1) The minimum hole size required to prevent crack initiation can be estimated with the relationship

$$\frac{\Delta K}{\sqrt{r}} = 26.7\sqrt{\sigma_y} \tag{8-1}$$

where

ΔK = stress intensity factor range, MPa-$\sqrt{m}$

r = radius of the hole, m

σ_y = yield stress, MPa

(For non-SI units,

$$\frac{\Delta K}{\sqrt{r}} = 10\sqrt{\sigma_y}$$

where r is in in., σ_y is in ksi, and ΔK is in ksi-$\sqrt{in.}$)

(2) ΔK is calculated considering the entire stress range (algebraic sum of the tensile and compressive stress), and the crack size a (see Equation 6-1) includes the extent of the hole. Equation 8-1 is valid for structural steel and provides reasonable results for moderate stress ranges (less than 40 MPa (6 ksi)) and crack sizes. For most practical cases regarding moderate crack size and stress range less than 40 MPa (6 ksi), a crack will not reinitiate from a hole if the hole diameter is at least one-fifth the total crack length (Keating 1994). Hole diameters of 20 mm (13/16 in.) and 27 mm (1-1/16 in.) are practical since these sizes are commonly used for installation of high-strength bolts. The following are appropriate steps to arrest a small crack in structural steel subject to moderate stress range:

(a) Determine the appropriate hole size (Equation 8-1).

(b) Locate the crack tip with dye penetrant testing.

(c) Drill hole with center at crack tip.

(d) Inspect drilled surface of hole with dye penetrant testing to verify complete removal of crack tip.

(e) In some cases, crack reinitiation may be inhibited by installing tightened bolts in the holes. This introduces local compressive stresses in the through-thickness direction that inhibits crack initiation from the hole.

(3) For larger crack sizes and stress range greater than 40 MPa (6 ksi) (often the case for hydraulic structures), the hole size required by Equation 8-1 is significant and is not practical. In these cases, the crack tip may be removed by drilling a hole and the remaining crack repaired by welding or bolted splice plates. The following are general guidelines for a welded crack repair:

(a) Clean area and determine extent of crack with dye penetrant testing (see paragraph 4-5b).

(b) Drill hole at crack tip location.

(c) Gouge out crack and prepare joint as a full-penetration groove weld in accordance with ANSI/AWS D1.1.

(d) Preheat and weld joint using runout tabs and backing as required per American National Standards Institute/American Welding Society (ANSI/AWS) D1.1.

(e) Remove backing and runout tabs.

(f) Grind weld smooth.

(g) Ream hole to remove weld metal and smooth edges.

(h) Verify removal of crack tip with dye penetrant testing.

(i) Inspect weld with appropriate nondestructive testing (ultrasonic testing or radiographic testing (paragraph 4-5)).

(4) Alternatively, a bolted repair of the fatigue crack can be installed after a hole is drilled to arrest the crack:

(a) Determine extent of crack with dye penetrant testing.

(b) Drill hole at crack tip location.

(c) Verify removal of crack tip with dye penetrant testing.

(d) Prepare and install bolted repair over the crack.

b. Weld toe grinding. Weld-toe grinding reduces the geometrical stress concentration and extends the fatigue life of undamaged details (Keating 1994). Grinding can be used to remove shallow fatigue cracks that may exist in the weld toe. Grinding should always be done in the direction of applied stress. A pencil or rotary burr grinder can be used. Magnetic particle inspection of the ground area should be conducted after grinding to ensure that embedded flaws are not exposed. (Penetrant inspection may reveal false indications due to grinding marks.)

c. Peening.

(1) Peening is effective as a retrofit for shallow surface cracks that commonly occur at fillet weld toes. Peening imposes compressive residual stresses resulting from the plastic deformation induced by the peening hammer and reduces the geometrical stress concentration similar to that with grinding. Air hammer peening is effective in arresting fillet weld toe surface cracks with a depth of up to 3 mm (1/8 in.) if the tensile stress range does not exceed 40 MPa (6 ksi). Peening can also be applied to uncracked fillet welds to improve the fatigue resistance of the detail. The expected benefit of peening under favorable conditions (low stress range, low minimum stress) is an increase in fatigue life approximately equivalent to one fatigue design category (Fisher et al. 1979).

(2) Peening should be done using a small pneumatic air hammer with all sharp edges of the peening tool ground smooth. Although peening intensity can be easily varied by changing air pressure, multiple-pass peening at lower air pressures is most effective. Initial passes of the peening hammer may reveal some cracks that were not initially visible, and peening should be continued until the weld toe is smooth and no cracks are apparent. Penetrant inspection of the peened area should be conducted after peening to ensure that embedded flaws are not exposed. Peening is most effective when performed under dead load so that the imposed compressive residual stress has to be effective only against the live load.

d. Gas tungsten arc remelting.

(1) The GTA remelting process is also an effective procedure for repair of shallow surface cracks that occur at fillet weld toes. This procedure is generally effective for surface cracks with a depth of up to

5 mm (3/16 in.) (slightly greater depths than peening) and is not limited to small stress ranges and minimum stress levels. Like peening, GTA remelting can also be used to improve the performance of uncracked fillet welds, approximately doubling the fatigue life. However, it is not as easily performed in the field, and it requires highly skilled welders and good accessibility.

(2) With the GTA remelting procedure, a small volume of the weld toe and base metal is remelted with a gas-shielded tungsten electrode. After the area cools, the geometric stress concentration is improved and nonmetallic inclusions that might exist along the weld toe are eliminated. When the procedure is applied to crack repair, sufficient volume of the metal surrounding the crack must be melted so that upon solidification, the crack is eliminated. The effectiveness of the procedure is dependent on the depth of the remelted zone, since insufficient penetration would leave a crack buried below the surface. Such a crack would simply continue to propagate, resulting in premature failure. Proper selection of shielding gas and electrode cone angle is crucial in obtaining maximum penetration of the remelted zone. Argon-helium shielding and an electrode cone angle of 60 deg were found to be most effective (Fisher et al. 1979). For any retrofit procedure, the depth of penetration should be verified by metallographic examination of test plates before the procedure is applied in the field.

8-5. Rivet Replacement

a. Missing, loose, or headless rivets and rivets with rosette heads should be replaced (Fazio and Fazio 1984). Deteriorated rivets missing more than 50 percent of the head should be replaced if the rivet is subject to an applied tensile force or tension resulting from prying action (Fazio and Fazio 1984). Rivet heads with rosettes and deteriorating projections should not be built up using weld metal or other materials (brazing, caulking), since these could aggravate rather than improve the condition.

b. Rivets that require replacement should be replaced with high-strength bolts. However, removing a deteriorated rivet is sometimes difficult. The most accepted method of rivet removal is to knock off the rivet head using a pneumatic rivet buster and then force the rivet shaft out of its hole using a powered impact tool (Birk 1989). If necessary, the rivet hole should then be drilled out to obtain an aligned hole through the connected parts. Then a high-strength bolt is installed and tightened by an accepted method such as the turn-of-the-nut method. When pneumatic rivet busters are not available, rivet heads can be burned off. This technique can cause thermal metallurgical damage to the adjacent steel, and may result in burn gouges that adversely affect fatigue strength and susceptibility to corrosion.

8-6. Repair Examples

a.   Crack repair procedures developed for a cracked miter gate.

(1) Description of condition. Figure 8-2 shows a crack in a tension flange of a girder on a miter gate (the photograph shows the inside face of the flange). The crack extends from the termination of a weld joining the flange of a diagonal bracing member and flange of the girder. Similar cracking occurred at perpendicular intersecting members (diaphragm and girder). Numerous through-thickness cracks similar to this occurred on the structure.

(2) Cause of cracking. In general, cracking is attributed to high stress fatigue damage of low fatigue strength details. Cyclic loading occurs due to opening and closing of the gate leaves and to variation in hydrostatic pool. Unusually high stress may have occurred due to unintended loading while the gate was opened and closed with silt buildup at the gate bottom. Most of the cracks occurred at terminations of welds that join intersecting members, similar to the condition shown in Figure 8-2. Considering girder flexure, the fatigue strength of such details is Category E.
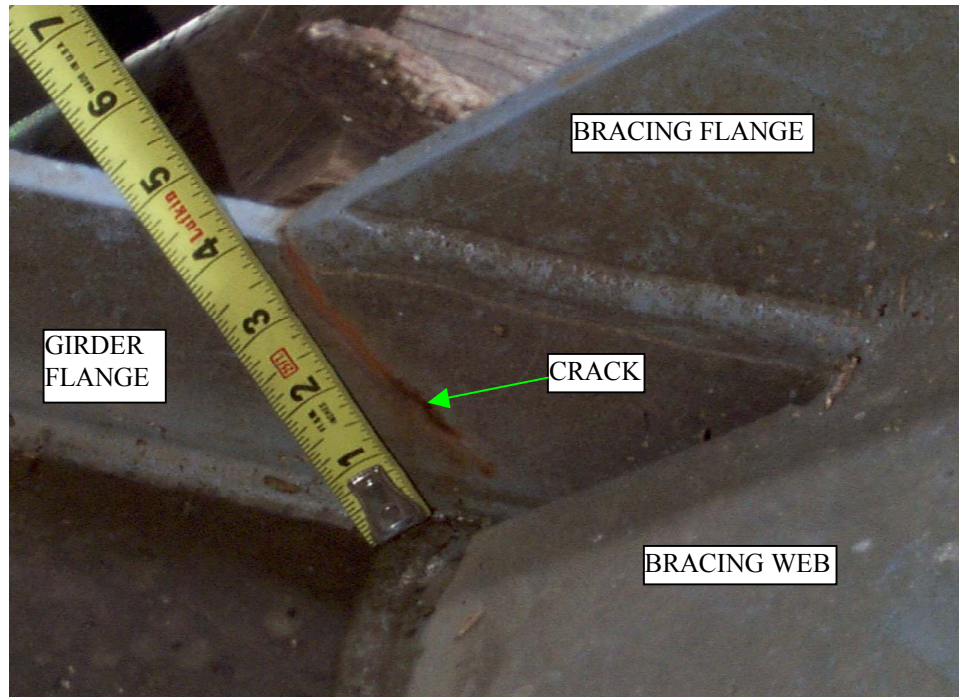
Figure 8-2. Crack in miter gate girder tension flange

(3) Repair alternatives. The following repair alternatives were developed for the miter gate. The types of cracks found on this structure are common to hydraulic structures that have experienced cracking. The presented alternatives are generally applicable to similar situations on all gates.

(a) Figure 8-3 shows a repair procedure that was developed for small cracks (less than 12 mm (1/2 in.)) located at re-entrant corners of perpendicular members. The area should be cleaned and prepared as necessary to locate and mark the crack tip using dye penetrant testing. The radius plate should then be installed using a full-penetration weld with welding in accordance with ANSI/AWS D1.1. The plate should be of the same (or similar) thickness as the adjacent plates (flanges). A 25-mm (1-in.) hole should then be drilled to encompass the crack and to remove the weld intersection. Penetrant testing should be conducted to verify removal of the crack tip, and the area should be repainted. Even if cracking has not occurred, this repair could be used to retrofit poor conditions found at intersecting perpendicular members (i.e., diaphragm and girder) on any structure. The retrofit shown (with radius of 15 cm (6 in.)) improves the fatigue strength from Category E to Category C.

(b) Figure 8-4 shows the selected repair for edge cracks greater than 25 mm (1 in.) The repair should be completed following the guidelines for welded crack repair given in paragraph 8-4*a*. Any type of full-penetration weld is acceptable. For edge cracks that extend into the web, a repair similar to that shown in Figure 8-4 is appropriate. However, some additional steps are required. A crack that extends into the web has a crack tip in the flange opposite that where the crack initiated and in the web. Holes should be drilled at both locations. Additionally, a weld access hole should be cut in the web to accommodate the full-penetration flange weld. The access hole should be proportioned in accordance with ANSI/AWS D1.1. Any type of full-penetration weld is acceptable.

b. Cracked girder, vertically framed miter gate.

(1) Description of condition. Figure 8-5 shows a connection bracket that is welded to the downstream flange of a vertical girder in a spare vertically framed miter gate. The gate consists of 3-m- (10-ft-) high welded modular sections that are stacked vertically and joined by bolts that extend through the connection
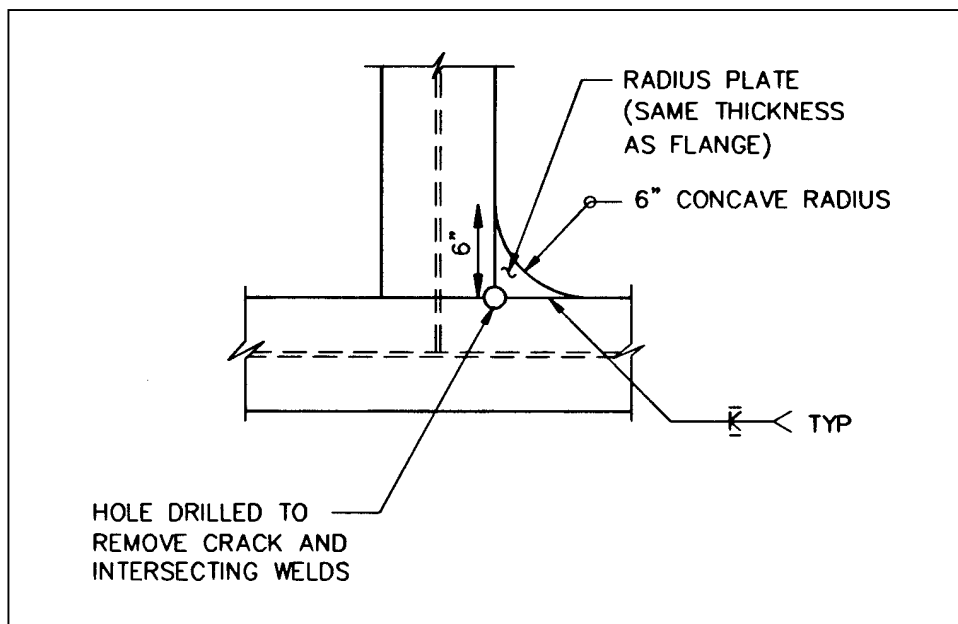
Figure 8-3. Retrofit to improve fatigue strength at intersecting perpendicular members (1 in. = 2.54 cm; 1 ft = 0.3 m)
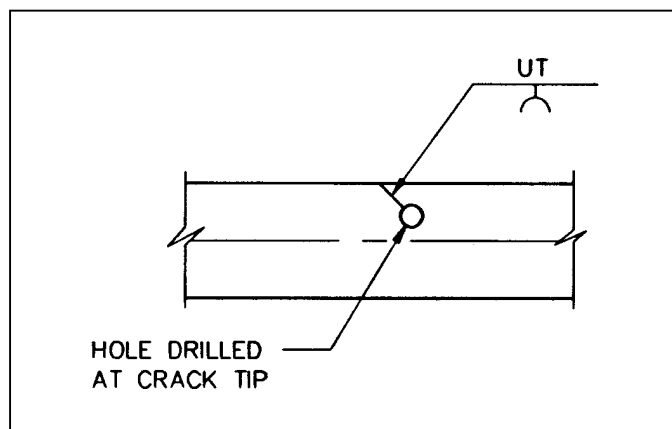

Figure 8-4. Weld repair for edge crack

bracket. The gate was fabricated in 1969 and had been installed several times for temporary use. While in service, the gate did not have any loading greater than the design load. In 1989, it was discovered that the downstream flanges on three of seven vertical girders were cracked as shown in Figure 8-5. In each case the crack extended through the 38-mm- (1-1/2-in.-) thick flange and approximately two-thirds of the way through the web.

   (2) Cause of cracking. The crack was located in the tension flange of the vertical girder at the intersection of the bracket plate and the flange plate. The weld that joins the bracket plate and flange plate is transverse to the direction of stress flow, and the intersection of the two plates creates a severe stress concentration for stress flow through the flange. This situation is similar to that at the end of a welded cover plate and would be classified as a category E fatigue detail. Considering the quality of weld, the actual condition is worse than a Category E. The general weld profile is rough and undercut, which essentially creates a small initial crack. The cracking in three of seven girders illustrates the adverse effects of this type of stress concentration.
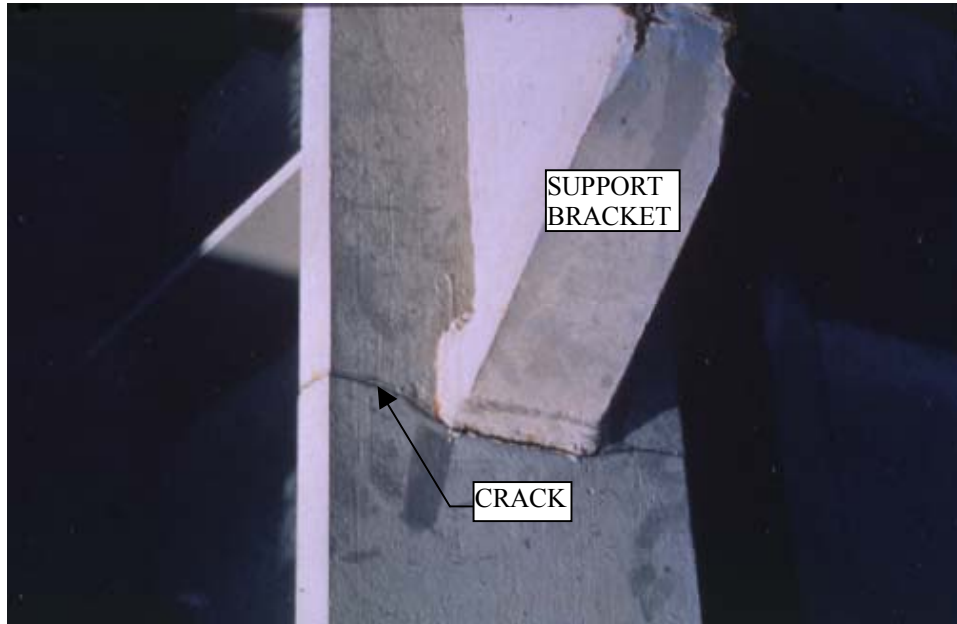
Figure 8-5. Cracked miter gate vertical girder tension flange

(3) Repair alternatives. Due to the general configuration and restrained geometry of this connection, a repair that restores the original intended strength may be difficult to achieve. However, the crack can be repaired using splice plates on the flange and web. The splice plates could be welded or bolted. A bolted repair would result in a Category B detail; however, due to the constrained geometry, the effective area considering the required bolts may be a concern. A welded repair would result in a Category E condition at the end of the splice plates. (However, with modern welding practices, the condition would be improved over that of the original connection.) To minimize the effect of the Category E, the splice plates could be extended into a region of low stress. For either a welded or bolted repair, a hole should be drilled at the crack tips. Prior to cracking, the condition could have been improved by grinding the weld profile smooth, or by retrofitting the welds by peening or GTA remelting procedures. A similar modification was undertaken on an extensive retrofit of the Yellow Mill Pond Bridge in the early 1980s (Fisher 1984).

c. Cracked girder and bracing members on a vertical lift gate.

(1) Description of condition. Figure 8-6 shows a connection between a vertical diaphragm, diagonal bracing members, and a main horizontal girder on a vertical lift gate. This type of connection (intersection of bracing members, diaphragms, and girders) is a very common occurrence on lift gates, miter gates, tainter gates, and bridges. Flanges of bracing members and the diaphragm were each welded directly to the girder flange. Cracking occurred completely through each bracing member and through the diaphragm flange and girder flange (at various locations on this particular structure). The girder is designed to resist flexural forces imposed by hydrostatic pressure, and under this condition, the down-stream flange is subject to tension. The bracing members are designed as members of a truss that resists vertical loads imposed by the gate weight and water pressure. Therefore, the bracing members are presumably subjected to axial tension or compression. Field measurements have shown that out-of-plane displacement and rigidity of end connections may also impose flexure in the bracing members (Commander et al. 1994).
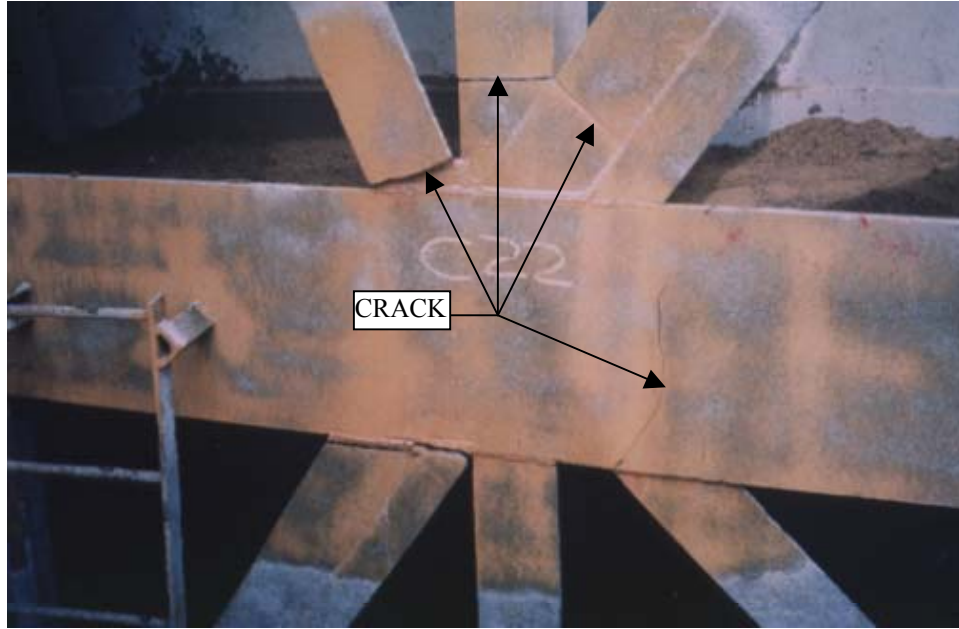
Figure 8-6. Cracked girder, diaphragm, and bracing in a lift gate

(2) Cause of cracking. The location and orientation of cracks indicate that cracking initiated at weld terminations and weld intersections. The re-entrant corners between members and the inferior weld geometry (overlapping welds, transverse to stress and not ground smooth) both create a critical stress concentration condition for the stress flow through the girder flange, diaphragm flange, and bracing members. The attachment to the girder tension flange is a Category E, and considering axial behavior of intersecting members, a Category C, D, or E situation exists depending on the thickness of joined elements. (With overlapping welds and poor weld profiles, the strength is likely less than that of a Category E detail.)

(3) Repair alternatives. It is necessary to restore the girder strength and to provide adequate connections of the intersecting members. To avoid future fractures, the repair details should improve the original condition if possible. Various alternatives could be used to repair the girder while improving the original condition:

(a) One alternative would be to drill holes at the ends of each existing crack and to add a bolted gusset plate as shown in Figure 8-7. The gusset plate would be sized such that the plate and connected flanges would resist the required forces considering the net area. This alternative would improve the fatigue strength to Category B; however, due to the number of bolts required and the resulting reduction in net area, a very large plate would likely be necessary.

(b) A second alternative would be to use a welded gusset plate. A gusset plate could be placed over the existing flanges and welded to each flange. This would provide a temporary patch; however, the fatigue strength considering bracing and girder stresses would be Category E (although with proper welding procedures and no intersecting welds, the situation would be improved over the original condition).

(c) A better detail is shown in Figure 8-8. This would require removing a specified length of flange from each of the intersecting members and replacing the flanges with a single gusset plate. All of the member flanges would be welded to the gusset plate with full-penetration groove welds, and the member
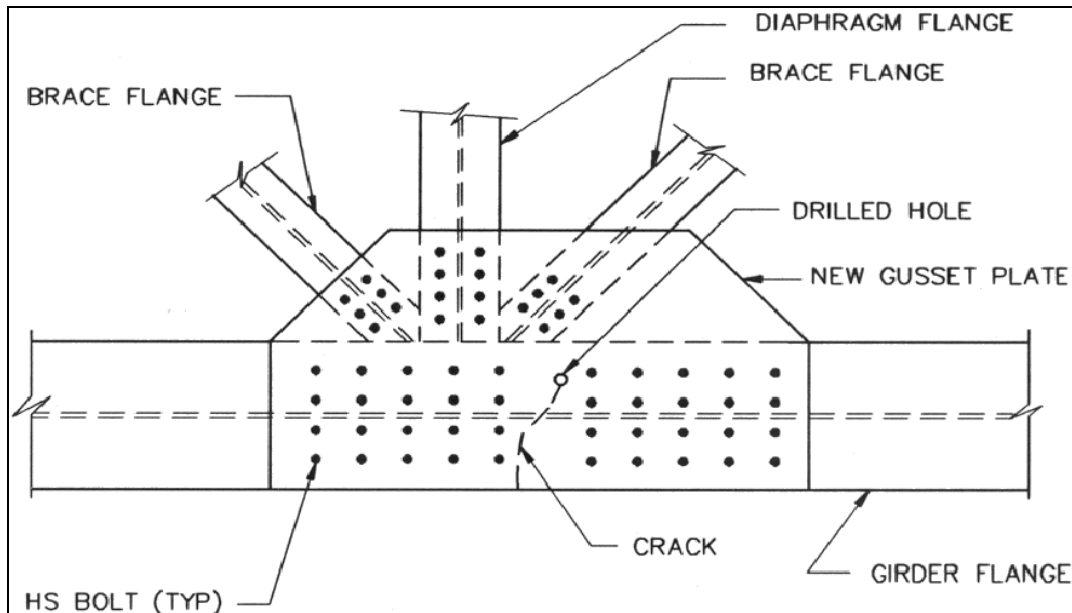
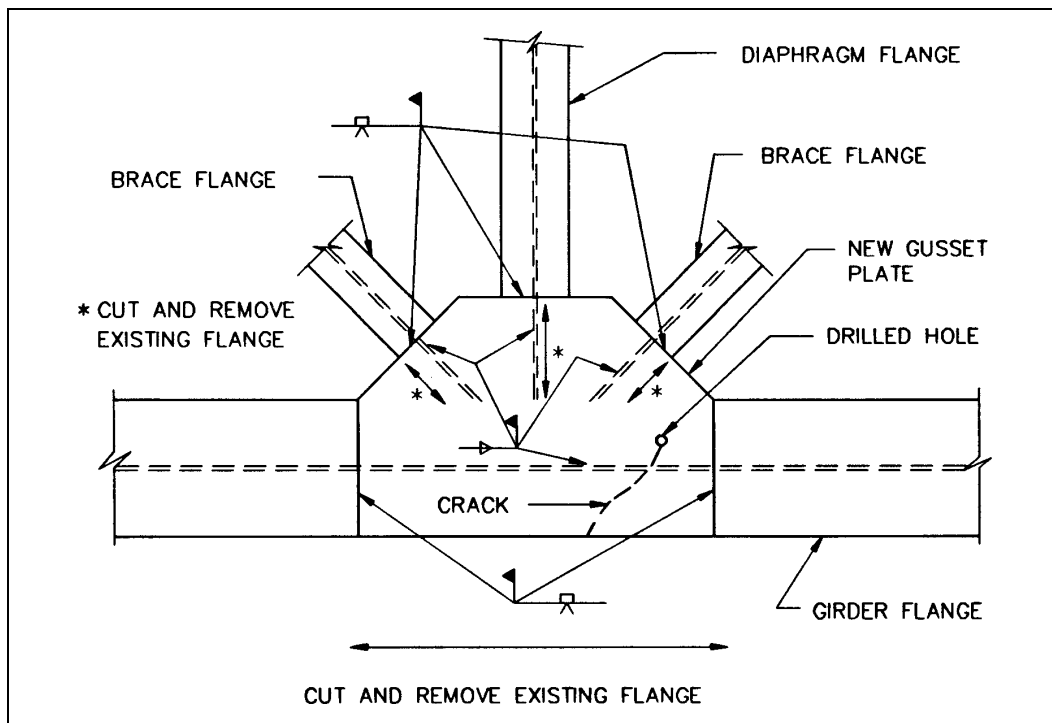**Figure 8-7. Bolted repair alternative for cracked lift gate**

Figure 8-8. Welded repair alternative for cracked lift gate

webs would be welded to the gusset plate with full-penetration or fillet welds. Web access holes are required at flange welds and should be prepared in accordance with ANSI/AWS D1.1. The exact configuration should be determined to avoid intersecting welds. With this approach, the detail would improve from a Category E to a Category C or B depending on weld profile and weld inspection requirements (see requirements for groove welded connections in Table 2-1).

    d. *Cracked bridge floor beam connection angle.*

    (1) Description of condition. Figure 8-9 shows a crack in a connection angle that attaches a floor beam to one web of a box girder in a USACE tied arch bridge. The crack extends from the upper edge of the connection angle downward along the fillet of the angle. The cracks were discovered after approximately 40 years of service. Similar cracks have been found in at least four connections. The cracks were repaired by drilling a hole at the end of the crack approximately 6 years ago. Recently, cracking through the hole was observed in at least one location.
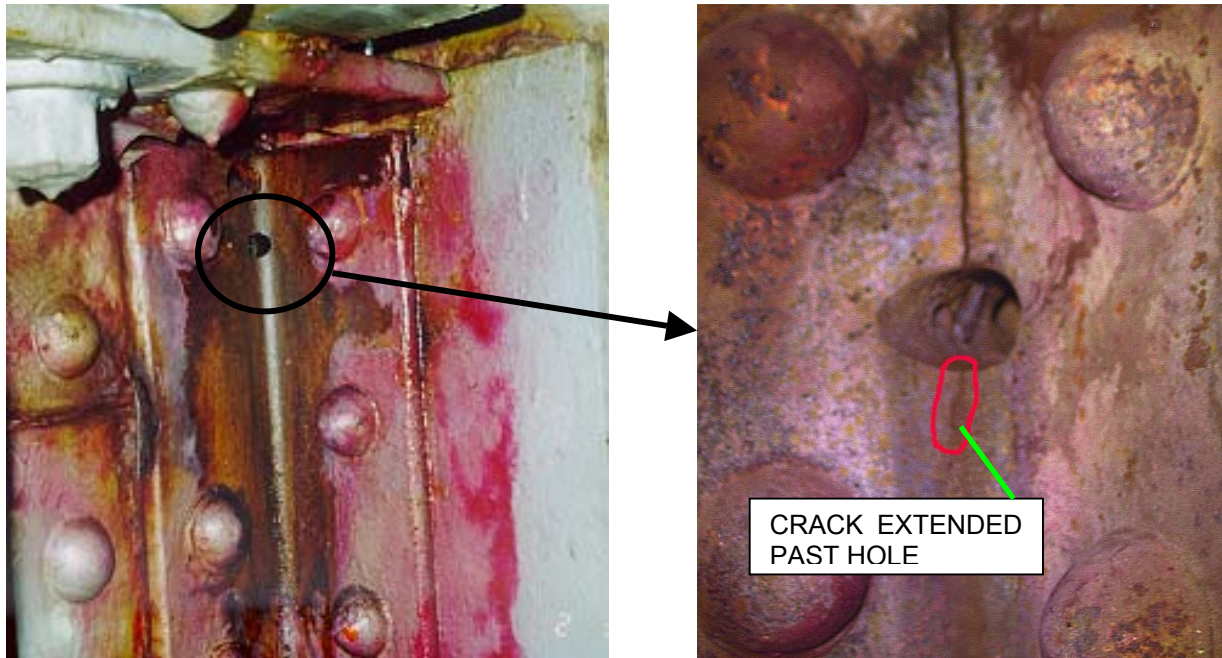

CRACK EXTENDED PAST HOLE

Figure 8-9. Crack in bridge floorbeam connection angle

    (2) Cause of cracking. For the purposes of this example, it is assumed that floor beam flexural forces cause unintended distortion of the connection angle that was not accounted for in the design. The connection is assumed to be a simple shear connection and was not designed to resist floor beam flexure. However, the angle actually resists out-of-plane forces due to connection rigidity, and the crack driving force is apparently due to the floor beam flexure. The prior repair, which consisted of drilling a hole at the end of the crack, served to arrest the crack temporarily. However, since the out-of-plane displacement is not restrained and the floor beam flexure still exists, the crack has reinitiated from the hole.

    (3) Repair alternatives. To eliminate the cause of cracking, the connection must be modified to reduce the inherent rigidity (to minimize bending forces) or to increase the rigidity (to minimize the out-of-plane displacement of the connection angle). Cases similar to this are discussed by Keating (1994) and Fisher (1984).

    (a) Simple connection. One alternative is to alter the floor beam connection detail to reduce the connection rigidity such that minimal flexure is imposed at the end of the floor beam. This would eliminate the driving force that causes the out-of-plane distortion of the angle. Although many repair details could be designed to serve this purpose, one possibility would be to remove rivets at the top of the angle and to cut away the corresponding length of angle to reduce the angle length. To account for the lost shear strength, a seat angle could be added at the bottom of the floor beam. This alternative would

maintain the required shear strength and would reduce the connection rigidity that causes crack driving force.

(b) Rigid connection. Another alternative would be to reinforce the connection to prevent the distortion. This could be done by attaching the top flange of the floor beam to the box girder web using a tee section with its flanges bolted to the box girder web and its web bolted to the top flange of the floor beam. The top portion of the existing connection angle would have to be removed to provide room for the tee flange. Although the displacement of the original connection angle would be controlled, large flexural forces would develop at the end of the floor beam due to the connection rigidity. This may result in other problems such as distress of the girder web, since the connection was designed as a simple connection.

e. Fractured bars on a trashrack.

(1) Description of condition. Figure 8-10 shows a trashrack used at an inlet structure on a dam. The trashrack is composed of a steel outer frame, two support beams, and several screen bars that span the frame across the support beams. The bars were attached on the upstream face of the rack with the edges of the bar welded directly to the support beams and frame with fillet welds. Seventeen out of twenty of the bars fractured completely as shown in Figure 8-10. In each of the fractured bars, the cracks initiated at the end of the weld that joins the bar to the supporting member (on the downstream edge of the bar).

Figure 8-10. Fractured screen bars on dam intake trashrack

(2) Cause of cracking. Design loads consisted of lateral hydrostatic loads that induce flexure in the bars. The direction of bending in the bar at the welds is such that the design stress is compressive on the downstream edge of the bar at the crack locations. Therefore, under design assumptions, cracking is not expected. The cracking is attributed to tensile fatigue stresses caused by out-of-plane distortion of the bars

as they are vibrated by passing water. The weld termination and abrupt change in geometry between the bar and supporting member create a severe stress concentration resulting in a detail with low fatigue strength. Even with vibration due to passing water, the cracking might not have occurred given connection details with higher fatigue strength.

(3) Repair alternatives.

(a) The attachment between the screen bars and supporting members creates a severe stress concentration condition that could be avoided by using a different type of connection. Similar trashracks have been designed where the supporting members have carefully sized holes through which the screen bars pass and there is no need for a welded attachment. This eliminates the stress concentration at the weld, and it is likely that the screen bars would have a significantly longer life. The actual repair for this case is shown in Figure 8-11. New screen bar supports with holes (retainer bars) were fabricated and attached to the existing channel support members with bolts. The bars were then threaded through the retainer bar holes and held in place by angles at the bar ends oriented perpendicular to the bars and attached to the existing frame with bolts.

(b) The selected repair eliminated the stress concentration and may have reduced the future number of load cycles. The fatigue strength has been improved from a detail similar to Category E to Category A. The repair may also decrease the vibration of the bars with passing water since the new screen bar edges were rounded on the upstream edge to minimize hydraulic disturbance. Additionally, the overall flexural stiffness of the bars has been reduced significantly since the bars are now free to rotate at the connection points. This affects the natural frequency of vibration of the bars and may reduce vibration as water passes.

 f.   Crack at diaphragm flange to girder flange intersection in a lift gate.

(1) Description of condition. Figure 8-12 shows a crack in the downstream girder flange of a vertical lift gate. The crack initiated at the end of the weld between a diaphragm flange and downstream girder flange and propagated into the girder flange. The fatigue strength of the girder flange at the weld termination is analogous to Category E. Under typical design assumptions, the girder is in flexure due to lateral hydrostatic forces and the downstream flange is subject to tensile stress. If cracking were to occur considering design assumptions, the expected direction of cracking in the girder flange would be transverse to the flange (perpendicular to flexural tensile stress). However, the crack is oriented at approximately 45 degrees to the horizontal girder flange.

(2) Cause of cracking. The crack is located at the re-entrant corner between flanges (a severe stress concentration condition), and tensile cyclic stress exists in the flange at this location. The cracking is attributed to fatigue cracking of a detail with low fatigue strength. It is also presumed that the condition was exasperated by out-of-plane distortion of the girder flange. Under vertical hydrostatic loading on the lift gate, the horizontal girder flanges displace in a vertical plane similar to a uniformly loaded simple beam as shown in Figure 3-5. The figure illustrates displacement of downstream girder and diaphragm flanges due to vertical loading. The ends of diaphragm flanges are forced to rotate with the displaced girder flanges causing out-of-plane flexure in the diaphragm flanges. This induces stresses acting parallel to the diaphragm flange with tension on one edge and compression on the other as shown in Figure 3-5. Experimental measurements of lift gate stresses verify this behavior (Commander et al. 1994). At the point of crack initiation, longitudinal tension stresses exist in both the girder flange (due to lateral hydrostatic loading) and diaphragm flange (due to out-of-plane distortion). The combined effect of these perpendicular tensile stresses results in a primary tensile stress that acts perpendicular to the direction of the existing crack.
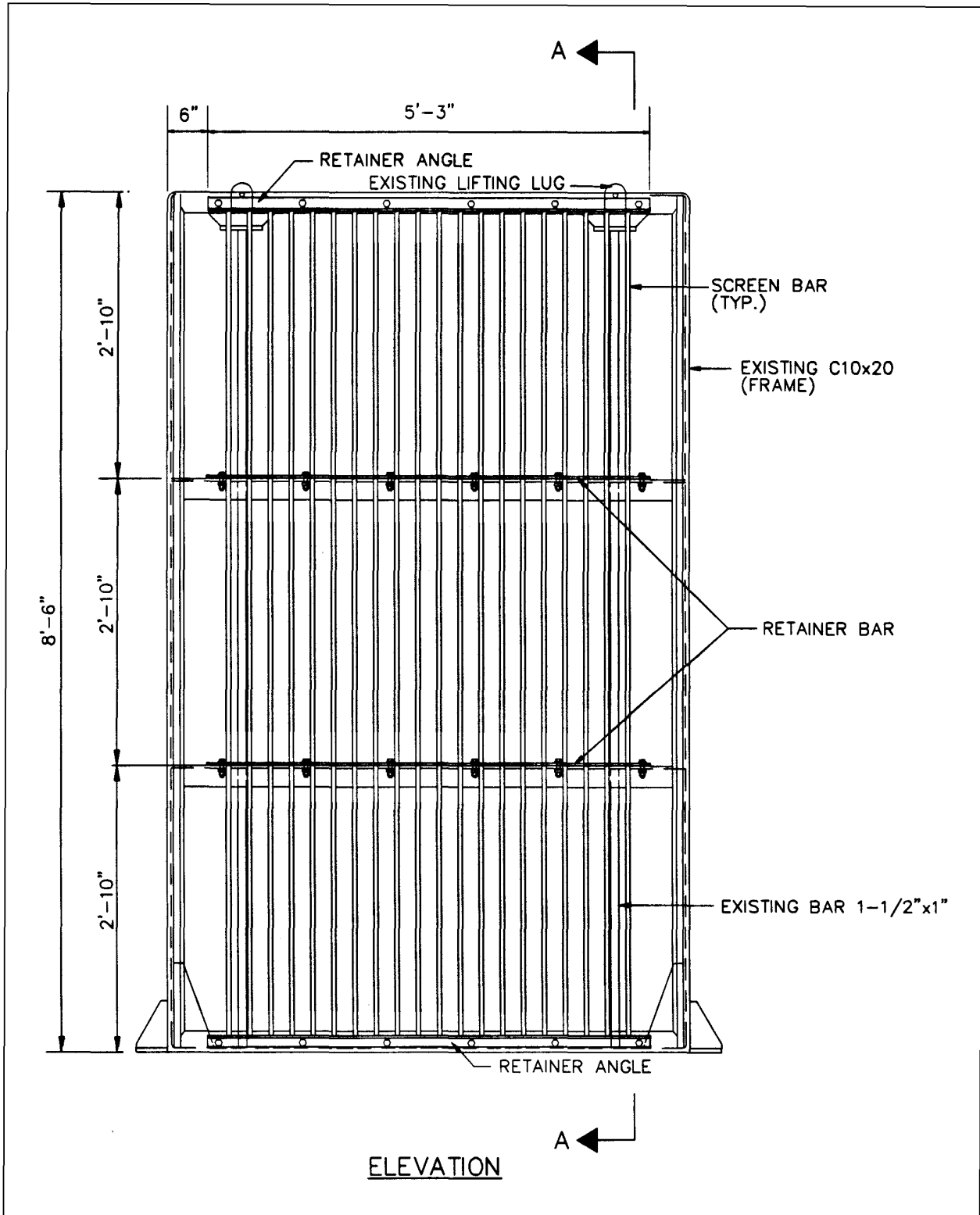
ELEVATION

Figure 8-11. Trashrack repair details (1 in. = 2.54 cm; 1 ft = 0.3 m) (Continued)

SECTION A-A

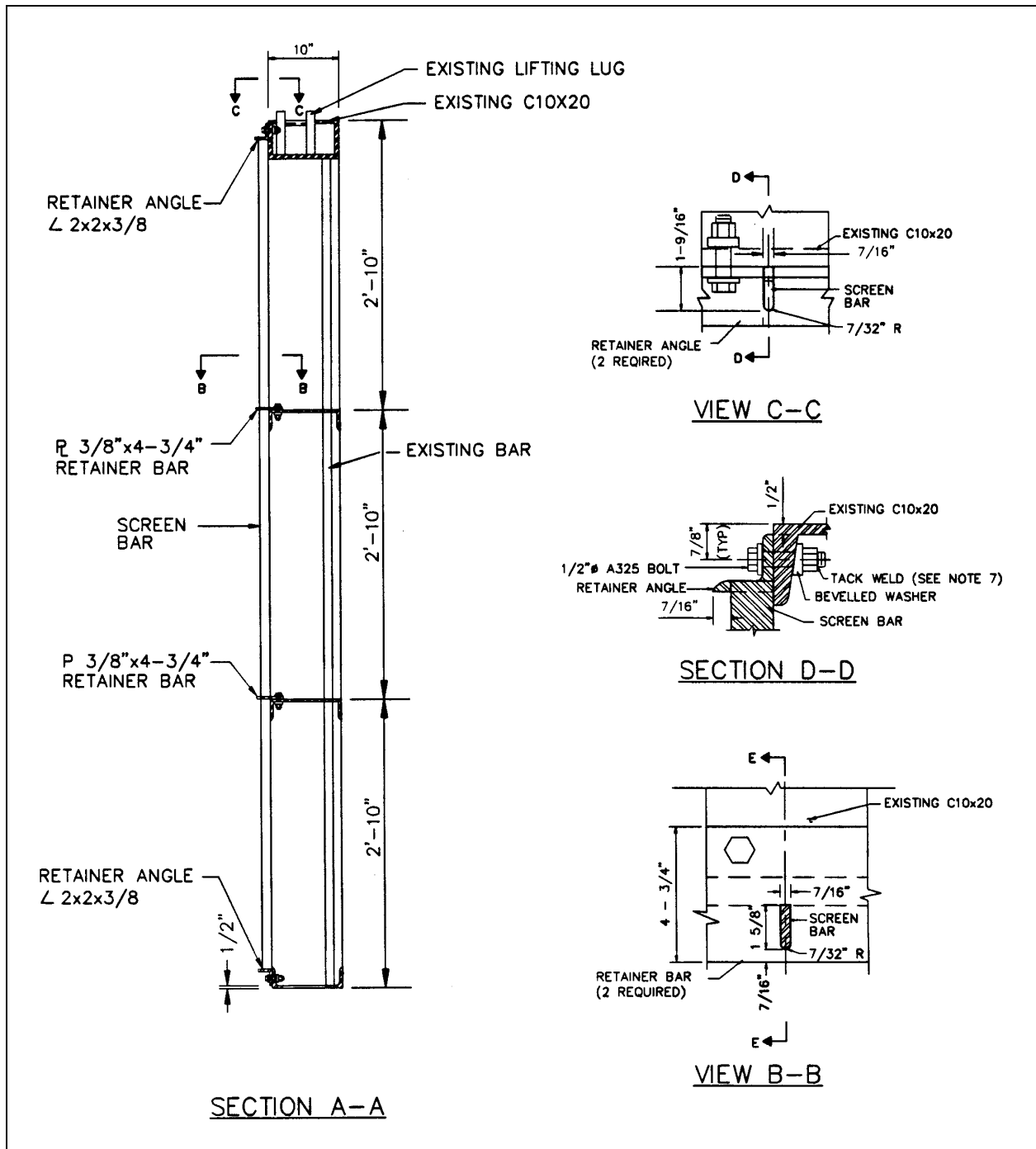VIEW C-C

SECTION D-D

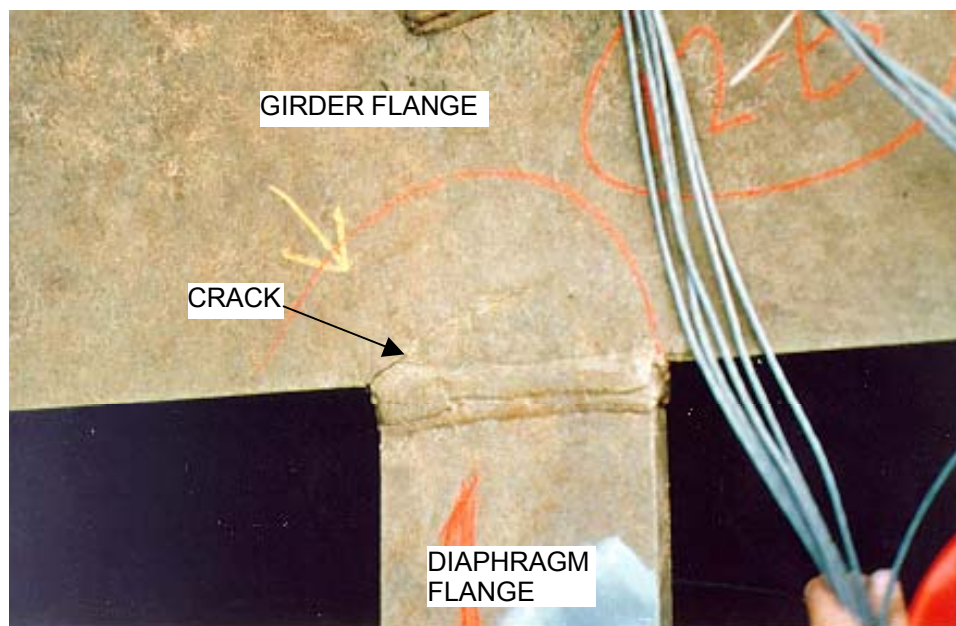VIEW B-B

Figure 8-11. (Concluded)

Figure 8-12. Cracked girder tension flange at diaphragm of a lift gate

(3) Repair alternatives.

(a) The ideal crack repair would also improve the fatigue strength of the detail and would eliminate the out-of-plane distortion. However, to eliminate the displacement shown in Figure 3-5 would require significant structural modification, and the cracking might not have occurred given connection details with higher fatigue strength. The fatigue strength of the detail would be improved by providing a smooth radius between the diaphragm flange and girder flange. This would improve the stress concentration condition and could theoretically improve the fatigue strength from Category E to Category B (see condition 16 of Table 2-1). The recommended repair is a combination of crack repair procedures shown in Figures 8-3 and 8-4. First, repair the crack according to Figure 8-4 while following the guidelines for welded crack repair given in paragraph 8-4*a*. Then add the radius plate and drill the hole as shown in Figure 8-3 and as described in paragraph 8-6*a*(3).

(b) Another possible alternative would be to install a bolted repair similar to that shown in Figure 8-7 (a similar repair is described in paragraph 8-6*c*(3)). Before the bolted repair is installed, the crack tip should be drilled and the diaphragm-flange-to-girder-flange weld should be removed to eliminate the stress concentration.

(c) In the design of new gates, the low fatigue strength details could be eliminated by installing a skin plate on the downstream face of the gate. This was done in a recent design of a vertical lift gate. Instead of downstream bracing members, the new design called for a skin plate on the downstream face of the gate.

g. Crack in vertical lift gate at uncoped web stiffener.

(1) Description of condition. A through-thickness crack that extends through the tension flange of a built-up girder on a vertical lift gate is shown in Figure 8-13. The structure had been in service for less than 2 years at the time the crack was discovered. The crack is located where an uncoped transverse web stiffener is attached. The crack apparently initiated at the intersection of the three welds (web-to-flange,

Figure 8-13. Cracked girder tension flange of a lift gate

stiffener-to-web, and stiffener-to-flange). Figure 8-14 shows the intersection of welds where the girder web, girder flange, and stiffener are joined.

(2) Cause of cracking. The three intersecting welds (web-to-flange, stiffener-to-web, and stiffener-to-flange) each contract during cooling and contain tensile residual stresses creating a state of triaxial tension stress. Under the condition of triaxial tensile stress, steel cannot yield and an extremely brittle condition exists. Additionally, at locations of intersecting welds, there is often a lack of fusion at the end of one or both stiffener welds. This results in an embedded discontinuity. The fatigue category considering girder flexure is a Category C for a stiffener coped per American Association of State Highway and Transportation Officials (AASHTO) requirements (minimum cope dimension is required to be at least 4 times the thickness of the web). However, the described condition has much lower fatigue strength due to the increased brittleness and likelihood of embedded discontinuities. The use of uncoped stiffeners should always be avoided; however, there are many such cases in existing USACE structures. A similar condition exists in many vertical lift gates and miter gates where built-up girders and diaphragms intersect. If the diaphragm web is not coped, intersecting welds exist (girder-web-to-girder-flange weld, diaphragm-web-to-girder-web weld, and the diaphragm- web-to-girder-flange weld).

(3) Repair alternatives. Prior to cracking, a general retrofit for uncoped stiffeners is to drill a hole in the stiffener adjacent to the intersection and grind all surfaces smooth. The drilled hole removes the weld intersection and effectively serves as a cope. A similar type repair has been completed on web connection plates that intersect with transverse web stiffeners (Fisher 1984). The actual repair of this condition consisted of a bolted splice plate (Figure 8-15). Ideally, the stiffener should have been drilled near the intersection (as previously described) before the splice plate was installed. Additionally, the crack tip should have been located and drilled out. With this repair, the crack is isolated and the fatigue strength is improved to Category B. It is possible that a welded repair (similar to that described in paragraph 8-6*a*(3) for a crack that extends into the web), could have been completed. However, such a weld repair would have been difficult or impossible with the existing stiffener located adjacent to the crack.
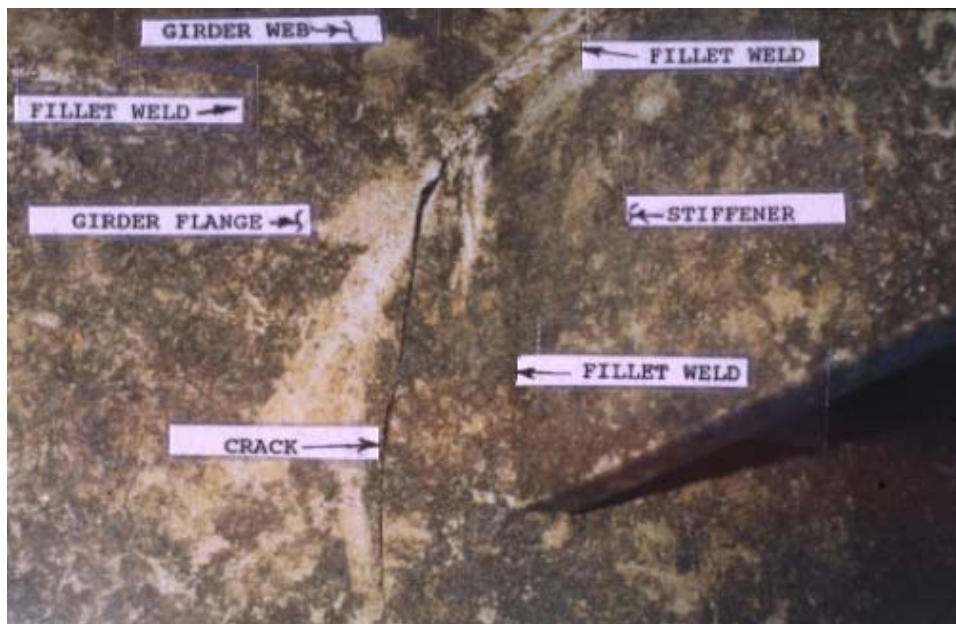
Figure 8-14. Intersecting welds at web stiffener of the girder shown in Figure 8-13

Figure 8-15. Bolted repair splice for the girder shown in Figure 8-13

h. Cracked handrails.

(1) Description of condition. After less than 2 years of service, severe cracking occurred at numerous locations on a welded steel handrail (Figure 8-16). The basic railing configuration is shown in Figure 8-17. All railing consists of 38-mm (1-1/2-in.) stainless steel pipe. The top rails are continuous and are fillet welded to the top of vertical posts. The bottom rails consist of segments of pipe fillet welded at each end to the vertical posts. Considering flexure in the rails, the fatigue strength of the rails at
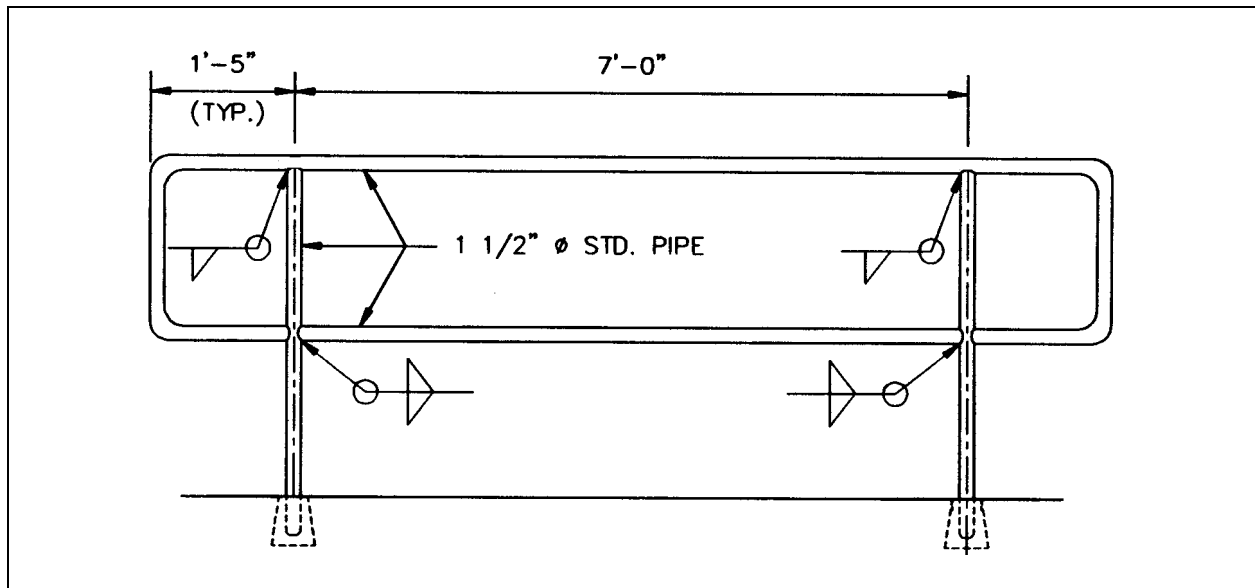
Figure 8-16. Cracked steel handrail

Figure 8-17. Steel handrail schematic (1 in. = 2.54 cm; 1 ft = 0.3 m)

the post is similar to Category C. Vertical cracks (perpendicular to the rails) located at the outer edges of the posts occurred in the top and bottom rails at numerous locations. Several of the cracks propagated through the pipe.

    (2) Cause of cracking. Cracking is attributed to high cycle fatigue. A laboratory analysis was conducted on one of the failed pipes to determine the cause of cracking. The analysis showed that the crack

initiated at the weld toe and propagated to failure under high cycle vibration loading. Field observations confirmed that the rails vibrated with significant midspan displacement when subjected to wind loading.

(3) Repair. The handrails were repaired with bolted tee and cross fittings fabricated to fit snugly around the intersecting pipes (Figure 8-18). The fittings consist of two pieces that sandwich the pipe like two halves of a sleeve to form a bolted splice. The first repair fittings were aluminum because steel fittings were not available. Therefore, corrosion was also a consideration since stainless steel and aluminum are dissimilar metals. To protect the aluminum from corroding, an electric isolater that consisted of a thick epoxy-based paint was applied to the inside surface of the fittings. After 2 to 3 years, the aluminum fittings had corroded significantly. The fittings have since been replaced with custom-manufactured stainless steel fittings.   This repair improved the original fatigue strength from Category C to Category B. In addition, the rails are now more flexible since their end connections are no longer rigid. This may improve the vibration problem (similar to the discussion of repair of the trashrack bars in paragraph 8-6*e*).

Figure 8-18. Bolted tee connection retrofit of fractured hand rail

Appendix A
References

A-1. Required Publications

ER 1110-2-100
Periodic Inspection and Continuing Evaluation of Completed Civil Works Structures

ER 1110-2-1150
Engineering and Design for Civil Works Projects

ER 1110-2-8157
Responsibility for Hydraulic Steel Structures

EM 1110-2-2105
Design of Hydraulic Steel Structures

EM 1110-2-2701
Vertical Lift Gates

EM 1110-2-2702
Design of Spillway Tainter Gates

EM 1110-2-2703
Lock Gates and Operating Equipment

EM 1110-2-3400
Painting: New Construction and Maintenance

CWGS 05036
Metallizing: Hydraulic Structures

CWGS 09940
Painting: Hydraulic Structures

American Association of State Highway and Transportation Officials 1996
American Association of State Highway and Transportation Officials. 1996. "Standard Specifications for Highway Bridges," Designation: AASHTO HB-16, 16th ed., Washington, DC.

ANSI/AWS B1.10
American National Standards Institute/American Welding Society. "Guide for the Nondestructive Inspection of Welds," Designation: ANSI/AWS B1.10-99, Miami, FL.

ANSI/AWS D1.1
American National Standards Institute/American Welding Society. "Structural Welding Code – Steel," Designation: ANSI/AWS D1.1-2000, Miami, FL.

ANSI/AWS QC1
American National Standards Institute/American Welding Society. "Standard for AWS Certification of Welding Inspectors," Designation: ANSI/AWS QC1-96, Miami, FL.

American Society for Nondestructive Testing 1980
American Society for Nondestructive Testing. 1980. "Recommended Practice No. SNT-TC-1A," Columbus, OH.

ASTM A36M-97
American Society for Testing and Materials. "Specification for Carbon Structural Steel," Philadelphia, PA.

ASTM A435/A435M
American Society for Testing and Materials. "Standard Specification for Straight-Beam Ultrasonic Examination of Steel Plates," Philadelphia, PA.

ASTM A514/A514M
American Society for Testing and Materials. "Specification for High-Yield-Strength, Quenched and Tempered Alloy Steel Plate, Suitable for Welding," Philadelphia, PA.

ASTM A517/A517M
American Society for Testing and Materials. "Specification for Pressure Vessel Plates, Alloy Steel High-Strength, Quenched and Tempered," Philadelphia, PA.

ASTM A572/A517M
American Society for Testing and Materials. "Specification for High-Strength Low-Alloy Columbium-Vanadium Structural Steel," Philadelphia, PA.

ASTM A577/A577M
American Society for Testing and Materials. "Standard Specification for Ultrasonic Angle-Beam Examination of Steel Plates," Philadelphia, PA.

ASTM D2688
American Society for Testing and Materials. "Standard Test Methods for Corrosivity of Water in the Absence of Heat Transfer (Weight Loss Methods)," Philadelphia, PA.

ASTM E4
American Society for Testing and Materials. "Practices for Force Verification of Testing Machines," Philadelphia, PA.

ASTM E8
American Society for Testing and Materials. "Test Methods for Tension Testing of Metallic Materials," Philadelphia, PA.

ASTM E10
American Society for Testing and Materials. "Test Method for Brinell Hardness of Metallic Materials," Philadelphia, PA.

ASTM E18
American Society for Testing and Materials. "Test Methods for Rockwell Hardness and Rockwell Superficial Hardness of Metallic Materials," Philadelphia, PA.

ASTM E23
American Society for Testing and Materials. "Test Methods for Notched Bar Impact Testing of Metallic Materials," Philadelphia, PA.

ASTM E30
American Society for Testing and Materials. "Test Methods for Chemical Analysis of Steel, Cast Iron, Open-Hearth Iron, and Wrought Iron," Philadelphia, PA.

ASTM E92
American Society for Testing and Materials. "Test Method for Vickers Hardness of Metallic Materials," Philadelphia, PA.

ASTM E94
American Society for Testing and Materials. "Guide for Radiographic Testing," Philadelphia, PA.

ASTM E110
American Society for Testing and Materials. "Test Method for Indentation Hardness of Metallic Materials by Portable Hardness Testers," Philadelphia, PA.

ASTM E114
American Society for Testing and Materials. "Practice for Ultrasonic Pulse-Echo Straight-Beam Examination by the Contact Method," Philadelphia, PA.

ASTM E142
American Society for Testing and Materials. "Method for Controlling Quality of Radiographic Testing," Philadelphia, PA.

ASTM E164
American Society for Testing and Materials. "Practice for Ultrasonic Contact Examination of Weldments," Philadelphia, PA.

ASTM E165
American Society for Testing and Materials. "Test Method for Liquid Penetrant Examination," Philadelphia, PA.

ASTM E190
American Society for Testing and Materials. "Test Method for Guided Bend Test for Ductility of Welds," Philadelphia, PA.

ASTM E208
American Society for Testing and Materials. "Test Method for Conducting Drop-Weight Test to Determine Nil-Ductility Transition Temperature of Ferritic Steels," Philadelphia, PA.

ASTM E214
American Society for Testing and Materials. "Practice for Immersed Ultrasonic Examination by the Reflection Method Using Pulsed Longitudinal Waves," Philadelphia, PA.

ASTM E242
American Society for Testing and Materials. "Reference Radiographs for Appearances of Radiographic Images as Certain Parameters Are Changed," Philadelphia, PA.

ASTM E350
American Society for Testing and Materials. "Test Methods for Chemical Analysis of Carbon Steel, Low-Alloy Steel, Silicon Electrical Steel, Ingot Iron, and Wrought Iron," Philadelphia, PA.

ASTM E399
American Society for Testing and Materials. "Test Method for Plane-Strain Fracture Toughness of Metallic Materials," Philadelphia, PA.

ASTM E709
American Society for Testing and Materials. "Guide for Magnetic Particle Examination," Philadelphia, PA.

ASTM E747
American Society for Testing and Materials. "Practice for Design, Manufacture, and Material Grouping Classification of Wire Image Quality Indicators (IQI) Used for Radiology," Philadelphia, PA.

ASTM E999
American Society for Testing and Materials. "Guide for Controlling the Quality of Industrial Radiographic Film Processing," Philadelphia, PA.

ASTM E1025
American Society for Testing and Materials. "Practice for Design, Manufacture, and Material Grouping Classification of Hole-Type Image Quality Indicators (IQI) Used for Radiology," Philadelphia, PA.

ASTM E1032
American Society for Testing and Materials. "Method for Radiographic Examination of Weldments," Philadelphia, PA.

ASTM E1290
American Society for Testing and Materials. "Test Method for Crack-Tip Opening Displacement (CTOD) Fracture Toughness Measurement." Philadelphia, PA.

ASTM E1316
American Society for Testing and Materials. "Terminology for Nondestructive Examinations," Philadelphia, PA.

ASTM G46
American Society for Testing and Materials. "Guide for Examination and Evaluation of Pitting Corrosion." Philadelphia, PA.

ASTM G96
American Society for Testing and Materials. "Guide for On Line Monitoring of Corrosion in Plant Equipment (Electrical and Electrochemical Methods)," Philadelphia, PA.

American Society of Mechanical Engineers 1978
American Society of Mechanical Engineers. 1978. "Rules for Inservice Inspection of Nuclear Power Plant Components." *ASME Boiler and Pressure Vessel Code, Section XI,* New York.

American Welding Society 1998a
American Welding Society. 1998a. "Standard Methods for Mechanical Testing of Welds," Designation B4.0, Miami, FL.

American Welding Society 1998b
American Welding Society. 1998b. "Standard Symbols for Welding, Brazing and Nondestructive Examination," Designation A2.4, Miami, FL.

British Standards Institution 1980
British Standards Institution. 1980. "Guidance on Some Methods for the Derivation of Acceptance Levels for Defects in Fusion Welded joints," Designation: BS PD6493, London.

Burdekin et al. 1975
Burdekin, F. W., Harrison, J. D., Kanazawa, T., Mashida, S., Ekwall, B., Knokoly, T., and Muncher, L. 1975. "Proposed Assessment Methods for Flaws with Respect to Failure by Brittle Fracture," *Welding in the World,* IIW-471-74(13).

Canadian Standard Association 1917
Canadian Standard Association. 1917. "Certification of Welding Inspectors," Designation: CSA W178.2, Rexdale, ON, Canada.

Greimann, Stecker, and Rens 1990
Greimann, L., Stecker, J., and Rens, K. 1990. "Management System for Miter Lock Gates," Technical Report REMR-OM-08," prepared by Engineering Research Institute, Ames, IA, for U.S. Army Construction Engineering Research Laboratories, Champaign, IL.

Pennsylvania Department of Transportation 1988
Pennsylvania Department of Transportation. 1988. "Guidelines for Fatigue and Fracture Safety Inspection of Bridges," Commonwealth of Pennsylvania, Department of Transportation, Bridge Management Systems Division.

A-2. Related Publications

American Institute of Steel Construction 1989
American Institute of Steel Construction. 1989. "Allowable Stress Design Manual of Steel Construction," 9th ed., Chicago, IL.

American Institute of Steel Construction 1994
American Institute of Steel Construction. 1994. "Load and Resistance Factor Design Manual of Steel Construction," 2nd ed., Chicago, IL.

American Railway Engineers Association 1992
American Railway Engineers Association. 1992. "Manual for Railway Engineering, Steel Bridges," Washington, DC.

ASTM A6/A6M
American Society for Testing and Materials. "Standard Specification for General Requirements for Rolled Steel Plates, Shapes, Sheet Piling, and Bars for Structural Use," Philadelphia, PA.

ASTM A7-33T
American Society for Testing and Materials. "Tentative Specifications for Steel for Bridges," Philadelphia, PA.

ASTM A7-39
American Society for Testing and Materials. "Standard Specifications for Steel for Bridges and Buildings," Philadelphia, PA.

ASTM A7-50T
American Society for Testing and Materials. "Standard Specification for Steel for Bridges and Buildings," Philadelphia, PA.

ASTM A7-67
American Society for Testing and Materials. "Specification for Steel for Bridges and Buildings," Philadelphia, PA.

ASTM A9-33T
American Society for Testing and Materials. "Tentative Specifications for Steel for Buildings," Philadelphia, PA.

ASTM A36-60T
American Society for Testing and Materials. "Tentative Specification for Structural Steel," Philadelphia, PA.

ASTM A94-25T
American Society for Testing and Materials. "Tentative Specifications for Structural Silicon Steel," Philadelphia, PA.

ASTM A140
American Society for Testing and Materials. "Specification for Steel for Bridges and Buildings," Philadelphia, PA.

ASTM A141
American Society for Testing and Materials. "Tentative Specifications for Structural Rivet Steel," Philadelphia, PA.

ASTM A195-36T
American Society for Testing and Materials. "Tentative Specifications for High-Strength Structural Rivet Steel," Philadelphia, PA.

ASTM A373-58T
American Society for Testing and Materials. "Tentative Specification for Structural Steel for Welding," Philadelphia, PA.

ASTM A502
American Society for Testing and Materials. "Standard Specification for Steel Structural Rivets," Philadelphia, PA.

ASTM A588/A588M
American Society for Testing and Materials. "Specification for High-Strength Low-Alloy Structural Steel with 50 KSI [345 Mpa] Minimum Yield Point to 4 in. [100 mm] Thick," Philadelphia, PA.

ASTM A898/A898M
American Society for Testing and Materials. "Specification for Straight Beam Ultrasonic Examination of Rolled Steel Structural Shapes," Philadelphia, PA.

ASTM E140
American Society for Testing and Materials. "Hardness Conversion Tables for Metals," Philadelphia, PA.

Barsom and Rolfe 1987
Barsom, J. M., and Rolfe, S. T. 1987. *Fracture and fatigue control in structures.* Prentice-Hall, Englewood Cliffs, NJ.

Birk 1989
Birk, J. D. 1989. "Economic Feasibility of a Tool to Remove Rivets from Railway Bridges," REU report, ATLSS Engineering Research Center, Bethlehem, PA.

Bower et al. 1992
Bower, J. E., Kaczinski, M. R., Ma, Z., Zhou, Y., Wood, J. D., and Yen, B. T. 1992. "Structural Evaluation of Riveted Spillway Gates," ATLSS Report No. 92-12, Lehigh University, Bethlehem, PA.

Commander et al. 1994
Commander, B. C., Schulz, J. X., Goble, G. G., and Chasten, C. P. 1994. "Field Testing and Structural Analysis of Vertical Lift Lock Gates," Technical Report REMR-CS-44, U.S. Army Engineer Waterways Experiment Station, Vicksburg, MS.

Ewins 1985
Ewins, D. J. 1985. "Hammer or Impactor Excitation," *Modal Testing: Theory and Practice,* Research Studies Press, Ltd. (A Division of John Wiley & Sons), Letchworth, Hertfordshire, England.

Fazio and Fazio 1984
Fazio, R. N., and Fazio, A. E. 1984. "Rivet Replacement Criteria," *Second Bridge Engineering Conference,* Volume 1, TRR 950, Transportation Research Board, Washington, DC.

Ferris 1953
Ferris, H. W., ed. 1953. "Iron and Steel Beams 1873 to 1952," American Institute of Steel Construction, Chicago, IL.

Fisher 1977
Fisher, J. W. 1977. "Bridge Fatigue Guide Design and Details," American Institute of Steel Construction, Chicago, IL.

Fisher 1984
Fisher, J. W. 1984. *Fatigue and Fracture in Steel Bridges,* John Wiley & Sons, New York.

Fisher et al. 1979
Fisher, J. W., Hausamann, H., Sullivan, M. D., and Pense, A. W. 1979. "Detection and Repair of Fatigue Damage in Welded Highway Bridges," National Cooperative Highway Research Program (NCHRP) Report 206, Transportation Research Board, Washington, DC.

Fisher et al. 1987
Fisher, J. W., Yen, B. T., Wang, D., and Mann, J. E. 1987. "Fatigue and Fracture Evaluation for Rating Riveted Bridges," National Cooperative Highway Research Program (NCHRP) Report 302, Transportation Research Board, Washington, DC.

Frank and Fisher 1979
Frank, K. H., and Fisher, J. W. 1979. "Fatigue Strength of Fillet Welded Cruciform Joints," *Journal of the Structural Division*, ASCE, Vol 105, No. ST9, pp 1727-1740.

Kayser and Nowak 1987
Kayser, J. R., and Nowak, A. S. 1987. "Evaluation of Corroded Steel Bridges," *Bridges and Transmission Line Structures,* American Society of Civil Engineers, New York, 35-46.

Kayser and Nowak 1989
Kayser, J. R., and Nowak, A. S. 1989. "Reliability of Corroded Steel Bridges," *Structural Safety,* Vol. 6. Elsevier Science Publishers, New York, 53-63.

Keating 1994
Keating, P. B. 1994. "Focusing on Fatigue," *Civil Engineering*, November 1994, 54-57.

Mlakar et al. 1989
Mlakar, P. F., Toussi, S., Kearney, F.W., and White, D. 1989. "Reliability of Steel Civil Works Structures," Technical Report REMR-CS-24, U.S. Army Construction Engineering Research Laboratory, Champaign, IL.

Pisigan and Singley 1985
Pisigan, F. A., and Singley, J. E. 1985. "Evaluation of Water Corrosivity Using the Langelier Index and Relative Corrosion Rate Models," *Materials Performance Journal*, April, 26-36.

Slater 1987
Slater, J. E. 1987. "Corrosion in Structures," *Metals Handbook,* 9th ed., ASM International, Metals Park, OH, 13, 1229-1310.

Stout and Doty 1953
Stout, R. D., and Doty, W. D. 1953. *Weldability of Steels*, 1st ed., Welding Research Council, New York.

Stout et al. 1987
Stout, R. D., and contributing authors Ott, C. W., Pense, A. W., Snyder, D. J., Somers, B. R., and Somers, R. E. 1987. *Weldability of Steels,* 4th ed., Welding Research Council, New York.

Tada, Paris, and Irwin 1985
Tada, H., Paris, P. C., and Irwin, G. R. 1985. *The Stress Analysis of Cracks Handbook,* Paris Productions, Inc., Saint Louis, MO.